US ARMY RESEARCH OFFICE

WORKSHOP

ON

SMART MATERIALS

August 15-17, 1994

The Martin Fisher School of Physics
Brandeis University
Waltham MA 02254

REPORT DOCUMENTATION PAGE

Form Approved
OMB No. 0704-0188

1. AGENCY USE ONLY (Leave blank)	2. REPORT DATE	3. REPORT TYPE AND DATES COVERED
		Final Aug 15-Aug 17, 1994

4. TITLE AND SUBTITLE

Workshop on Smart Materials

5. FUNDING NUMBERS

DAAH04-94-G-0309

6. AUTHOR(S)

Robert B. Meyer and Edward Chen

7. PERFORMING ORGANIZATION NAME(S) AND ADDRESS(ES)

Brandeis University
Department of Physics
415 South Street
Waltham, MA 02254

8. PERFORMING ORGANIZATION REPORT NUMBER

9. SPONSORING / MONITORING AGENCY NAME(S) AND ADDRESS(ES)

U.S. Army Research Office
P.O. Box 12211
Research Triangle Park, NC 27709-2211

10. SPONSORING / MONITORING AGENCY REPORT NUMBER

ARO 33608.1-MS-CF

11. SUPPLEMENTARY NOTES

The views, opinions and/or findings contained in this report are those of the author(s) and should not be construed as an official Department of the Army position, policy, or decision, unless so designated by other documentation.

12a. DISTRIBUTION / AVAILABILITY STATEMENT

Approved for public release; distribution unlimited.

12b. DISTRIBUTION CODE

13. ABSTRACT *(Maximum 200 words)*

Proceedings of a workshop on Smart Materials, reviewing the research sponsored by the ARO program in Smart Materials and Systems. Extended abstracts from 18 investigators and 2 invited speakers are included.

14. SUBJECT TERMS

Smart materials, biosystems, optics, polymers, solid state

15. NUMBER OF PAGES

16. PRICE CODE

17. SECURITY CLASSIFICATION OF REPORT	18. SECURITY CLASSIFICATION OF THIS PAGE	19. SECURITY CLASSIFICATION OF ABSTRACT	20. LIMITATION OF ABSTRACT
UNCLASSIFIED	UNCLASSIFIED	UNCLASSIFIED	UL

Table of Contents

Forward

In August,1994, a Workshop on Smart Materials was held at Brandeis University. The general purpose of the workshop was to review the work done under the auspices of the ARO's URI program in Smart Materials and Structures, which has funded research at a number of universities for several years. All the available principal investigators were invited to participate. Two keynote speakers were also invited, to highlight important topics. In addition to ARO representatives, a number of Army Research Laboratory scientists attended.

The history of Smart Materials and the ARO's role in this field is short and exciting. Early on, the ARO recognized its potential, and in 1988 they sponsored the first workshop in this field at VPI, on " Smart Materials, Structures and Mathematical Issues." This was followed by the ARO U.S.-Japan Workshop on Smart/Intelligent Materials and Systems in 1990. In FY 1989, the ARO made a major commitment to funding research in this field through the DoD URI program. The ARO concepts of Smart Structures and Smart Materials are as follows: A Smart Structure is viewed as a structure or structural component on which are attached/embedded sensors and actuators whose signals and actions are coordinated through a control system to provide suitable responses to external stimuli. A Smart Material, on the other hand, has the sensor, actuator and control elements as part of the structure of the material itself. This typically involves the design, synthesis, and processing of Smart Materials at the molecular level, and often the use of intimate combinations of materials, as layered structures, or composites. A workshop on Smart Structures was held in September, 1993, at the University of Texas at Arlington. The workshop at Brandeis was intended to review Smart Materials, rather than Structures. The workshop also took on the role of a final program review, since the URI program on Smart Materials and Structures will unfortunately be concluding in FY 1995.

The program of the workshop included a general presentation of the ARO program, its purpose, its projects, and its accomplishments, followed by a discussion of what had been learned and what we could look forward to. It was intended to include all the currently active ARO research programs on Smart Materials. The detailed program that grew out of this plan is presented in the following section. It involves introductory remarks by Dr. Crowson, keynote addresses, and the division of the presentations by principle investigators into four sub-areas, for convenience of organization. These sub-areas are represented both in the presentations, and in the reports that constitute the main summary of the follow-up discussion. The general summary of the workshop that follows the program includes ideas drawn from the final discussion session and from the separate group reports.

Robert B. Meyer
Brandeis University

Edward Chen
U.S. Army Research Office

ARO Workshop on Smart Materials

Brandeis University
August 15-17, 1994

Program

Monday, August 15

0830 Registration opens

0850 Welcoming Remarks, Dr. Robert B. Meyer
0910 Introduction to the Workshop, Dr. Andrew Crowson
0940 Invited Lecture, Dr. Masuo Aizawa

1025 Coffee Break

Session 1: Biosystems, Chairman, Dr. Kenneth A. Marx

1045 Dr. Pill-Son Song
1120 Dr. Wesley E. Stites
1155 Dr. H. Ti Tien

1230 Lunch

1345 Dr. Kenneth A. Marx

Session 2: Optical Systems, Chairman, Dr. Robert E. Meyer

1420 Dr. Mark G. Kuzyk
1455 Dr. Michael L. Myrick

1530 Break

1550 Dr. Yang Zhao
1625 Dr. Robert B. Meyer

1700 End of First Day

Tuesday, August 16

0830 Opening Announcements, Dr. Robert B. Meyer
0840 Invited Lecture, Dr. R.A. Pethrick

Session 3: Polymer Systems, Chairman, Dr. M. Shahinpoor

0925 Dr. William J. Brittain
1000 Dr. Darrell H. Reneker

1035 Coffee Break

1100 Dr. William Rosen
1135 Dr. M. Shahinpoor

1210 Lunch

Session 4: Solid State Systems, Chairman, Dr. A. Peter Jardine

1310 Dr. William B. Carlson
1345 Dr. Walter A. Schulze
1420 Dr. Craig J. Eckhardt

1455 Break

1515 Dr. John E. Furneaux
1550 Dr. Russell Pinizzotto
1625 Dr. A. Peter Jardine

1700 End of Second Day

Wednesday, August 17

0830 Meetings of the four area groups to formulate presentations

Presentation of Group Reports

0930 Biosystems report
0950 Optical systems report

1010 Coffee Break

1030 Polymer systems report
1050 Solid State systems report
1110 General Discussion and Conclusions

Departure; lunch is available on campus

General Summary

The workshop produced a stimulating atmosphere, characterized by an open exchange of information and mutual interest in a broad range of topics. It was clear that the definition of Smart Materials included a number of conceptions of both the words "Smart" and "Materials." However, as distinct from Smart Systems in general, the projects in this workshop all concentrated on materials development, and phenomena taking place in materials which could play an essential role in the basic functions of sensing, computing, and actuating that are at the heart of of Smart Materials or Systems. In many cases, all three basic functions were integrated into a material system, without external computation or power supply. Extended abstracts of the presentations by the principal investigators follow the summary reports.

In each of the following group summary reports, various issues are addressed. For each project, some things have been learned, and new ideas and insights have been generated. Progress has been made in each project, and each project surely has the potential of further accomplishments. By continuing research on the projects presented at the workshop, we could add to our general knowledge about smart materials, by generating examples from which one might generalize.

However, it is also clear that in addition to these specific conclusions and prospects for future work, one must say that the field of smart materials is still in an early stage of development. In all areas, there were suggestions for future work that implied very basic investigations of new or well known materials, new combinations of materials, and new ways of taking advantage of material properties that have not yet been exploited. I was clear that in many cases, these new investigations implied cooperation among scientists from very different backgrounds, such as enzymology, polymer synthesis and semiconductor technology. In other cases, even though only one classical discipline was involved, it was clear that one had to gain a deeper understanding of the structure and function of some material before one could hope to control or modify it in a useful way to achieve a particular goal in Smart Materials. Despite this clear need for vast amounts of knowledge, the encouraging thing was that there is already an enormous range of imagined devices and applications that have only just begun to be explored. There is no shortage of potential for the field of Smart Materials.

In addition to the obvious need for continued funding, there is also a need for expanded communication and cross-disciplinary interaction among scientists working on Smart Materials. There is also a need for flexibility in research administrative structures, so that as new needs for collaboration arise, the mechanisms exist to address those needs, both in terms of funding and in terms of making the appropriate connections among scientists.

In conclusion, this Workshop on Smart Materials served to review the ARO program, to educate the participants, and to help us look to the challenges of the future.

ARO WORKSHOP ON SMART MATERIALS

BRANDEIS UNIVERSITY AUGUST 15-17, 1994

BIOSYSTEMS GROUP REPORT

Prepared by Prof. K.A. Marx, Chairman

with Prof. M. Aizawa
Prof. P.S. Song
Prof. A. Ottova
Prof. H. Ti Tien
Dr. J. Akkara

Biological systems at the molecular and supramolecular levels both inspire and inform us in unique ways about smart materials and smart structures. Nature has achieved an exquisite sensitivity to stimuli and control over organismal/cellular response through the directed evolution of these molecular level systems as integrated components of living cells. An excellent example of a naturally occuring smart system teaching us is that presented by Prof. Meyer on smart reflectors being found as the surface exoskeleton coating of certain species of iridescent beetles.

The Biosystems Group felt quite strongly the importance of having interdisciplinary teams(from molecular biologists all the way to computer scientists and engineers)study the fundamental mechanisms of how biological macromolecules carry out their sensing/actuating, signal transduction functions. Many such signals are sensed and transduced by cells, including: thermal, electrical, mechanical, light and chemical signals. Most of the macromolecular systems involved in detecting these signals are unexplored or minimally studied. Only by very specifically controlling and channeling the energy involved in these sensing/transduction functions do these biological macromolecular systems achieve their high sensitivity, specificity and efficiency as smart materials.

For the ARO to be able to best utilize these molecules, their rationally modified forms or their fundamental mechanisms in optimized biomimetic approaches, considerably more fundamental study of important systems needs to be done. Only by understanding the underlying principles involved will real 'engineering' of these biosystems be possible. This involves both experimental as well as systems based modelling approaches to describe the fundamental interactions between components involved in carrying out the smart material/structure function. Of special interest in modelling is to understand potential emergent properties of complex systems comprised of coupled associative components. Such an understanding could lead to the *de novo* design of signal transduction pathways or to natural smart biological systems being incorporated into new cellular environments or cell types.

Another important concensus of the Biosystems Group involved the realization that both Molecular Biology and Materials Science represent disciplines that have

matured to the point that they may be merged successfully to create smart materials and structures. One example of this is manifest in the development of 'toolkits' in molecular biology. Provided by suppliers, once complicated molecular systems that themselves were the object of fundamental research investigation 10 years ago are now being supplied as off the shelf components or reagents for investigators to use in the next level of experimental questions being addressed. These include methodologies to rationally alter nucleic acid and protein sequences to create new and useful properties. The Biosystems Group felt that an appropriate methodology to merge the two disciplines is through thin film, monolayer, bilayer formats that immobilize ordered biological macromolecules, in nanoscale to mesoscale structures on the surface of Si based substrates. In doing so, great cooperative advantage can be gained from the current depth of understanding of Si based microelectronics measurements.

To carry out the successful merging of Molecular Biology and Materials Science in Si based thin film smart materials, an entirely novel interfacial technology must be developed to connect the smart materials/structures components from each discipline. This interfacial technology may involve a number of different approaches capable of ordering the individual bound components. These approaches include: LB trough monolayer films and multilayer build up; BLM(immobilized Black Lipid Membranes) and SAMs (self-assembling monolayers). In developing novel interfacial technology, the use of polymeric materials to bind the elements from both disciplines and provide mechanical stability, durability, and useful interfacial optoelectronic properties(such as conducting polymers) will be of particular importance. An added advantage of the thin film, monolayer, bilayer, BLM, SAM formats is that from these techniques multilayer structures may be designed and created that can involve biological macromolecules/organics/inorganics in various combinations. Nature continues to teach us the value of this alternating layer or laminate structure approach for building smart or emergent properties into systems found in living cells or whole organisms.

One example of a compelling direction to take the novel interfacial technology to be developed for merging Molecular Biology and Materials Science is to utilize it coupled with the immobilized, miniaturized combinatorial chemistries(peptide, nucleic acid) that have been developed recently for rational accelerated drug discovery and selection of macromolecules for optimized binding affinities. This approach could be used to select the fundamental building blocks of smart molecular materials from biological systems by highest affinity selection for the desired interactions and properties. Also this technology could be used to test for the compatibility of different organic/polymeric and inorganic materials with biological macromolecules. That is, to create or evolve new interfacial technology.

Optical Systems Group Report

Submitted by Robert B. Meyer

Other Group Members:
Dr. Mark G. Kuzyk
Dr. Michael L. Myrick
Dr. Yang Zhao

The Optical Systems group discussion covered the applications and advantages of optical systems for smart materials and structures. The discussion then moved to consideration of the future, and to the requirements for significant progress in the projects under way.

The recognized advantages of optical systems include their intrinsic rapid response, or high bandwidth, the possibility of unique architectures, including parallel processing, and the use of light to sense, to compute, and to actuate. With optical power to run the system, in fact complete systems can be constructed that are entirely based on the interaction of light with smart material structures.

The applications taking advantage of these properties of optical systems include materials and systems for protection against laser weapons, smart surfaces including smart reflectors and smart camouflage systems, and even decontamination systems. In support of such applications there are important projects in the development of components, including sensors, computation systems, and actuators. For interaction with humans, optical display components and systems are also of fundamental importance.

In reviewing the projects reported at the workshop, it was clear that the challenge in most cases lay in the necessity to collect and utilize information, techniques, and materials from a wide range of sources. For a single investigator or even a team working on a project to make significant progress after an initial exploratory period usually requires the optimization of at least one essential part of the design. This often requires, for example, materials selection or development requiring specialized knowledge and techniques. Or it may require major computations, or micro-fabrication facilities, or specialized analytic or testing methods. In any case, the ability to find the solutions to such problems was recognized as crucial to the success of smart materials and system development.

Some specific examples come out of the workshop. For several of the projects, interaction of light with materials at the optical wavelength scale was essential, since the materials depended on diffraction effects for their function. This requires changes either in material dimensions or in indices of refraction as the mechanism for modulating the interaction of the material with light. After some demonstration of the feasibility of this kind of modulation to provide the desired

smart response, using whatever material could be obtained for initial studies, it became clear that specialized materials and specialized fabrication methods were usually required. Thus, for smart reflectors based on liquid crystals, for example, a list of properties for the optimum material could be developed, but obtaining that material would require collaboration with a synthetic organic chemist with the right kind of experience and motivation toward materials development. For laser goggles based on nonlinear optical response of a bragg-scattering layered structure, selection of the appropriate nonlinear optical materials, and the fabrication of the layered structure are crucial. For each material candidate, specialized fabrication methods must be considered. For light actuated feedback controlled interferometric devices based on spatially modulated optical fibers, the fiber material and the modulation techniques must be chosen properly to optimize performance. For chameleonic skin, the requirements for the liquid crystal display device that is the actuator are different from those for ordinary information display. In all these examples, expert knowledge must be sought and evaluated, and the appropriate collaborations formed.

Beyond the questions of how to proceed with development of current projects, there is the larger question of how to conceive of whole new approaches and methodologies for smart systems and materials, and of new kinds of tools and techniques to employ. This will surely require the merging of ideas and information from a variety of different fields. Surely there is still much to be learned about how biological systems utilize and interact with light, for example. Experts in optics, provided with such information, might conceive of whole new approaches to optical smart systems and materials. Developing such systems might also require further interaction with biologists for materials development (novel proteins) or nanoscale fabrication.

Even though the discussion focused on optical systems, on which we were expert, it seemed obvious that the same problems must arise with all the materials and systems being explored. A major conclusion of our discussion was that resources for ongoing information exchange, mechanisms for identifying and making contact with experts in other fields, and flexibility in funding methods to accommodate new collaborations were all essential.

ARO Workshop on Smart Materials
August 17, 1994
Brandeis University

Summary Report of Polymer Systems Break-Out Group

"Future Directions in Polymeric Smart Systems"

submitted by William J. Brittain

other committee members: Darrell Reneker, William Rosen & M. Shahinpoor

- transform use of polymers in smart materials from "matrix" to essential functions of the system

Many uses of functional polymers systems simply employ the polymer as a physical matrix with embedded functional components. The polymer provides physical integrity and the function of the material relies on the added molecular components. The next generation of polymeric smart structures should use the polymer chains to enhance the action of the functional components and provide a higher organizational structure to the overall system.

- exploit known principles of phase transformation, phase segregation and crystallization/morphology

While biological systems demonstrate amazingly complex behavior and function in response to external stimuli, it is difficult with current polymer chemistry expertise to control structural hierarchy at the same level. However, much is known about morphology and phase segregation in block copolymer and crystalline systems. These phase separated morphologies provide many ways to create more highly organized structures for smart systems. Many functional responses rely on a geometrical arrangement of molecular architecture; this geometry can be created/enhanced by the use of phase segregation. In addition, phase separation can be used to impart improved physical properties to polymeric systems.

- improve fabrication and processing approaches to polymeric smart structures

New fabrication methods are needed. These might exploit current techniques of thin film deposition (LB, self-assembly) and spontaneous phase separation. One goal is to chemically arrange the monomeric or oligomeric building blocks during polymer formation to create long-range order in the polymer molecule during polymerization. Another goal is to build polymers which spontaneously (by the application of heat or a potential field) organize into stable structures having macroscopic ordering. For this type of processing, it will be important to control the placement of functional components to enhance the tendency toward large scale organization.

- improve understanding of some currently known responsive systems

Some of the current responsive polymers (e.g., polyelectrolytes that change shape in response to pH) are not fully understood. Better molecular design to enhance macroscopic effects, and molecular characterization (monomer sequence, molecular weights, phase morphology, degree of cross linking) will help pave the way for the next generation of improved and more sophisticated polymers.

OVERALL, the goal of future work should be to use macroscopically ordered polymers as functional systems to help improve responses to external stimuli, provide an inherent tendency toward geometrical alignment of functional components, and develop new fabrication procedures that mitigate the need for multiple-processing steps in the building of smart structures.

The areas of interest that these structures may impact include: laser eye protection, thermal signal reduction, dynamic camouflage, semi-permeable membranes, new fabrication/processing technology, stress and failure sensors, and electrostrictive gels. The uses for the smart structures include both civilian and military applications; e.g. an exoskeleton to enhance the mobility of "land warrior" can also lead to an active prosthesis for the disabled.

ARO Smart Materials Workshop

Group Report on Solid State Systems

Submitted by Dr. A. Peter Jardine

Other Group Members:

Dr. William B. Carlson
Dr. Craig J. Eckhardt
Dr. John E. Furneaux
Dr. Russell Pinizzotto
Dr. Walter A. Schulze

Summary:

The technologies reported here range from fundamental materials studies of solid state materials for sensor/actuator combinations to overall system integration using solid state electronics. Each sensor/actuator combination effectively controls one physical parameter , for example, on a structure. There is an obvious need to both improve the effectiveness of the sensor/actuator combination as well as to introduce local autonomous control at that particular site, thereby minimizing the amount of external control to be imposed on a structure. However over a large structure, that physical parameter may change significantly, and therefore the external control of the structure becomes problematic. The ARO workshop seeks to address these issues in terms of local and global systems.

I have arranged the topics and speakers in terms of a bottom-up approach, looking first at synthesis issues at the atomic level and then introducing subjects on a more macroscopic scale or for more global applications:

Towards the molecular design of smart materials;

Ekhardt (Nebraska University) has investigated the synthesis of smart molecular materials in some clever ways. The key was to find molecules which would crystallize into a desired unit cell, and thereby use known structure-property relations to infer the likely active or adaptive properties of the system. For three dimensional crystals, the search for a precursor is difficult due to the large number of geometrical combinations available. By restricting the material to two dimensions, there is a better correspondence between the precursor states and

final structure. In addition, the design of two dimensional precursors (so-called amphiphiles) to form the required 2-dimensional net is more facile. A Monte-Carlo based atom-atom simulation was developed so that the likely 2-D net could be predicted, thereby saving expensive synthesis time. Of real interest was that synthesis of both chiral 2D nets and photoferroelectric 2D nets was reported. Thus, there is a methodology in place to begin the synthesis of previously unexplored 2D nets by the molecular design of amphiphiles. The net results of the syntheses are Langmuir-Blodgett films that have similar properties over a macroscale region, which can thus be used to both sense and actuate, and can also be interrogated by micro-scale to macroscale devices.

Strain-temperature piezo smart materials:

Carlson and Shulze (Alfred University) have investigated synthesis and manufacturing techniques of Positive Temperature Coefficient Resistors (PTCR's) based on doped $BaTiO_3$ ceramics. Using a piezoelectric material, PTCR's exhibit both temperature-resistance and temperature-voltage relations, hence serving as a smart piezoresistor. The ability to produce such materials in reasonable quantities has interesting implications, especially as a material to modify the strain response of another material to a thermal event, such as protecting and controlling the position of a platform to thermal drifts, in friction brake applications etc. As a PTCR material, piezoresistors can be used as self-tripping electrical relays in case of overheating of modules. These types of materials, unlike mechanical relays, have no moving parts and therefore will be more reliable and possibly less expensive than their mechanical counterparts.

Local Control based on Ferroelastic and Ferroelectric Heterostructures:

Jardine (SUNY Stony Brook) reported on the successful synthesis of sensor-actuator materials using ferroelastic TiNi and ferroelectric PZT coupled via a TiO_2 layer. The use of the superelastic phase transformation in TiNi to engineer the dampened structural response to shock phenomenon has been established in cavitation-erosion studies. By coupling TiNi to PZT via an RC network composed of a thin film of TiO_2, the final composite material can sense and actuate to dampen structural vibrations without the use of external control, making these truly "smart" composite materials. By using thin-film TiNi, an unexpected payoff was the discovery of fast-acting TiNi cantilevers, which responded at 520 Hz, a 10 time increase in response rate from previously reported TiNi actuators.

At present the work has centered around the development of macroscale panels based on porous TiNi coupled to PZT. However, continuum of scale synthesis is also of interest, and PZT coated microballoons have been investigated as a suitable substrate on which to grow these heterostructures. As the material properties change dramatically in going from nanoscale to macroscale, the idea

of using these large heterostructures based on smaller structures may generate interesting structural response based on cooperative phenomena.

Optically based dimensionally self regulating structures:

As presented by Aifer (Boston U.), the work of Furneaux (U.Oklahoma) and Goldberg (Boston U.) , a modulation doped Field Effect Transistor (MODFET) was developed, which has a self-tuning capability for 10-12 mm wavelength IR radiation. Although the GaAs/AlGaAs based device is fixed with respect to the structural features (such as wires, mesa etc.) lithographically defined into the structure, the controllable gate voltage of the device controls the electron density at the interface and therefore the profile of the potential well patterned into the material. These potential wells defined by the line spacing will cause 2-D sub-bands in the device to be split. If the well is symmetric, then the splitting is a function of the well width only. However, if an asymmetric potential well is used then the curvature of the asymmetric well is involved in the splitting, which is controlled by the gate voltage. Thus the "smartness" of the device is in defining the potential well profile, which in turn changes the spectroscopic features of the device, by changing the splitting of the 2-D sub-bands.

Towards the signal processing of highly redundant systems:

Pinnizzotto (U.North Texas) reported on "Genius" chip type technologies which could be used to make comprehensive simulations of smart material interactions on a global scale. This would be important in highly redundant systems where the sensor/actuator interactions may be easily predictable for one device but would be difficult to predict on a global level where cooperative phenomenon will affect the final state of the structure. The project has developed from productive industrial partnerships, with work in progress based on the development of suitable ferroelectric films which can be lifted-off of a substrate to build the requisite 3-D geometry. The idea of generating devices which simulate neurons is exciting, due to the ability to produce interesting interconnection patterns between "neurons" which could be either hard-wired or soft-wired depending on the system state, thus generating a primitive type of learning.

Synergies of Technologies:

LB films can be used as flexible systems which can be interrogated optically, which could therefore provide remote sensing information. Also, LB films could replace ferroelectrics in some cases; for instance, a flexible Genius-type chip might be made using LB films.

INTELLIGENT MOLECULAR MATERIALS

Masuo Aizawa
Department of Bioengineering, Tokyo Insitute of Technology, Nagatsuta, Midori-ku, Yokohama 227

DESIGN CONCEPT OF INTELLIGENT MATERIALS

The design concept of intelligent materials has emerged from a view point of integration of sensing, information processing and actuating functionalities within material [1-2]. The intelligent materials may be endowed with environmental adaptability, self-repair, self-degradability, learning ability and other intelligent characteristics. The new technology will change the current philosophy of material design and usher in a new material age.

The intelligent molecular materials are designed on the model of the biological systems which involve the molecular systems and structures with the intelligent characteristics such as environmental adaptability and self-repair. The biological systems provide us with the design principles in three defferent manners.

1. Protein Molecular Network : Receptor proteins embedded in cellular membranes are coordinated with adjacent protein molecules in non-covalent manner to transduce extracellular molecular information into innercellular one for regulating the cellular functions. These protein molecular networks are characterized by the intelligent molecular material which can undergo information process through intermolecular coordination. Several intelligent molecular materials have been designed after the protien molecular networks in the biological systems.

2. Growing Processes : Sea urchin spines are porous single crystals of calcium carbonate. Their growth is apparently controlled by acidic proteoglycans which absorb strongly to the crystal surface. These molecules when present in solution, can act as growth inhibitors, or, when absorbed to a surface, can act as nucleating agents. These polymers are incorporated into the crystal when it grows and harden the crystal. These biological growing processes can be mimicked.

3. Intelligent Biological Structures : Various unique structures are found in biological systems including bones, tooth and bamboo, which may indicate design principle of intelligent materials.

In our laboratory several intelligent molecular materials have been designed and processed on the basis of the design concept described above.

STIMULI-RESPONSIVE PROTEIN ASSEMBLIES

Calcium-binding protein, calmodulin, has covalently been conjugated with such a protein as phosphodiesterase with retain-

Calcium-binding protein, calmodulin, has covalently been conjugated with such a protein as phosphodiesterase with retaining both binding affinity and enzyme activity [3-4]. The sensing and actuating functions are portioned in the calmodulin and enzyme parts of the protein assembly, respectively. The protein assembly responds to calcium ion in such a manner as the enzyme is activated. It is postulated that calcium ion is bound with calmodulin with a resulting change in its conformation, which is followed by a conformational change of phosphodiesterase. Two different parts of molecular functions have successfully been coordinated in a single protein assembly.

The stimuli-responsive protein assemblies have been fabricated in a membrane form to regulate the pore-size of the membrane with responding to the environment, which appears promissing in application in a wide field.

MOLECULAR NETWORK TO RESPOND ENVIRONMENTAL POLLUTANTS

An extremely sophisticated molecular network has been constructed and implimented in bacterial cells [5]. The major part of the molecular network is TOL plasmid which carries a series of genes required in the digestion of benzene derivatives. In the plasmid, the gene product, xyl R protein, stimulates the transcription of the following genes by activating the promoter. We succeeded in introducing the firefly luciferase gene to the TOL plasmid. The recombinant plasmid, pTSN316, was incorporated in E.coli.

The xyl R protein shows strong affinity to benzene derivatives such as xylene and toluene to form comoplexes, which is followed by activation of the promoter for the luciferase gene. In result, firefly luciferase is produced in a cell with responding benzene derivatives. When the cells are in contact with luciferase, the cells exhibit luminescence to benzene and toluene.

ORDERED ANTIBODY ARRAY FOR BIOSELECTIVE MOLECULAR COUNTING BY AFM

Biosensing technology has made a marked progress specifically in this decade with a great success in implementation of biological selectivity into electronic and optoelectronic devices. One of the ultimate goals of biosensing technology may be to emerge a new technology to quantitate selectively a specific molecule in a specific site.

We have succeeded in fabricating an ordered array of antibody on the solid surface and quantitating selectively the corresponding antigen molecules on the antibody array by atomic force microscopy (AFM). Protein A (Prot A), which has a specific binding affinity to the Fc part of antibody, was found to form a monolayer on the water surface. A monolayer film of Prot A was deposited on the solid surface by LB film technique. Antiferritin antibody was then self-assembled on the Prot A layer. Each protein layer was characterized in ordered structure by AFM. In the further step, ferritin was self-assembled on the antibody

array. Ferritin molecules self-assembled on the antibody nano-array was quantitated by AFM.

ELECTRO-SENSITIVE ENZYME MEMBRANES

Another intelligent biomaterial is an activity-controllable enzyme membrane. A redox enzyme is immobilized in a conductive polymer membrane on the electrode surface [6]. Electron transfer between the active center of the enzyme and the electrode surface is extremely enhanced through a molecular wire of conductive polymer. Enzyme activity of molecular-wired enzyme was found modulated by a change in electrode potential. The membrane is applicable to an intelligent bioreactor in which its catalytic activity could be electrically modulated in response to the reaction conditions.

INTELLIGENT MOLECULAR MACHINE

Ribosome is an subcellular organelle which translates the codes of mRNA to amino acid sequence of a peptide. Cell-free protein synthesis has been performed with an immobilized mRNA on which ribosomes are attached. The ribosome worked as an intelligent molecular machine on the immobilized mRNA, which was followed by incorporation of the corresponding tRNA and peptide bonding of amino acids [7].

ARTIFICIALLY DESIGNED NEURON NETWORKS ON SOLID SURFACE

There have been striking attempts to the cultured neurons by patterning their outgrowth. It would be useful to construct 2-dimentional *in vitro* models that mimic the architecture observed *in vivo*. These attempts have simply been verified to aid in the study of developmental and computational properties of neural systems.

Our serial investigation have shown that the proliferation of mammalian cells cultured on the electrode surface is electronically regulated. In the line of the investigations 2-dimentional *in vitro* neural network have been constructed on the potential-controlled and patterned electrode surface as was designed.

Fibroblast cells (PC12C) were plated on the surface of an optically transparent electrode coated with collagen. The electrode is placed at the bottom of a culture vessel with a counter electrode and a Ag/AgCl, the cells differentiated to neurites. In sharp contrast, differentiation was markedly inhibited around 0.4V vs. Ag/AgCl.

The findings have encouraged us to construct an electrically controlled 2-dimentional *in vitro* neuronetwork model. The PC12 cells were placed on the surface of the patterned electrode plate. Potential controlled culture was continued for 14 days in the presence of NGF. The neurites were growth in the direction of the glass stria. The electrode prevented the neurites from growing. This should be the first step to control the direction

of neuronetwork formation.

References

1) The Concept of Intelligent Materials and Guidelines on Their R&D Promotion, Science and Technology Agency in Japan, Nov. 30 (1989) (published in English in Jan., 1990)

2) T.Takagi, Proc. 1st Int. Conf. Intelligent Materials, 3-8 (1993)

3) T. Miwa, N.Damrongchai, H.Shinohara, Y.Ikariyama, and M.Aizawa, J.Biotechnol., 20, 141-150 (1991)

4) T.Miwa, E.Kobatake, Y.Ikariyama, and M.Aizawa, Bioconjugate Chem., 2, 271-274 (1991)

5) Y.Ikariyama, S.Nishiguchi, E.Kobatake, M.Aizawa, M.Tsuda, and T.Nakazawa, in "Biolumin. and Chemilumin." (ed. A.A.Szalay, L.J.Kricka, and P.Stanley) John Wiley, Chichester (1993) pp.420-424.

6) G.F.Khan, H.Shinohara, Y.Ikariyama, and M.Aizawa, J.Electroanal.Chem., 315, 263 (1991)

7) E.Kobatake, Y.Ikariyama, and M.Aizawa, Biotechnol.Bioeng., 37, 723-728 (1991)

NEW PHOTOSENSOR MOLECULES OF SINGLE CELL CILIATES

Nengbing Tao and Pill-Soon Song

Center for Materials Research and Analysis and Department of Chemistry
University of Nebraska, Lincoln, NE 68588-0304

Introduction. Most organisms ranging from bacteria to mammals directly or indirectly react to light irradiation, eliciting a wide variety of responses. These processes are initiated by the absorption of light of specific wavelength by the photosensor molecules involved. However, only a few biological photosensor molecules have been structurally identified and characterized. The best known photoreceptors are those containing retinal as a chromophore. Although retinal-containing photoreceptors are used in nature, most notably rhodopsin in animal vision, other rhodopsin-like photoreceptor molecules have also been found widely distributed outside the animal kingdom.[1,2,3] Another class of well-studied photoreceptors belong to the tetrapyrrole family which includes phytochrome, phycobilins and chlorophylls. Phytochrome serves as a main photosensory pigment and regulates many processes and activities in plants.[4] It has been found in green algae as well as in spermatophytes, ferns and mosses.[5] The phycobilins are accessory pigments which absorb visible wavelength light and transfer excitation energy to chlorophylls.[6] Chlorophylls are Mg^{2+}-containing tetrapyrrole molecules and occur in all photosynthetic organisms primarily to harvest light energy for photosynthetic carbon dioxide fixation. In addition, flavins have been implicated to represent a major group of blue light receptors.[7,8] We recently reported a new class of photoreceptor molecule, stentorin found in *Stentor coeruleus*,[9] confirming its hypericin-like structure.[10,11] Interestingly, the photosensor molecule blepharismin in *Blepharisma japonicum*, a heterotrichous protozoan closely related to *Stentor coeruleus*, has also been proposed to be hypericin-like.[10,12,13,14] Thus these photosensor molecules represent a novel class of photoreceptor molecules with significantly different chromophore structure from the well-known photoreceptors. Here we report our attempt to characterize the photosensor molecules and their function in *Stentor coeruleus* and *Blepharisma japonicum.*

Results and Discussion. When stentorin crude extract was developed on a normal phase thin layer chromatographic plate, usually only streaky bands were observed for most common solvents tried. Fractionation through a reverse phase C18 column, with an eluent consisting of 80% methanol, 20% ethyl acetate and 0.05% TFA, afforded a major fraction, stentorin.

Stentorin has a very similar absorption spectrum to that of hypericin.[10,11] This is shown in Figure 1. We observed a red shift of 7 nm for the longest wavelength absorption peak from hypericin (588 nm) to stentorin (595 nm). However, this red shift is reduced greatly under acidic conditions. In fact, the λ_{max} for stentorin and hypericin are 577 and 578 nm respectively under acidic condition. These results clearly indicate that stentorin has a naphthodianthrone skeleton. It should also be noted that stentorin exhibits a weak hyperchromic effect, whereas hypericin shows hypochromism in acidic condition. This absorbance difference, along with the λ_{max} difference, can be taken as an indication of structural distinction between them.

The solid line in Figure 2 shows the absorption spectrum of red blepharismin, which was extracted from *Blepharisma* cells with methanol. When *Blepharisma* cells are exposed to light of moderate intensity (3 to 30 Wm^{-2}),[17] their color turns green. The extract (oxidized blepharismin) from these cells has a spectrum shown as a dotted line in Figure 2. Though blepharismin has a distinct absorption spectrum, its oxidized form does have a similar spectrum to that of hypericin (Figure 1). It is concluded that blepharismin is also analogous to hypericin.

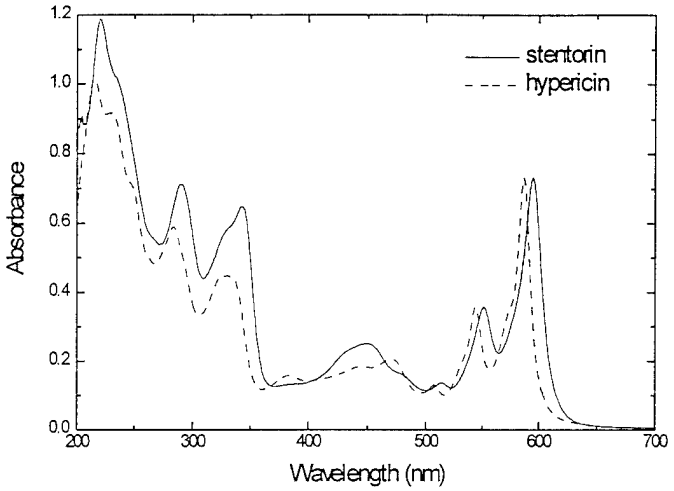

Figure 1. Absorption spectra of stentorin and hypericin.

The IR spectra for stentorin and hypericin have been recorded. It was not difficult to identify the resemblance between them. Particular attention should be paid to the peaks at 1575 (stentorin) and 1590 cm^{-1} (hypericin). They are the absorptions characteristic of hydrogen-bonded quinone carbonyl groups.[18] Hypericin hexaacetate and stentorin octacetate both showed two carbonyl absorptions, one from non-hydrogen-bonded quinone carbonyls (1684 and 1676 cm^{-1} respectively), the other apparently from the ester carbonyls (1766 and 1774 cm^{-1} respectively).

In negative ion mode, fast atom bombardment of stentorin produced a $(M-1)^-$ at 591.1304, which is in accord with $(M-1)^-$ of the molecule $C_{34}H_{24}O_{10}$ ($(M-1)^-$ calculated to be 591.1291). However, stentorin and hypericin in various matrices, did not show appreciable signals in positive ion mode. Derivatization with acetic anhydride gave a series of ions at m/Z 593, 635, 677, 719, 761, 803, 845, 887, 929 with the most abundant one at 929. This ion series for stentorin clearly establishes the presence of eight hydroxyl groups in the molecule. A similar ion series was also observed for acetylated hypericin, which is in agreement with the previous report on hypericin hexaacetate EI spectrum.[19]

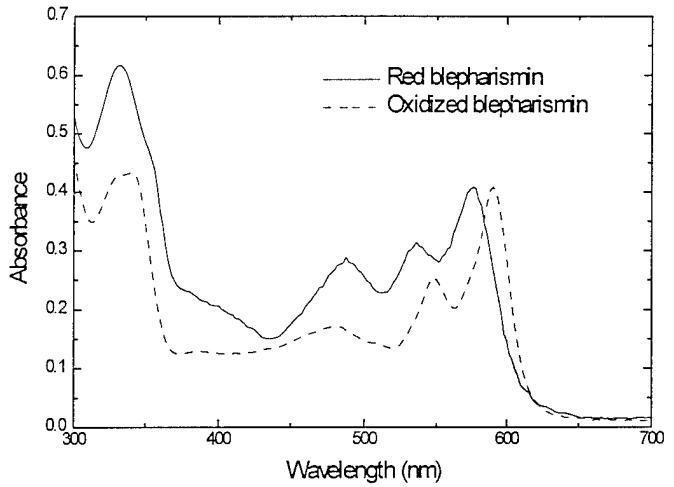

Figure 2. Absorption spectra of red blepharismin and oxidized blepharismin.

This ion series could come from the fragmentation of $(M+1)^+$ or they can be $(M+1)^+$ themselves produced by incomplete acetylation. It turned out to be the latter since fractionation of acetylated stentorin by HPLC afforded stentorin octaacetate dominately, and heptaacetate and hexaacetate to lesser amounts. However, fragmentation of stentorin octaacetate was also observed under the same measurement conditions.

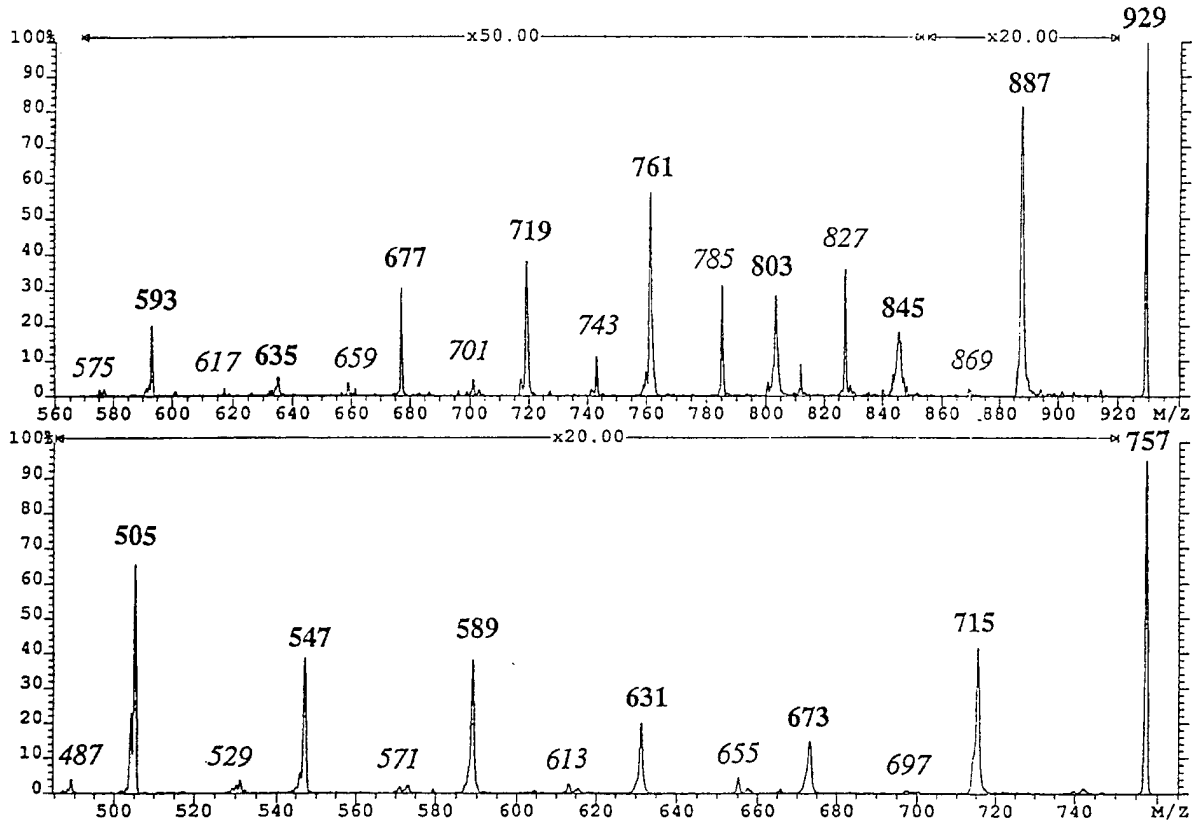

Figure 3. CAD-MS spectra of stentorin octaacetate (top panel) and hypericin hexaacetate (bottom panel).

The collisionally activated decomposition (CAD) spectrum of the $(M+H)^+$ of stentorin octaacetate shows fragmented ions with the loss of up to eight ketene (42 u) units from the parent ion, as is expected. It also shows the loss of acetic acid (60 u) from $(M+H)^+$, though not as facile as from fragments formed by ketene elimination from stentorin octaacetate. Although this is unexpected for acetylated phenol-like functionalities, it did occur for hypericin hexaacetate as well as for 2,2'-diacetoxybiphenyl. However it did not happen for 4,4'-biphenol diacetate. This expulsion of acetic acid is probably anchimerically assisted by adjoining acetoxy groups, a novel proximity effect. This has been further studied and confirmed.[20] The loss of acetic acid is consistent with a structure having OH (OAc) groups at positions 2, 2', 7, 7'.

Structural elucidation of stentorin was particularly challenging as we had very limited starting material. We finally accumulated sufficient amounts of material (ca. 1 mg) to acquire 1-D and 2-D ^{1}H NMR spectra.

We determined the ^{1}H chemical shifts for protons in stentorin and hypericin. Stentorin

must have a symmetry element, such as a 2-fold rotation axis (as in hypericin), or an inversion center or a mirror plane. The two singlets at δ 15.3 and 14.7 for stentorin are characteristic of hydrogen-bonded hydroxyl groups and are comparable to those of hypericin.[21,22] This result further supports that stentorin has a naphthodianthrone skeleton. Along with UV-visible absorption and IR spectra, this result points to the presence of four peri-hydroxyl groups in the stentorin chromophore.

Stentorin has only a single aromatic resonance at δ 6.9, whereas hypericin shows two peaks at δ 7.38 (H-6, H-6', adjoining the methyl groups) and δ 6.53 (H-3, H-3', adjoining the OH groups). By comparison, we conclude that stentorin has only two aromatic protons at any two positions of 3, 3', 6, or 6'. The resonances at δ 4.0 (septet, J = 7 Hz, 1 H) and δ 1.5 (doublet, J = 7 Hz, 6 H) imply the presence of isopropyl groups. As expected, the 2D NMR spectrum clearly demonstrated a strong coupling between those protons. Furthermore, no coupling between these and other protons was observed, indicating that they are not adjacent to other protons. The isopropyl groups are very likely located at two of the four positions at 3, 3', 6, or 6' not occupied by protons. This confirms that there are only two aromatic protons for stentorin.

In the published NMR spectra of hypericin,[21,22] there was no mention of the hydroxyl protons at positions 2, 2'. However, a very broad peak at δ 3.7 is attributable to them by comparison to similar broad peaks found in the NMR spectra of 3,4,8-trihydroxy-1-methylanthra-9,10-quinone-2-carboxylic acid methyl ester, 2,2'-dihydroxybiphenyl and 2,2',4,4'-tetrahydroxybiphenyl.[23] There is a similar broad peak for stentorin at approximately δ 5.4. However, integration of this peak gives an area that is too large to be accounted for by only four hydroxyl protons at 2, 2', 7, 7' positions. This large integration is possibly due to water contained in the stentorin sample, though the sample was dried extensively. It was recently reported that the site of deprotonation in hypericin is the hydroxyl protons at 2 or 2' positions.[24] The proton exchange of those hydroxyl groups and water molecules, complicated by the possible involvement of intra- and inter-molecular hydrogen bonding, may be the reason for the peak broadening.

From the results presented above, the structure of stentorin could be either one of three possible symmetrical arrangements of two protons and two isopropyl groups at 3, 3', 6, 6', namely, 2,2',4,4',5,5',7,7'-octahydroxy-3,3'-diisopropylnaphthodianthrone (**1**), 2,2',4,4',5,5',7,7'-octahydroxy-3,6'-diisopropylnaphthodianthrone (**2**), or 2,2',4,4',5,5',7,7'-octahydroxy-3,6-diisopropylnaphthodianthrone (**3**). However, the last choice (**3**) may be excluded by considering the usual routes of biosynthesis, since hypericin is produced by joining two emodin units, which are synthesized *in vivo* through the polyketide pathway.[25] The reagent di-*tert*-butylsilyl ditriflate, which was believed to react with OH groups at 7,7' if structure **1** is correct and with those at 2,2' and 7,7' if structure **2** is correct, was tried in the hope that **1** and **2** could be distinguished. However, it appears to us that the reagent is not sufficiently selective to distinguish between structures **1** and **2**. For biosynthetic reasons, we favor structure **1** over structure **2**. However, the choice between **1** and **2** must await the crystallographic determination.

Interestingly, a fossil pigment called fringelite D[26,27] found in a fossil sea lily of Jurassic age, 2,2',4,4',5,5',7,7'-octahydroxymesonaphthodianthrone, has a very similar structure to

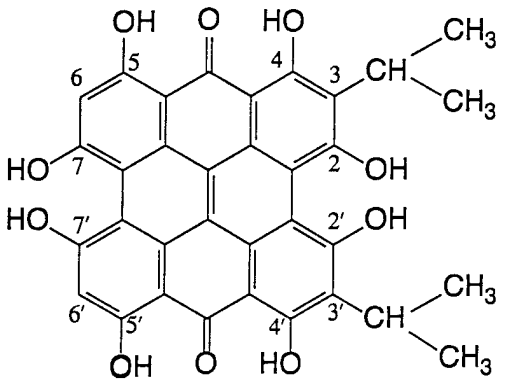

1

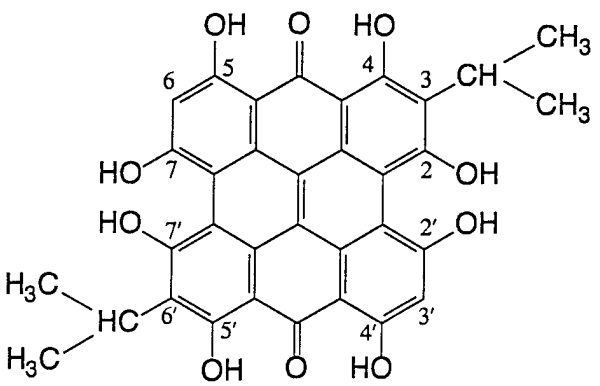

2

stentorin, but it lacks the two isopropyl groups. Stentorin may be synthesized via a pathway similar to that for fringelite. Nevertheless, the question whether or not the isopropyl group is introduced via an isoprenoid remains to be answered.

Similar studies with the photosensor blepharismin from *Blepharisma japonicum* indicate that the blepharismin chromophore is structurally different from the stentorin chromophore. A detailed account of structure determination for blepharismin will be reported at the ARO Workshop-Waltham.

Functional implications. *Stentor coeruleus* and *Blepharisma japonicum*, are both primitive single cell ciliates, and yet they are able to detect light (with respect to intensity and wavelength) with high efficiency.[13,15,17,29] The nature of the primary photoprocess involved in the photosensory transduction is still unknown.[30,31] We proposed that light irradiation of the cells generates a pH gradient which activates the Ca^{2+} influx and eventually leads to the ciliary stroke reversal.[11,28,29] Time-resolved fluorescence decay studies of the stentorin and blepharismin chromoproteins indicated that a primary event occurs from the excited singlet state of the photoreceptor molecules within a short time period (a few picoseconds[32] for stentorin, and 200-500 picoseconds for blepharismin[33]). The ultrafast process in stentorin was confirmed by recent pump-probe spectroscopy study, also suggesting that intermolecular proton transfer to an appropriately situated amino acid residue(s) of the apoprotein represents the radiationless decay mode in the primary photoprocess of the pigment molecule.[34] The stimulus light signal in *Stentor*, and possibly in *Blepharisma*, is transduced in the form of an intracellular pH gradient, *vide supra*, which is eventually amplified by a transient influx of calcium ions into the cell.[35] Preliminary studies suggest that photo-signal transduction in both organisms utilizes G-protein(s) as an initial transducer and a cGMP-phosphodiesterase as the effector system,[16,36] analogous to the visual system of higher animals.

Acknowledgements. This work was supported by a grant from the U.S. Army Research Office (No. 28747-LS-SM). We thank Dr. Rich Shoemaker for assistance with NMR

measurements and Dr. Michael Gross for MS measurements. This work is based on Nengbing Tao's Ph.D. dissertation supported by the ARO grant 29597-EPS.

References.

1. D. Oesterhelt and W. Stoekenius, "Rhodopsin-like protein from the purple membrane of *Halobacterium halobium*," *Nature: New Biol.* **233**, 149-152, 1971.
2. K. W. Foster, J. Saranak, N. Patel, G. Zarilli, M. Okabe, T. Kline, and K. Nakanishi, "A rhodopsin is the functional photoreceptor for phototaxis in the unicellular eukaryote *Chlamydomonas*," *Nature* **311**, 756-759, 1984.
3. J. L. Spudich, "Color discriminating pigments in *Halobacterium halobium*," In *Biophysics of Photoreceptors and Photomovements in Microorganisms* (F. Lenci, F. Ghetti, G. Colombetti, D.-P. Häder and P.-S. Song, eds), Plenum Press, New York, pp. 243-248, 1991.
4. M. Furuya and P.-S. Song, "Assembly and properties of holophytochrome," In *Photomorphogenesis in Plants,* 2nd Ed. (R. E. Kendrick and G. H. M. Kronenberg, eds), Kluwer Academic Publishers, Dordrecht, pp. 105-140, 1994.
5. P. Eilfeld and W. Haupt, "Phytochrome", in *Photoreceptor Evolution and Function* (M. G. Holmes, ed.), pp. 203-239. Academic Press, London, New York, 1991.
6. H. Scheer and S. Schneider (Eds.), *Photosynthetic Light-Harvesting Systems: Organization and Function.* W. D. de Gruyter, Berlin, 1988.
7. B. Diehn and B. Kint, "The flavin nature of the photoreceptor pigment for phototaxis in *Euglena*," *Physiol. Chem. Phys.* **2**, 483-488, 1970.
8. P. Galland, "Forty years of blue-light research and no anniversary", *Photochem. Photobiol.* **56**, 847-853, 1992.
9. N. Tao, M. Orlando, J.-S. Hyon, M. Gross, and P.-S. Song, "A new photoreceptor molecule from *Stentor coeruleus*," *J. Am. Chem. Soc.* **115**, 2526-2528, 1993.
10. K. M. Möller, "On the nature of stentorin," *Compt. Rend. Trav. Lab. Carlsberg, Ser. Chim.* **32**, 472-497, 1962.
11. E. B. Walker, T. Y. Lee, and P.-S. Song, "Spectroscopic characterization of the *Stentor* photoreceptor" *Biochim. Biophys. Acta* **587**, 129-144, 1979.
12. A. C. Giese, "The photobiology of *Blepharisma*," *Photochem. Photobiol. Rev.*, **6,** 139-180, 1981.
13. T. Matsuoka, "Negative phototaxis in *Blepharisma japonicum*", *J. Protozool.*, **30**, 409-414, 1983.
14. M. R. Sevenants, "Pigments of *Blepharisma undulans* compared with hypericin," *J. Protozool.* **12**, 240-245, 1965.
15. P.-S. Song, D.-P. Häder, and K. L. Poff, "Phototactic orientation by the ciliate *Stentor coeruleus*," *Photochem. Photobiol.* **32**, 781-786, 1980.
16. H. Fabczak, N. Tao, S. Fabczak, and P.-S. Song, "Photosensory transduction in ciliates. IV. Modulation of the photomovement response of *Blepharisma japonicum* by cGMP", *Photochem. Photobiol.* **57**, 889-892, 1993.
17. G. Checcucci, G. Damato, F. Ghetti, and F. Lenci, "Action spectra of the photophobic response of blue and red forms of *Blepharisma japonicum*," *Photochem. Photobiol.* **57**, 686-689, 1993.
18. W. Mammo, E. Dagne, and W. Steglich, "Quinone pigments from *Araliorhamnus*

vaginata," *Phytochemistry*, **31**, 3577-3581, 1992.
19. H. Brockmann and D. Spitzner, "Die konstitution des pseudohypericins", *Tetrahedron Lett.*, 37-40, 1975.
20. M. Orlando, M. George and M. L. Gross, "Elimination of acetic acid from protonated 4,5-diacetoxyphenanthrene and 2,2'-diacetoxybiphenyl: an example of an ion chemistry proximity effect", *Org. Mass Spectrometry*, **28**, 1184-1188, 1993.
21. M. Gill, A. Gimenez, and R. W. McKenzie, "Pigments of fungi, part 8. Bianthraquinones from *Dermocybe austroveneta*" *J. Nat. Prod.* **51**, 1251-1256, 1988.
22. H. Falk and G. Schoppel, "On the synthesis of hypericin by oxidative trimethylemodin anthrone and emodin anthrone dimerization: Isohypericin," *Monatsh. Chem.* **123**, 931-938, 1992.
23. Pouchert, C.J.(ed.) *The Aldrich Library of NMR Spectra*; edition II, **1983**.
24. H. Falk, J. Meyer, and M. Oberreiter, "Deprotonation and protonation of hydroxyphenanthroperylenes," *Monatsh. Chem.* **123**, 277-284, 1992.
25. R. H. Thomson, *Naturally Occurring Quinones*, Academic Press, London, pp. 2-3, 1957.
26. M. Blumer, "The organic chemistry of a fossil. I. The structure of the fringelite-pigments," *Geochim. Cosmochim. Acta* **26**, 225-230, 1962.
27. M. Blumer, "Organic pigments: Their long-term fate," *Science* **149**, 722-726, 1965.
28. P.-S. Song, "Protozoan and related photoreceptors: Molecular aspects," *Ann. Rev. Biophys. Bioeneng.* **12**, 35-68, 1983.
29. P.-S. Song, "Photosensory transduction in *Stentor coeruleus* and related organisms," *Biochim. Biophys. Acta* **639**, 1-29, 1981.
30. I.-H. Kim, J. S. Rhee, J. W. Huh, S. Florell, B. Faure, K. W. Lee, T. Kahsai, P.-S. Song, N. Tamai, T. Yamazaki, and I. Yamazaki, "Structure and function of the photoreceptor stentorins in *Stentor coeruleus*. I. Partial characterization of the photoreceptor organelle and stentorins," *Biochim. Biophys. Acta* **1040**, 43-57, 1990.
31. D. Gioffre, F. Ghetti, F. Lenci, C. Paradiso, R. Dai, and P.-S. Song, "Isolation and characterization of the presumed photoreceptor protein of *Blepharisma japonicum*," *Photochem. Photobiol.* **58**, 275-279, 1993.
32. P.-S. Song, I.-H. Kim, S. Florell, N. Tamai, T. Yamazaki, and I. Yamazaki, "Structure and function of the photoreceptor stentorins in *Stentor coeruleus*. II. Primary photoprocess and picosecond time-resolved fluorescence," *Biochim. Biophys. Acta* **1040**, 58-65, 1990.
33. T. Yamazaki, I. Yamazaki, Y. Nishimura, R. Dai, and P.-S. Song, "Time-resolved fluorescence spectroscopy and photolysis of the photoreceptor blepharismin," *Biochim Biophys. Acta* **1143**, 319-326, 1993.
34. S. Savikhin, N. Tao, P.-S. Song, and W. Struve, "Ultrafast pump-probe spectroscopy of the photoreceptor stentorins from the ciliate *Stentor coeruleus*," *J. Phys. Chem.* **97**, 12379-12386, 1993.
35. D. C. Wood, "Membrane permeabilities determining resting, action and mechanoreceptor potentials in *Stentor coeruleus*," *J. Comp. Physiol.* **146**, 537-550, 1982.
36. H. Fabczak, P.-B. Park, S. Fabczak, and P.-S. Song, "Photosensory transduction in ciliates. II. Possible role of G-protein and cGMP in *Stentor coeruleus*," *Photochem. Photobiol.* **57**, 702-706, 1993.

Protein-Protein Interactions

Wesley E. Stites
Dept of Chemistry and Biochemistry, University of Arkansas, Fayetteville AR

Introduction

The long range goals of our research program are to better understand and apply the principles of protein association. Much of the "intelligence" that biomolecules show is mediated by protein-protein interactions. For example, when biological systems respond to changes in environmental conditions, much of the flow of information about those conditions is conveyed by the interactions of various proteins. The chemotaxic behavior of bacteria provides a specific example of this behavior. The interaction of about ten proteins allow bacteria to sense chemical gradients of specific molecular species in their environment and guides the bacteria in swimming along that chemical gradient. The more one reflects on this system the more impressive it seems. A very sophisticated and specific response to the environment is mediated by astonishingly few components. The individual components of such a system are relatively simple. It is the interplay between them that imparts the "intelligence" to the system. It is our long-term goal to allow similar systems to be designed to respond as desired.

We are undertaking the construction of a *de novo* protein-protein complex from monomers that prior to modification have little affinity for one another. Much of the knowledge of protein-protein interfaces needed for this endeavor will come from the study of crystal structures. A number of surveys of available crystal structures of interacting proteins have been carried out. Some of the results of these studies are summarized below.

Analysis of Crystal Structures

a. Interface Size and Number of Amino Acids Involved in Interface

The surface area involved in interactions can be easily measured in crystal structures. In dimeric proteins, the size of the interface area per subunit was found[1] to range from 670 to 4890 Å^2. This represents slightly more than 12%, on average, of the accessible surface area of the individual monomers, but there is a wide range of 6.6 to 23.3%[2]. Crystal structures of protease-inhibitor complexes[3] and antibody-protein antigen complexes[4] show 600 to 1000 Å^2 buried per individual protein, for a total surface area buried in the complexes of 1600 +/- 350 Å^2. The percentage of the accessible surface area of the proteins that was buried ranged from 5 to 20 percent. The lower limit of observed interface area agrees well with a theoretically based estimate of 1200 Å^2 of buried surface area required to allow stable association of a dimer, 600 Å^2 per monomer[5]. A more useful or at least more graspable measure than surface area buried is the number of residues involved in the interface. In 15 protease-inhibitor complexes and 4 antibody-antigen complexes this number was 34 +/- 7 residues (in both proteins in the complex, 17 per monomer). Any residue with an atom within 0.5 Å of an atom across the interface was counted as a contact residue[3].

b. Types of Amino Acids Involved in Interfaces

Argos[2] found the amino acid composition of oligomeric protein interfaces to be generally intermediate between the composition of the protein interior and exterior. The number of both charged and uncharged polar residues in the interface was intermediate between the numbers found for interior or exterior as was the number of non-aromatic hydrophobic residues. However, the aromatic hydrophobic residues were as well represented at interfaces as in the protein interior. He noted a preference for larger residues in form of the aromatics and also, interestingly, arginine.

Using a different definition for subunit participation, Janin *et al*[1] found that the amino acid composition of oligomeric protein interfaces, while intermediate between the composition of the interior and exterior, more closely resembled the protein's interior rather than the surface exposed to solvent. However, in marked contrast to the protein interior was the high number of charged residues

found buried in interfaces. The number of charged residues found in the interior of protein is quite low.[6] However, a disproportionate number of arginines were found at interfaces.

On the other hand, when Janin and Chothia[3] examined interfaces in protease-inhibitor and antibody-protein complexes they found little difference between interface surfaces and solvent exposed surfaces in the percentages of polar, non-polar and charged surfaces. In antibodies, they found that nonpolar residues were disproportionately aromatic in character. Padlan[7] examined the complementarity-determining region (CDR) of seven Fab structures that have been crystallographically determined. He also found that aromatic residues, in particular tyrosine, were more likely to be in the binding pocket than elsewhere in the molecule. (No distinction was made between the interior or exterior of the rest of the Fab.) However, histidine and asparagine were the most favored, by a factor of eight, to appear in the CDR relative to the rest of the Fab. Serine residues, though only slightly more likely to be found in the CDR than elsewhere in the Fab, were still the most common residue in the CDR, comprising 14.7%. Next most common at 13.13% of the residues in the CDR, was tyrosine. Asparagine was third at 8.32%. Although no explicit analysis of percent surface areas was made, it is clear from size and prevalence that tyrosines form the largest part of the surface of the CDRs.

Calmodulin binds to many different proteins. It has been noted that the binding site of calmodulin has eight methionines exposed. It has been proposed that the flexibility of the methionine sidechain[8] and the high polarizability of the sulfur (which increases the favorable enthalpy when interacting with non-polar surfaces)[9] allows the plastic interaction of this binding site with different sites. It is worth noting that the data of Janin *et al.*[1] show that, while composing only 3.9% of oligomeric subunit interface surface areas, methionine is significantly more prevalent in interfaces than elsewhere in the proteins. This result is buttressed by data from Padlan's analysis of Fab CDRs[7], where methionine was the only small nonpolar (i.e. non-aromatic) residue that was more likely to be in the CDR than elsewhere in the molecule.

The Model Protein

The model protein we are using in our studies is staphylococcal nuclease. It is difficult to imagine a better model system for any study of protein structure and function. It has been used extensively for just this purpose. The crystal structure of nuclease has been refined by modern methods to a resolution of 1.65 angstroms.[10,11] Nuclease is a small protein, 149 amino acids, and has a single domain containing both alpha helix and beta sheet. The protein is purified in a single chromatographic step, folds and unfolds reversibly, and contains no disulfides, indeed, no cysteines at all. There is a single tryptophan residue in the wild type protein which provides a sensitive fluorescence probe that distinguishes between the native and denatured states. It is possible to quickly, accurately and reproducibly determine the free energy of the native state to 0.1 kcal/mol. The gene has had numerous restriction sites cloned in and is in an overexpressing system that makes it possible to produce even highly unstable mutant proteins in yields of tens of milligrams of purified protein per liter of cell culture.[12] Literally hundreds of mutants of nuclease have been made using standard methods of site directed mutagenesis.[13,14] Using the insights from naturally occurring protein-protein complexes and molecular modeling we are currently designing interfaces in staphylococcal nuclease that we believe will promote specific association of the molecule.

Dimer Design

Using the design principles inferred from the study of protein-protein complexes we carried out a series of "mutations" and energy minimizations using the *Discover* software package. We began by making substitutions of polar and charged residues with aromatics and methionine in the center of the desired new interface. Around the periphery charged residues of opposite signs were placed to encourage specificity of interaction. Energy minimization identified unfavorable interactions in the monomer which were addressed in further rounds of mutation and minimization.

We arrived at a final design that placed 6 phenylalanines, 2 tryptophans, 3 methionines, and 1 leucine in solvent exposed sites. This hydrophobic patch was surrounded by 6 arginines on one side

and by 5 glutamic acids on the other. Although clustered together in three dimensional space, the sites of these mutations are at three separated locations in the primary sequence of the protein. Accordingly, we broke the design into three segments and carried out the mutations.

We have successfully incorporated all three mutant segments into nuclease at this point although there was some extended difficulty with the first segment due to a synthesis error on the part of the company supplying the mutagenic oligonucleotide. Purification of the first and second segments has proven unexpectedly difficult. There appear to be two reasons for this. One, the mutations proved more destabilizing than expected. This violation of protein folding dogma is interesting in itself but rather annoying in hindering progress on our problem. We have therefore had to incorporate a series of stabilizing mutations elsewhere in the protein. Second, and much more encouragingly, these proteins aggregate. While we indeed want them to aggregate in a specific fashion when native the purification normally occurs under denaturing conditions. Here it appears that the protein aggregates in a non-specific fashion and the result is a largely insoluble mess. We were forced to work out new methods of protein purification because of this. We believe that we have found a method that will purify these proteins and hope to soon characterize them.

Hydrophobic Surface Residues

As detailed above, we know from crystal structures that aromatic residues are common in interfaces. The presence of hydrophobic residues on the surface of proteins in general is rare. We have nearly completed a project substituting phenylalanine residues for forty-eight surface sites in nuclease. The stability of these mutations to thermal and solvent denaturation has been investigated. Of thirty-five mutants examined by solvent denaturation to date, fifteen have a stability difference from wild-type of less than 0.5 kcal/mol, six are between 1 and 0.5 kcal/mol less stable than wild-type and thirteen are more than 1.0 kcal/mol less stable than wild-type. It was somewhat surprising that this many mutants have been found to be destabilized since little change in stability is generally found upon substituting surface sites.

We have also been examining the effects of surface aromatic residues on protein-protein interactions. The association constants for the homodimeric association of the protein are measured by analytical ultracentrifugation. Wild-type nuclease has a very weak association of 5.06×10^2. In every case measured so far a single phenylalanine increases this association constant by an order of magnitude. In a few cases the increase in association constant is three orders of magnitude. The tightest association constant measured to date is 9.71×10^5 for the mutant lysine 49 to phenylalanine. This is a marked change in association for a single substitution. We believe there is a good chance several mutations that are as of yet uncharacterized will show even tighter association. We expect to finish characterizing these mutations and their effects on protein-protein interaction by the end of the year.

Cysteine Crosslinked Proteins

We have introduced many surface cysteine residues into staphylococcal nuclease. There were several reasons for our interest. These cysteines can then be used to link the protein into a homodimer either via disulfide linkage or via alkylation with a bifunctional electrophile. These crosslinked proteins would serve as good standards and controls for the achievement of protein dimerization. As a result of an earlier ARO workshop we met Dr. C. Broomfield of the USAMRICD. It occurred to us that mustard gas could possibly serve as a bifunctional electrophile. We have been investigating the effect of mustard treatment on nuclease in collaboration with Dr. Broomfield.

The mode of action of mustard is still not clear.[15] It is clear that its potent alkylating ability is key to its toxicity but the exact target(s) that are critical to cause vesication is still uncertain. DNA crosslinking certainly can account for at least some of the toxic effects of mustard[16] but not all.[17] It has long been known that mustard can alklyate proteins,[18, 19] but the precise site(s) of alkylation have remained unknown.

Small scale reaction of single cysteine substitution mutants of nuclease with mustard was carried out at both pH 7.4 and pH 8.8. As much as 10% of the protein formed dimers. Wild-type protein, containing no cysteines, formed detectable, but negligible amounts of dimer, despite the large numbers of potentially nucleophilic lysines. This is strong evidence that the site of mustard modification in proteins is at cysteine residues.

Eight singly-substituted cysteine mutants and wild type have been treated with sulfur mustard on a large scale (reaction of 15 mg in 100 mM Tris HCl, pH 8.8). Proteins were purified under denaturing and reducing conditions (2 M GuHCl, 15 mM BME). Relative dimer yields were small, on the order of 1% as detected by peak areas from gel filtration chromatography.

All eight monomers, K70C dimer, and wild type were purified and subjected to an Ellman's assay as well as denatured with GuHCl. Results are shown below.

Mutant	% Free Thiol	ΔΔG treated and untreated protein in .5mM TCEP
WT + mustard	0 ± 9	-0.2
G29C monomer	30 ± 8	---
G50C monomer	6 ± 9	-0.8
E57C monomer	8 ± 4	-0.3
A60C monomer	30 ± 6	-0.4
K70C monomer	20 ± 10	---
K70C dimer	8 ± 10	---
K78C monomer	45 ± 4	-0.7
A112C monomer	16 ± 11	-0.9
K134C monomer	44 ± 5	-0.2
A112C untreated	91	
K134C untreated	77	

The results of the Ellman's assay show that most of the purified monomers contain substantial amounts of mustard alkylation. Many, though not all of the monomers, show significant changes in protein stability.

Clearly modification of cysteines with mustard can result in changes in protein stability and function. The crosslinking of proteins also has potential to cause widespread metabolic damage. Therefore, we believe this set of experiments is strong evidence for further investigation of mustard-protein reaction as an important factor in mustard toxicity.

Several other interesting observations have been made. A curious cleavage reaction of the dimer is occurring and it appears to escalate with increasing temperature as seen through an experiment with K134C mustard crosslinked dimer. Three incubations were performed with the purified dimer; one at -20°C, one at 37°C and one at 80°C, all overnight. Compared to the frozen sample both the high temperature incubations showed significant amounts of monomer. Another sign that there was some type of cleavage occurring was observed when the dimer band of K78C was excised from an SDS PAGE gel and electroeluted. The product revealed a mixture of monomer and dimer. The mechanism of this cleavage is unclear.

We are in the process of performing amino acid analysis on various samples to investigate the presence of modified cysteine in proteins as a long-term biochemical marker for individuals who have come in contact with mustard agent.

References

[1] J. Janin; S. Miller; C. Chothia *J. Mol. Biol.* 1988, **204**, 155.
[2] P. Argos *Prot. Eng.* 1988, **2**, 101.

[3] J. Janin; C. Chothia *J. Biol. Chem.* 1990, **265**, 16027.
[4] D. R. Davies; E. A. Padlan; S. Sheriff *Annu. Rev. Biochem.* 1990, **59**, 439.
[5] A. V. Finkelstein; J. Janin *Prot. Engineering* 1989, **3**, 1; J. Janin; C. Chothia *Biochem.* 1978, **17**, 2943; C. Chothia; J. Janin *Nature* 1975, **256**, 705.
[6] A. A. Rashin; B. Honig *J. Mol. Biol.* 1984, **173**, 515.
[7] E. A. Padlan *Prot., Struct. Funct. Genet.* 1990, **7**, 112.
[8] K. T. O'Neil; W. F. DeGrado *Trends Biochem. Sci.* 1990, **15**, 59; K. T. O'Neil; S. Erickson-Viitanen; W. F. DeGrado *J. Biol. Chem.* 1989, **264**, 14571.
[9] S. H. Gellman *Biochem.* 1991, **30**, 6633.
[10] P. J. Loll; E. E. Lattman *Prot. Struct. Funct. Genet.* 1989, **5**, 183.
[11] T. R. Hynes; R. O. Fox *Prot. Struct. Funct. Genet.* 1991, **10**, 92.
[12] W. E. Stites; A. G. Gittis; E. E. Lattman; D. Shortle *J. Mol. Biol.* 1991, **221**, 7.
[13] J. Sondek; D. Shortle *Prot. Struct. Funct. Genet.* 1990, **7**, 299.
[14] D. Shortle; W. E. Stites; A. K. Meeker *Biochem.* 1990, **29**, 8033.
[15] A. P. Watson; G. D. Griffin *Environ. Health Perspect.* 1992, **98**, 259.
[16] B. Papirmeister; C. Gross; H. Meier; J. Petrali; J. Johnson *Fundam. Appl. Toxicol.* 1985, **5**, S134; C. Gross; H. Meier; B. Papirmeister; F. Brinkley; J. Johnson *Appl. Pharmacol.* 1985, **81**, 85.
[17] C. Broomfield, personal communication.
[18] M. Dixon; D. M. Needham *Nature* 1946, **158**, 432.
[19] J. L. Hambrook; D. J. Howells, C. Schock *Xenobiotica* 1993, **23**, 537.

Extended abstract for the Workshop on Smart Materials, sponsored by the Materials Science Division of the USARO, August 15-17, 1994, Brandeis University, Boston, MA.

SELF-ASSEMBLED LIPID BILAYERS AS A SMART MATERIAL FOR NANOTECHNOLOGY

H. Ti Tien, Membrane Biophysics Laboratroy (Giltner Hall), Physiology Department, Michigan State University, East Lansing, MI 48824

Project Overview From Prior USARO Support

The Principal Investigator (PI) has been supported by the USARO during the past three and one-half years. Since 1990, the PI has reported the results of his ARO-supported research in 15 publications, in 10 presentations given at national and international meetings, and in 25 seminars given at various universities and industrial laboratories. Fruitful collaborative research with Associate Professors Angelica Ottova, Vladimir Tvarozek (Department of Microelectronics, Slovak Technical University, Slovak Republic), Prof. Tibor Hianik (Department of Biophysics, Commenius University, Slovak Republic) and their colleagues have been carried out by the PI under the support of the U.S. Agency for International Development. Collaborative research has also been carried out with Prof. L.-G. Wang and his colleagues (Physics Department, Nankai University, PRC).

A. Introduction

In the past few years there have been a number of reports on self-assemblies of molecules as 'advanced materials' or 'smart materials'. Without questions, the inspiration for these exciting work comes from the biological world, where, for example, the lipid bilayer of cell membranes plays a pivotal role. The seminal work on the self-assembly of lipid bilayers (or bimolecular lipid membranes, BLMs for short) in vitro was carried out by Rudin and his colleagues in the early 1960s [1]. They showed that a BLM formed from the brain extract was self-sealing to puncture with the following electrical characteristics: capacitance (C_m) = 1 $\mu F/cm^2$, resistance (R_m) greater than 10^8 ohm cm^2 and dielectric breakdown (V_b) at about 250,000 V/cm. Further, upon modification with suitable proteins, this otherwise electrically 'inert' structure of 6 nm thick became excitable displaying characteristic features similar to those of action potential of the nerve membrane.

Since the mid 1960s, our work has been motivated by the desire to explain the living system in physical, chemical and physiological terms. The area chosen for investigation is membrane biophysics, where the cell membrane plays a crucial role in signal transduction, energy conversion and information processing. This is owing to the fact that most physiological acitivties involve some kind of lipid bilayer-based ligand-receptor contact interactions. Outstanding examples among these are ion sensing, antigen-antibody binding, light conversion and detection, and gated channels, to name a few. Our present approach to study these interactions in vitro is facilitated by employing self-assembled bilayer lipid membranes (BLMs) of 4-6 nanometer in thickness. We have focused the efforts on ion and/or molecular selectivity and specificity using newly available BLMs on solid support (i.e., s-BLMs), whose enhanced stability greatly aids in research areas of membrane biophysics, biochemistry and molecular cell biology as well as in biosensor designs and molecular devices development. It should be noted that the dimensions of a typical s-BLM under investigation is about 2×10^{-5} cm^2 and 5 nm thick.

Since its inception in 1960, the conventional BLMs have been used as models of biological membranes In particular, the BLMs have been used to elucidate the molecular mechanisms of biomembrane function [2-4]. The conventional BLM system, however, has one major drawback in that it is notoriously unstable, rarely

lasting more than a few hours. As a result, many attempts have been made to stabilize this extremely delicate lipid bilayer structure for fundamental studies and practical applications. In this connection, the first report was published in 1978 describing the formation of supported BLMs in polycarbonate filters with much improved stability to both chemical and mechanical disturbances [5,6]. For practical biosensors, a self-assembled bilayer lipid membrane (s-BLM) on nascent metallic surface was later developed [7,8 see Ref. 9 for a review]. Other researchers have reported similar and/or related systems [10-13]. This new type of s-BLM-based probes is destined for micro-electronic fabrication. The present paper is mainly concerned with our recent experiments and the work on s-BLMs carried out in close collaboration with others [14-25].

B. Accomplishments

1. Immobilization of ferrocene on s-BLMs. To test the versatility of s-BLMs as a 'smart material', an amperometric sensor was constructed for ferri-/ferrocyanide ions. The results have shown that (i) ferrocene can be very easily immobilized in the lipid bilayer on the tip of a metallic wire (s-BLM) system, and (ii) ferrocene in a BLM increases about two orders of magnitude of potassium ferri-/ferrocyanide ion sensitivity than that of the platinum electrode. This demonstrates that the s-BLM system offers a novel approach to the electrode modification by simple way of immobilization of compounds within a lipid bilayer [14].

2. Hydrogen peroxide-sensitive s-BLMs. The insertion of appropriate active molecules (modifiers) into the matrix of the lipid bilayer should be able to impart the functional characteristics of s-BLMs. We chose TCNQ (tetracyanoquinodimethane) and DP-TFF (dipyridyl-tetra-thiafulvalene), because of their properties as typical electron acceptor and donor molecules, respectively. It was found that DP-TTF could improve not only the stability but also increased the range of s-BLM's sensitivity to hydrogen peroxide. In contrast, TCNQ-containing s-BLMs did not show much responses to H_2O_2 [15].

3. Modified s-BLMs as pH sensors. Of all the ions crucial to the functioning of cellular processes is the hydrated hydrogen ion (H_3O^+) which plays a leading role in enzyme catalysis and membrane transport. To test our concept, we incorporated a number of quinonoid compounds (chloranils) into s-BLMs and found that, indeed, s-BLMs containing either TCOBQ (tetrachloro-o-benzoquinone) or TCPBQ (tetrachloro-p-benzoquinone) responded to pH changes with a nearly theoretical slope [16,17]. This new pH-sensitive s-BLM offers prospects for ligand- selective probe development using microelectronic technologies (see Item #9 below).

4. Modified s-BLMs as ion sensors. S-BLMs containing six different kinds of crown ethers were investigated using cyclic voltammetry. In particular, s-BLMs formed from a liquid crystalline aza-18-crown-6 ether and cholesterol-saturated n-heptane solution was found sensitive to K^+ in the concentration range of 10^{-4} to 10^{-1} M with theoretical Nernstian slope. The specificity for three alkali metal cations and NH_4^+ of five different kinds of bis-crown ethers in BLMs were also investigated. The order of specificity for most of these bis-crown ethers was found to follow hydrated radii of cations, i. e., $NH_4+ > K^+ > Na^+ > Li^+$ [18,19]. The results obtained with these s-BLMs compare favorably with conventional BLMs containing similar compounds such as valinomycin [21].

5. Modified s-BLMs as Molecular sensors. Many authors have reported sensors for the detection of glucose using glucose oxidase [20]. Interestingly, using s-BLMs containing redox compounds and electron mediators but without the enzyme, glucose was detected in buffered solution. The results are preliminary and further experiments are in progress. If highly conjugated compounds such as TCNQ is incorporated in the s-BLM forming solution, the resulting s-BLM was able to detect the presence of ascorbic acid, which is consistent with the findings obtained with conventional BLMs [16].

6. Molecular recognition in a s-BLM. S-BLMs can be employed to immobilize a

host of compounds such as enzymes, antibodies, protein complexes (receptors, membrane fragments or whole cells), ionophores and redox species for the detection of their counterparts, respectively, such as substrates, antigens, hormones (or other ligands), ions, and electron donors or acceptors [21]. In the present work we report a feasibility study of an antigen-antibody reaction using s-BLMs as the probe with electrical detection. The antigen (HBs-Ag or hepatitis B surface antigen) was incorporated into a s-BLM, which then interacted with its corresponding antibody (HBs-Ab or Monoclonal antibody) in the bathing solution. This Ag-Ab interaction resulted in some dramatic changes in the electrical parameters (conductance, potential and capacitance) of s-BLMs. The magnitude of these changes were directly related to the concentrations of the antibody in the bathing solution. The linear response was very good ranging from 1 to 50 ng/ml of antibody, demonstrating the potential use of such an Ag-Ab interaction via the s-BLM as a transducing device [22].

7. Electron transfer experiments in s-BLMs. The early experiments in the field of electron transfer processes in BLMs were first conducted in the late 1960s to understand the primary step in natural photosynthesis [2,4]. It was discovered that light-driven electron transfer process between donor and acceptor species can occur across the thickness of a pigmented bilayer lipid membrane. This finding has subsequently led to the view that the reaction center of natural photosynthesis functions similar to that of a photovoltaic device of molecular dimensions. In the mid 1980s, electron transfer in the dark was seen in BLMs doped with either organic 'metals" or semiconducting nanoparticles formed in situ. These phenomena were explained in terms of light-induced charge separation, field-driven charge transport and subsequent redox reactions on opposite sides of the BLM. In the absence of light, the theory of electron tunneling was invoked (see above on TCNQ or TTF containing BLMs). When a s-BLM doped with Zn-phthalocyanine was excited by light, a voltage and a current were recorded, with the action spectra paralleled closely to that of the absorption spectrum of the photoabsorber [2,9,21]. Thus, we have shown that a pigmented s-BLM can function as a light transducer or photon-activated switch or detector.

8. S-BLMs deposited on piezoelectric quartz crystals. Smell and taste (olfaction and gustation) are among living organisms two most vital sensing systems; the biophysics of which have been increasingly elucidated at the molecular level [23]. Here again the crucial receptors are bilayer lipid membranes. In our preliminary experiments several kinds of BLMs were successfully deposited on AT-cut quartz resonators [24]. These were verified by observing frequency (f_m), potential (E_m), capacitance (C_m) and I/V curves. Frequency change (vs. that in air) ranged from 9 to 16 KHz, and no redox peaks could be observed or the peak was largely damped in the presence of $Fe(CN)_6^{-3}$. E_m and C_m also showed characteristic values. But the exact values of these parameters were found to be related to the lipid solution, pH of the bathing solution, and the scan time of voltammograms. If the BLM failed to form or broken, obvious changes in these parameters were observed. In this case, f_m increased several KHz (frequency decreased to about 6 KHz, which corresponds to that induced only by pure viscous loading); C_m and E_m also increased largely and characteristic redox peaks were observed. Our findings show that BLMs can be formed on piezoelectric quartz crystals and the piezoelectric techniques can be applied as a powerful tool to characterize the s-BLM system.

9. S-BLMs on interdigitated structures by microelectronic techniques. The fact that a lipid bilayer structure can be deposited on a solid substrate is intriguing. This novel manner of lipid bilayer formation overcomes two basic obstacles in the way of the constructive utilization of the BLM structure, namely: (i) its stability and (ii) its compatibility with a standard microelectronic technology. As has been repeatedly demonstrated by us and others [19,21], that the solid supported BLM system (s-BLMs) not only possesses the advantages of a conventional BLM structure, but gains additionally the new important properties, besides its long-term stability, such as (a) an anisotropic, highly ordered, yet very dynamic liquid-like structure, and (b) two

asymmetric interfaces, one of which is metallic. With this metallic connection, this type of probes solves the interfacing problem and is predestined for microelectronic technology. On this last mentioned property, we have extended the experiment described above (Item #3) to the interdigitated structures (IDS). IDS are finger-like electrodes made by microelectronic technologies and used in micro-chip applications [25]. By forming s-BLMs on IDS made of platinum with a window of 0.5 mm x 0.5 mm, we obtained the following interesting results. First, when an IDS coated with a BLM formed was from asolectin, it responded to pH changes with only 15 $\pm$ 2 mV/decade slope. The conductance of s-BLMs on IDS was about 50 times higher than the usual s-BLMs. Second, when an IDS coated with a BLM formed from asolectin doped with either TCOBQ or TCPBQ, the pH response was linear with a slope close to theoretical value [16,17,25].

C. Possibilities for the Future

The development of BLMs and later s-BLMs has made it possible for the first time to study, directly, electrical properties and transport phenomena across a 6 nm ultrathin biomembrane element separating two interfaces. As a result of these extensive studies, biomembranes have now been recognized as the basic structure of Nature's sensors and molecular devices. For example the plasma membrane of cells provides sites for a host of ligand-receptor contact interactions. To impart relevant biofunctions in BLMs, a variety of compounds such as ionophores, enzymes, receptors, etc. have been incorporated. Some of these incorporated compounds cause the BLMs to exhibit non-linear phenomena. A modified or reconstituted BLM (or s-BLM) is viewed as a dynamic system that changes in response to environmental stimuli and as a function to time. This is best described by the dynamic membrane hypothesis as a basis of the biomembrane function. The self-assembled lipid bilayer, the basic component of biomembranes, is in a liquid-crystalline and dynamic state. A functional biomembrane system based on self-assembled lipid bilayers, proteins, carbohydrates and their complexes should be considered in molecular and electronic terms; it can support ion or/and electron transport and is the site of cellular activities in that it functions as a 'device' for either energy conversion or signal transduction. Such a system, as we know it intuitively, must act as some sort of a transducer capable of gathering information, processing it, and then delivering a response based on this information. In the past, we were limited by our lack of sophistication in manipulating and monitoring such a system. Today, membrane biophysics is a matured field of research as a result of applications of many elegant techniques including bioelectrochemistry, patch-clamp, spectroscopy, acoustics, and membrane reconstitution. We now know a great deal about the structure of cell membranes, 'ion pumps', electroporation, and membrane channels. In membrane reconstitution experiments, the evidence is that intracellular signal transduction begins at membrane receptors. The work described here offers new and exciting opportunities for the preparation of a variety of supported lipid bilayer (BLM) probes with applications in membrane biophysics and biotechnology. For example, the membranes can function in such important processes as electron-transfer, signal transduction and cellular environmental sensing. Specifically, the following experiments, some of which are in progress, are delineated below:

1. On the basis of our findings and experiments in close collaboration with our colleagues as summarized above, we have established that supported BLMs (s-BLMs) are smart materials that can function as probes in membrane biophysics and biotechnology. The work is invaluable in providing the fundamental insight necessary for the design of biosensors and biomolecular electronic devices. The s-BLM as a smart material is classified as an ultrathin film which can transduce a ligand-receptor contact interaction into an electrical response (i.e., changes in capacitance, potential, conductance, or dielectric breakdown or in voltammogram).

2. IDS are finger-like electrodes made by microelectronic techniques and used in micro-chip applications. When an IDS coated with a BLM containing TCOBQ (or TCPBQ), it responded to pH changes linearly. This very interesting finding suggests that (i) the lipid bilayer, the fundamental structure of all biomembranes, can be attached to an IDS with responses not unlike those found in glass pH electrodes, (ii) this type of structure (i.e., s-BLM on interdigitated electrodes) can be used to investigate ligand-receptor contact interactions, and (iii) s-BLMs on an IDS can be manufactured using microelectronic technologies which already exist without the explicit need of special modification. We consider this finding as a major 'breakthrough' in biosensor development. In this connection it should be mentioned that the experiment on IDS-chip modified with a BLM is based on a common basic aspiration. That is to self-assemble a lipid bilayer containing membrane receptors, natural or synthetic, so that a host of physiological activities, such as ion/molecular recognition can be investigated. At the molecular level, most of these activities may be termed collectively as receptor-ligand contact interaction. The structures we will be reconstituting are inherently dynamic. (see Concluding Remarks). Receptors and ligands in such close contact normally will vary as a function of time, frequently resulting in non-linear behavior. With IDS-chip modified with BLMs, we now have at last a most unique system for extensive experimentation which will be only limited by our imagination. Thus, insight gained from these studies will guide the preparation of functional BLMs on IDS support. Our aim is to take advantage of microelectronic techniques and apply them to biochemical and neurosciences research.

3. Supported BLMs or lipid bilayers are ultrathin films of nanometer thickness, as such the interior of a BLM is strongly influenced by the close proximity of its interfaces. At the nanometer dimension, the quantum size effects come into play. Thus, the properties of BLMs depend strongly on their constituent molecules and interfaces. Remarkable changes in the electrical, optical and electromechanical properties are observed. For example, the rate of electron transport across BLMs by quantum tunneling is one such phenomenon. We plan to study size quantization using s-BLM doped with semiconducting nano-particles formed in situ.

In concluding, it should be reiterated that the proposed research is highly interdisciplinary. Emphasis has been and will be placed on fundamental research Our past work has been benefited by cross fertilization of ideas among various branches of sciences. It seems likely that the devices based on smart materials may be constructed in the form of a hybrid structure, for example, utilizing both inorganic semiconducting nanoparticles and synthetic lipid bilayers. The biomimetic approach to materials science is unique and should be continued. In this connection, the rationale of our work in membrane biophysics has been to understand the living organisms in physical and chemical terms. Hence, in a sense, we have been mimicking Nature's approach to 'smart' materials science or life, as we understand it, which may be summarized by one word 'trial and error'. This approach was fine for Nature but not a viable one for us now, since we do not have unlimited time and resources at our disposal. Nevertheless, we can glean the design principles from Nature's successful products and apply to our search for better materials from which advanced devices ultimately depend. So, the approach of our proposed research is a biomimetic one. The success of our past work is evidenced by self-assembled lipid bilayers, photoelectric effects in pigmented BLMs, TCNQ-based BLM rectifiers, and most recently supported BLMs on interdigitated structures as biosensors by microelectronic techniques. We plan to continue this biomimetic approach to materials science research in the years to come.

REFERENCES

[1] P. Mueller, D. O. Rudin, H. T. Tien and W. C. Wescott, Nature, 194, 979 (1962).

[2] H. T. Tien, "Membrane bioenergetics as viewed from reconstitution experiments," in Redox Chemistry and Interfacial Behavior of Biological Molecules, G. Dryhurst and K. Niki, eds., Plenum Publishing Corp., New York, NY, 1988. pp. 529-556.

[3] P. Vassilev and Tien, H.T. (1989), in Artificial and Reconstituted Membrane Systems, Subcellular Biochemistry, Vol. 14, eds., Harris, J.R. and Etemadi, A.-H., Plenum Press, N.Y. 97-143.

[4] H. T. Tien, "Electronic Processes and Redox Reactions in BLMs", in Adv. Chem. Series, No. 235 --Biomembrane Electrochemistry, ACS, Washington, DC, 1994. Chapter 24.

[5] J. M. Mountz and H. T. Tien, "Photoeffects of pigmented BLMs in a microporous filter", Photochem. Photobiol., 28, 395-400 (1978).

[6] M. Zviman and H. T. Tien, "Formation of a BLM on rigid supports: An approach to BLM-based biosensors", Biosensors & Bioelectronics, 6, 37-42 (1991).

[7] H. T. Tien, "Self-assembled lipid bilayers for biosensors and molecular electronic devices," Advanced Materials, 2, 316-318, June 1990.

[8] H. T. Tien, in Interdisciplinary Research in Smart Materials, (A. Crowson and J. A. Bailey, eds.), USARO, Research Triangle Park, NC, 1993. 81 pp.

[9] A. Ottova-Leitmannova, T. Martynski, A. Wardak and H. T. Tien, "Self-assembling bilayer lipid membranes on solid support: Building blocks of future biosensors and molecular devices", in Molecular Electronics and Bioelectronics (R. Birge, ed.) Adv. Chem. Series No. 240, ACS, Washington, D. C. (1994).

[10] K. Yoshikawa, H. Hayashi, T. Shimooka, H. Terada and T. Ishii, Biochem. Biophys. Res. Commun., 145, 1092 (1987).

[11] W. Schulmann, S.-P. Heyn and H. E. Gaub, Adv. Materials, 3, 388 (1991).

[12] K. T. Kinnear and H. G. Monbouquette, Langmuir, 9, 2255 (1993).

[13] T. Hianik, J. Dlugopolsky and M. Gyepessova, Bioelectrochem. Bioeng., 31, 99 (1993).

[14] H. T. Tien, Z. Salamon, W. Liu and A. Ottova, Analyt. Lett., 26, 819 (1993).

[15] W. Liu, A. Ottova-Leitmannova and H. T. Tien, in "Polymer/Inorganic Interfaces", Vol. 304 (R. L. Opila, F. J. Boerio and A. W. Czanderna, eds) Materials Research Society, Pittsburgh (1993).

[16] A. L. Ottova, D.-L. Guo and H. T. Tien, Proc. Conf. on Smart Sturctures and Materials, Orlando, FL., in press, 1994.

[17] W. Ziegler, D. Remis, A. Brunovska and H. T. Tien, in Proc. 7th C-S Conference on Thin Films, (V. Tvarozek and S. Nemeth, Eds.) pp. 304-311.

[18] Z.-H. Tai, T. Li and Z.-C. Yang, Prog. Biochem. Biophys., 19, 306, 391 (1992).

[19] Y.-E. He, M.-G. Xie, S.-K. Liu and H. T. Tien (to be published).

[20] J. Kotowski, T. Janas, and H. T. Tien, "Immobilization of glucose oxidase on a polypyrrole-lecithin bilayer lipid membrane," J. Electroanal. Chem., 253, 277-282 (1988).

[21] A. Ottova-Leitmannova and H. T. Tien, Prog. Surface Science, 41(4) 337-445 (1992).

[22] L. G. Wang, Y.-H. Li and H. T. Tien, Bioelectrochem. Bioenerg. Submitted (1994).

[23] M. Zviman and H. T. Tien, "Reconstituted olfactory receptors in BLMs", Bioelectrochem. Bioenerg. in press (1994).

[24] A. L. Ottova, W. Liu, T.-A. Zhou and H. T. Tien, Proc. Materials Reseach Society (MRS) 1993 Fall Meeting. in press (1994).

[25] V. Tvarozek, H. T. Tien, I. Novotny, T. Hianik, J. Dglugopolsky, W. Ziegler, A. Leitmannova-Ottova, J. Jakabovic, Rehacek and M. Uhlar, Sensors and Actuators B, 19, 597 (1994).

INTELLIGENT MATERIALS AND STRUCTURES BASED ON ORDERED ASSEMBLIES OF DNA AND PROTEIN INCORPORATED WITHIN ELECTROACTIVE POLYMERIC SYSTEMS (28749-LS)

Prof. Kenneth A. Marx, P.I.
Center for Intelligent Biomaterials
Department of Chemistry
University of Massachusetts Lowell
Lowell, MA. 01854
tel. (508) 934-3658
fax (508) 458-9571

OBJECTIVE

Our ultimate objective is to create novel, ordered thin film and LB monolayer film structures possessing unique integrated smart properties. The structures will be comprised of two basic materials: 1) new types of conducting polymers and 2) native or bioengineered biological macromolecules(DNA; enzymes-horseradish peroxidase, laccase, alkaline phosphatase and other phosphatases; chromophore containing proteins-phycobiliproteins, bacteriorhodopsin). We hope to integrate the signal transduction capabilities of the highly evolved biological macromolecules with the interesting electronic and optical properties of the conducting polymers. As a result the biological macromolecules' superior properties may be exploited in the creation of new classes of smart materials.

APPROACH

We are creating new classes of conjugated polymers, using synthetic methodology involving new monomers. These conjugated polymers possess interesting conducting, optical and non-linear optical properties. Synthesis is carried out both in bulk (polyalkylthiophenes, electropolymerized polypyrrole) and enzymatically in the monolayer at the air-water interface of a Langmuir-Blodgett(LB) trough (alkyloxyphenols, alkylanilines, alkylazomethine, alkyldiazophenol, benzoporphyrins). Structural and functional properties of the synthesized polymers are being characterized routinely by UV-Vis, fluorescence, FT-IR, NMR spectroscopies and thermogravimetric analysis. Monolayer stability and the kinetics of different enzymatic catalysts, substrates and temperature on the LB monolayer polymerization process are being investigated. Molecular modelling of the polymeric products is being carried out as well as spectroscopic characterization by fluorescence and polarized FT-IR and FT-Raman.

DNA binding kinetics to electropolymerized polypyrrole is being followed using scintillation counting of radiolabelled DNA. These measurements are being correlated with high resolution TEM, SEM, AFM and electron diffraction of the polymer surface and interior. The polyalkylthiophene polymers are being chemically derivatized by biotin so that they can be used in LB monolayer and thin film formats to form a generic cassette system utilizing the classical biotin streptavidin complexation interaction to attach any

biotinylated or streptavidinylated macromolecule. We have demonstrated these cassette complexes in monolayer form for antibodies as well as a number of other chromophoric proteins bound to the polymer monolayer. LB trough isotherm characterization, Brewster Angle Microscopic analysis of the LB film, ellipsometry, high resolution TEM and AFM surface characterization as well as fluorescence measurements of protein chromophores are being utilized. We have begun to demonstrate the ability of these biotinylated polymer complexes to coat silanized optical fibre surfaces and transduce chemilueminescence signals to photon counters. Sol-gel chemistries for entrapment and immobilization of chromophoric proteins are being pursued also.

ACCOMPLISHMENTS

In the area of conducting polymers, synthesis of polyalkylthiophene has been extended to include synthesis of the C6, C8, C11 and C18 derivatives. The UV-Vis spectra, conductivities and GPC size analyses have been carried out on these materials. A modification of the synthetic route has been developed that improves polymer solubility. This is to create tosylate derivatives of hydroxymethylthiophene to which biotinic acid is added. The biotinylated derivative is then reacted with the alkylthiophenes in the presence of ferric chloride to form the same block copolymer species. In synthesis of an alternating copolymer, the monomer species formed from coupling a lithiated hydroxymethylthiophene with brominated(Grignard Chemistry) alkylthiophene monomer has been created. This monomer species has been confirmed by NMR and elemental analysis. Success in making a true alternating copolymer would eventually result in biotinylated derivatives with better defined electronic, optical and structural properties.

Studies of DNA binding to polypyrrole and polyalkylthiophenes have been carried out. DNA binding has been shown to occur to these polymers at levels reflected in their conductivities, which indicates that binding occurs by virtue of the interaction of negatively charged DNA phosphate residues with the positive charged defects of the polymer that give rise to its electronic conduction. It has been shown that both single and double stranded DNA penetrate polypyyrole films in a time dependent manner. These molecules may achieve equilibrium distributions in the polymer matrix through a combination of an adsorption effect and diffusion through micropores of varying sizes. The smooth(electrode facing) and rough surfaces of electropolymerized polypyrrole have been characterized by AFM, SEM, high resolution TEM and electron diffraction.

The cassette nature of the LB monolayer biotin lipid-streptavidin system has been demonstrated; that is, the ability to add any biotinylated species to the streptavidin binding sites pendant in the aqueous subphase. It has also been shown that both biotinylated phycobiliproteins and IgG protein alter the LB isotherms of the biotin lipid by increasing the surface pressure. This is indicative of their binding to the lipid film. In the case of the phycoerythrin, a laser fluorescence emission spectrum of the monolayer of fluorescent protein was clearly recorded, conclusively proving that the cassette system works to specifically bind biotinylated molecules. Furthermore, the high sensitivity of a monolayer of these high quantum yield fluorescent proteins suggests their utility for signal transduction purposes in potential device applications.

The LB isotherm behavior of newly synthesized polyalkylthiophene derivatives have been characterized. While most of the derivatives formed good isotherms, of special interest were the biotinylated derivatives which formed good isotherms and bound

streptavidin which subsequently bound biotinylated phycoerythrin based on a dramatic isotherm shift to higher surface pressures [poly(3-undecylthiophene-co-3-thiophenecarboxaldehyde-biotin-LC-hydrazone)]. This was confirmed by a subsequent measurement of the phycoerythrin fluorescence. High resolution TEM of these monolayers has shown streptavidin binding on the polymer film. Structures which may correspond to the two phases in this system on the fluorescence LB mini-trough have been identified. Multilayers of these phycobiliprotein-biotinylated alklypolythiophene LB films with as many as 10 monolayers have been created. Current studies are underway to incorporate bioengineered phycobiliproteins into the LB monolayer polyalkylthiophene films

Cassette technology has been further expanded to allow self-assembly of a biotinylated polythiophene on silanized(hydrophobic) surfaces of a bare optical fibre. The monolayer formed provides a functionalized surface for further binding of streptavidin conjugated biomolecules. However, our best studied system to date has been the self-assembly on hydrophobic inner surfaces of glass capillaries of the biotinylated undecylthiophene polymer discussed above followed by binding of the enzyme alkaline phosphatase as the streptavidin conjugate. We demonstrate the activity of a new commercially available chemileuminescent substrate, chloro-3-(4-methoxy spiro{1,2 dioxetane-3-2'-tricyclo-{3.3.1.1.}-decan}-4-yl)phenyl phosphate (CSPD), for this immobilized enzyme by detecting its broad visible chemileuminescence signature. This eliminates the need for laser light sources to generate an optical signal. We then demonstrated that organophosphate pesticides inhibited the enzymatic activity toward CSPD which generates chemileuminescence. Lineweaver-Burk plots of the data show a mixed type of inhibition. Using this approach the pesticide paraoxon was able to be detected down to 500 ppb in a 0.1 ml capillary. We have also demonstrated the use of alkaline phosphatase in solution as a metal ion detector for Zn(II), Be and Bi using the CSPD chemileuminescent substrate. The Zn(II) detector activity is based upon prior metal ion removal from the enzyme and its reconstitution in Zn(II) containing solutions. A 3 ppb detection limit has been achieved . Be and Bi can be detected at around 1 ppm by inhibition of the native enzyme. These experiments are now being repeated for the immobilized alkaline phosphatase.

In the area of enzyme catalyzed polymerization of LB monolayer(comprised of oriented monomers) films it was demonstrated that laccase and horseradish peroxidase(HRP) catalyze polymerization of oriented monolayers composed of 4-tetradecyloxyphenol or 4-hexadecylaniline mixed with excess ethyl phenol, phenol or aniline. The polymers were characterized by isotherm, UV-Vis spectroscopy and TGA(thermogravimetric) and were shown to be extremely thermostable. Third order nonlinear optical susceptibilities of the polymers have been determined and were found to be in the range of 10^{-9} esu compared to 10^{-10}-10^{-11} esu for the bulk synthesized polymers.

Enzyme polymerized LB monolayers analyzed by polarized FT-IR spectroscopy have demonstrated functional group orientation in the polymer. Molecular modelling of the polymer chain has produced a low energy structure in which all OH groups are pendant in the LB trough subphase, which agrees with the polarized FT-IR data. Also, AFM and ellipsometry studies were carried out on the polymer picked up on a solid substrate yielding an appropriate thickness for the monolayer film.

Recent experiments have demonstrated the enzymatic polymerization of LB monolayers comprised of the following oriented phenolic monomer compounds: tetra-meso(p-hydroxyphenyl)benzoporphyrin, tetradecyl azomethine, tetradecyldiazophenol

and the l-isomer of hexadecyl tyrosine all with an excess of phenol. Characterization of these LB polymer films, including their optical properties, has begun. We are obtaining initial evidence for ordered chromophore arrays on ITO surfaces for LB films picked up from the LB trough surface.

In experiments to investigate fluorescent proteins and their possible incorporation into photovoltaic devices, initial results measuring the photovoltage/photocurrent characteristics of phycobiliproteins in Au/Phycoerythrin/Au cells has been extended. The system appears to follow Onsager's law of geminate recombination. The photocurrent varies exponentially with temperature, the system exhibiting an activation energy of 300 meV. A theoretical modelling of the dielectric loss will yield charge transport mobility information on this system. Also, a nonempirical electronic structure calculation of the tetrapyrrole chromophores in phycobiliproteins has been completed. These calculations reasonably predicted the absorption maxima for the protein bound chromophores.

A novel three-dimensional optical memory system based on the light transducing protein bacteriorhodopsin was proposed. The system uses the non-linear optical properties of bacteriorhodopsin to accomplish reading and writing operations. A nondestructive method of reading information in three-dimensional optical memory that uses second harmonic generation was demonstrated. This method has the advantage of fast speed, is nondestructive, and has the potential for parallel access.

Using room temperature hydrolysis, condensation and densification steps, sol-gel derived glassy networks with controlled pore size have been produced. Photodynamic proteins and alkaline phosphatase have been incorporated and immobilized in these matrices. Their native fluorescence spectra and catalytic activity have been preserved in this process and environment. Avidin-biotin complexation has been used to specifically bind photodynamic proteins in the post cured system. This approach will provide fundamental advantages in immobilization and other sensing related applications.

FUTURE RESEARCH OPPORTUNITIES

The research accomplishments presented here suggest a number of promising areas for future development. Thin film and monolayer attachment strategies for biological macromolecules by self-assembly onto hydrophobic surfaces using the biotinylated alkylthiophene copolymers or onto LB monolayer films(and multilayers by build up) of the same polymers are generic cassette methodologies which we are continuing to perfect. The signal transduction and sensing capabilities of phycobiliproteins and alkaline phosphatase(chemileuminescence) have been most widely studied by us and continue to promise interesting future results. In our experiments, bacteriorhodopsin continues to show promise in new ways as a rugged and sophisticated optical system comprised of highly ordered elements. Enzymatic synthesis of novel 2-dimensional polymer films at the air-water interface of the LB trough is promising because it results in polymers with higher third-order nonlinear optical properties and superior processing properties compared to bulk solution synthesized branched polymers.

The foregoing activites form part of a strong collaborative effort between the University of Massachusetts Lowell and the Biotechnology Division, U.S. Army Natick Laboratories. The present collaboration has resulted in a number of patent applications and awarded patents and the publications listed below. Also listed below are the personnel and Ph.D. students supported and trained by this Grant.

Smart Photomechanical Polymer Devices

Mark G. Kuzyk
Department of Physics, Washington State University, Pullman, WA 99164-2814

July 6, 1994

1 Abstract

We are investigating photomechanical effects in polymer optical fibers and have found several mechanisms that can result in light-induced length changes. We have demonstrated that the photothermal heating mechanism responds on millisecond time scales and results in displacements of several microns while the electrostrictive response has a sub-nanosecond response time with a 10ns displacement. We have built several devices with polymer fibers including an optical actuator, stabilizer, and digital positioner. We have designed miniaturized devices with 80μm diameter and sub-millimeter lengths and are in the process of fabrication and characterization studies. Future studies are aimed at fabricating sheets of miniature device arrays that would form a smart fabric and could potentially be used as smart aircraft skin and active vibration suppressors.

2 Experiment

We report on two separate experiments; the demonstration of a stabilized photomechanical positioner and a fast actuator.

2.1 Positioner/Stabilizer

Figure 1 shows a schematic representation of a device that acts as a photomechanical actuator, stabilizer, and digital positioner. A mirror is suspended from a polymer optical fiber in an evacuated chamber. The hanging mirror defines one arm of an optical interferometer. The other arm is defined by a stationary mirror. The light intensity leaving the interferometer, which is related to the length of the hanging fiber, is directed to the fiber. Because the light intensity inside the fiber carries information about the fiber length, this forms a feedback loop that forces stabilization of the hanging mirror: if the mirror moves, the intensity leaving the interferometer changes and affects a length change in the fiber to restore it to its original position.

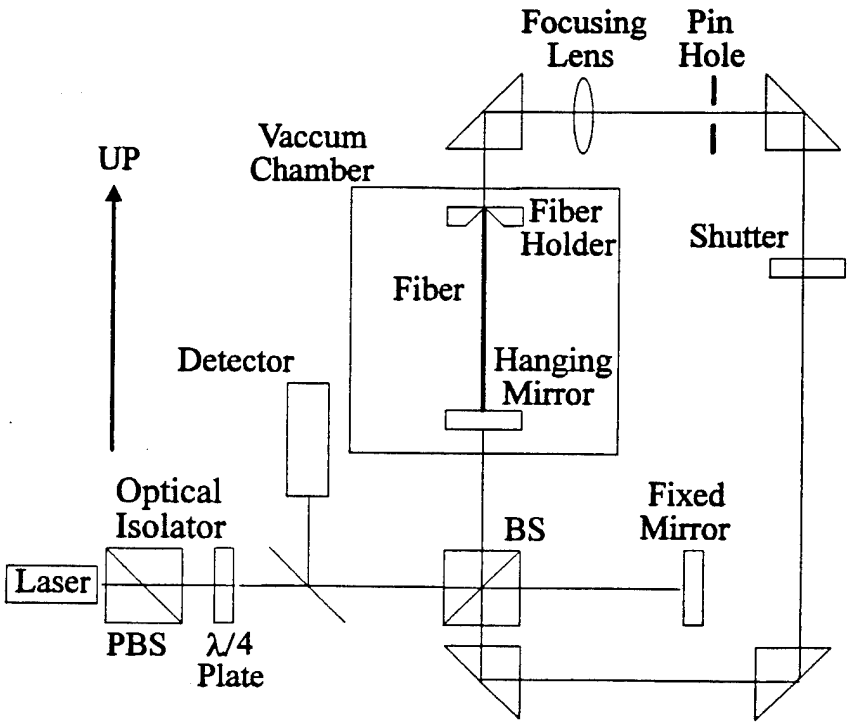

Figure 1: All-optical photomechanical stabilizer and positioner (digital and analog).

This device, then, acts as both a positioner and a stabilizer. The fiber length can be controlled by varying the laser intensity. For a fixed laser intensity, mechanical vibrations are actively eliminated. Figure 2 shows the output intensity of the interferometer as a function of time. Note that the light intensity is related to the length of the fiber. It is clear that when the shutter is closed so that no light is feed into the fiber, its length drifts with time. When the shutter is turned on to allow feedback, the fiber length stabilizes to a value that is determined from the laser intensity. We have found that this device keeps the mirror position fixed to within a few nanometers.

For a fixed laser intensity, the stabilizer is found to have several distinct equilibrium lengths. Figure 3 shows the light intensity as a function of time and the arrows show times at which mechanical agitation is applied to the system. The fiber length can be induced to hop to successively longer lengths when the magnitude of the mechanical agitation exceeds some critical value. Note that the stabilizer becomes more resistant to external mechanical impulse for each successive stable length. The data in Figure 3 shows that the step size is on the order of 300nm. This digital positioner is thus capable of a total travel of about 4μm in 300nm steps in which the position is accurate to a couple of nanometers. Digital stepping can also be induced with a pulse of light. We are in the process of making an all-optical digital positioner.

In summary, the device in Figure 1 acts as a continuous positioner that is controlled by the laser intensity and as a discrete positioner when the laser intensity is fixed. In both

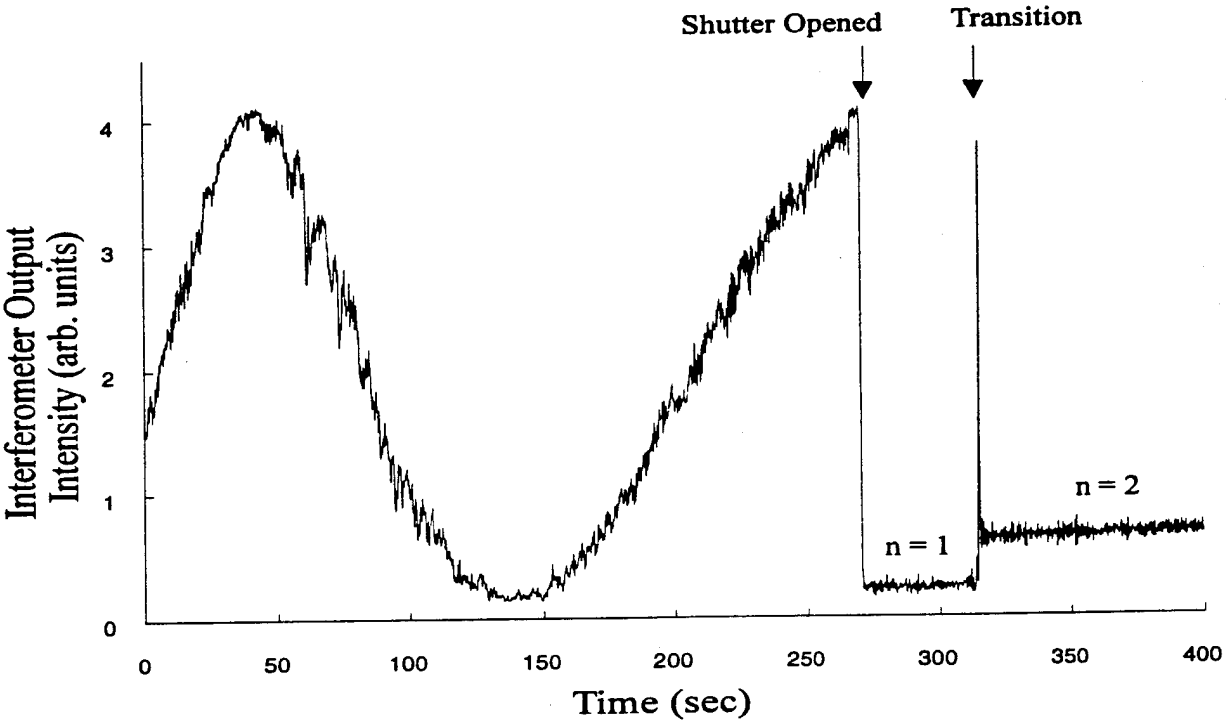

Figure 2: Intensity leaving interferometer as a function of time. Fiber length stabilizes when feedback is turned on.

cases, the position is stabilized to within about 2nm.

2.2 Fast Actuator

Figure 4 shows the fast photomechanical actuator experiment. An intense near infra red laser beam is launched into a KDP crystal to form a small amount of green second harmonic light. The infra red light is directed to a fiber that supports a hanging mirror while the low intensity green light is sent to an interferometer that is used to probe the position of the hanging mirror. The probe beam is first split into two separate pulses that are delayed relative to each other and recombined to form two temporally translated pulses. The experiment is timed in the following sequence. The first probe pulse hits the hanging mirror just before the arrival of the pump beam. The second pulse arrives just after the pump beam so that the pump-pulse-induced change in fiber length can be determined.

Figure 5 shows the fractional change of the probe intensity as a function of time. Because the length change is proportional to the fractional intensity change, the data points in the figure represent the length change as a function of time. The solid curve shows the pump intensity in the fiber. There are apparently two mechanisms of length change. One mechanism is ultrafast and follows the pump pulse profile. This implies that its temporal response time is much faster than the 5ns laser pulse width. The second mechanism decays with a time constant of about 12ns. Assuming that the response time is 5ns, we place a

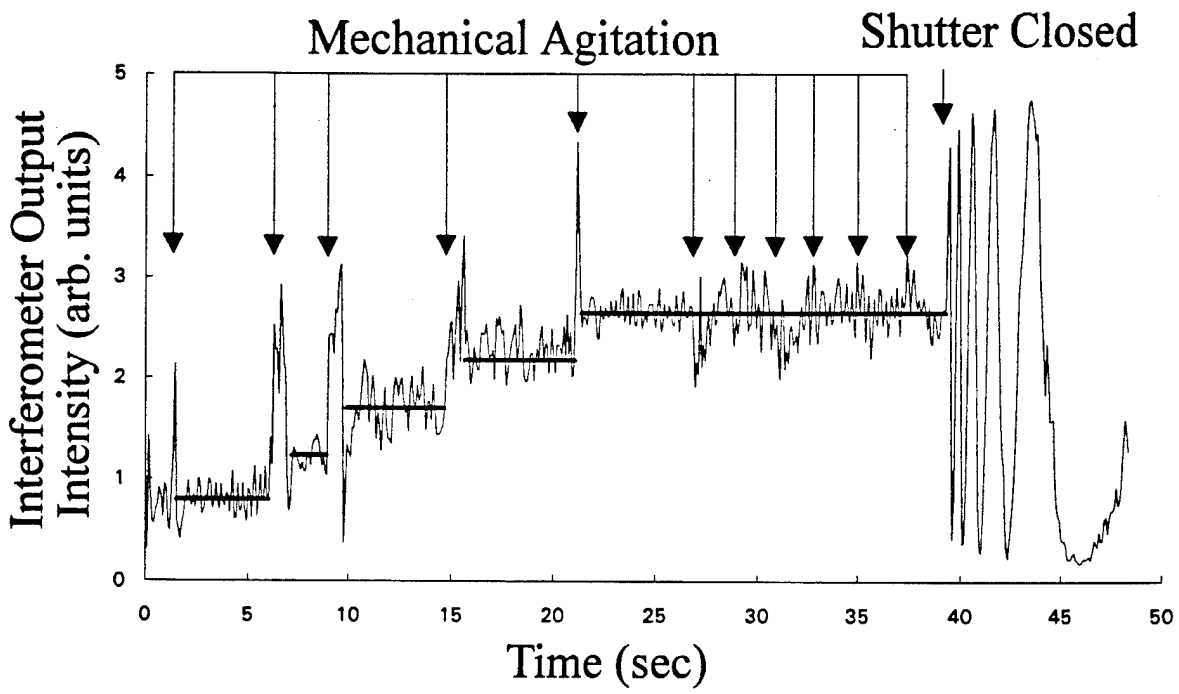

Figure 3: Interferometer output as a function of time during mechanical agitation. When the feedback shutter is closed, the fiber relaxes.

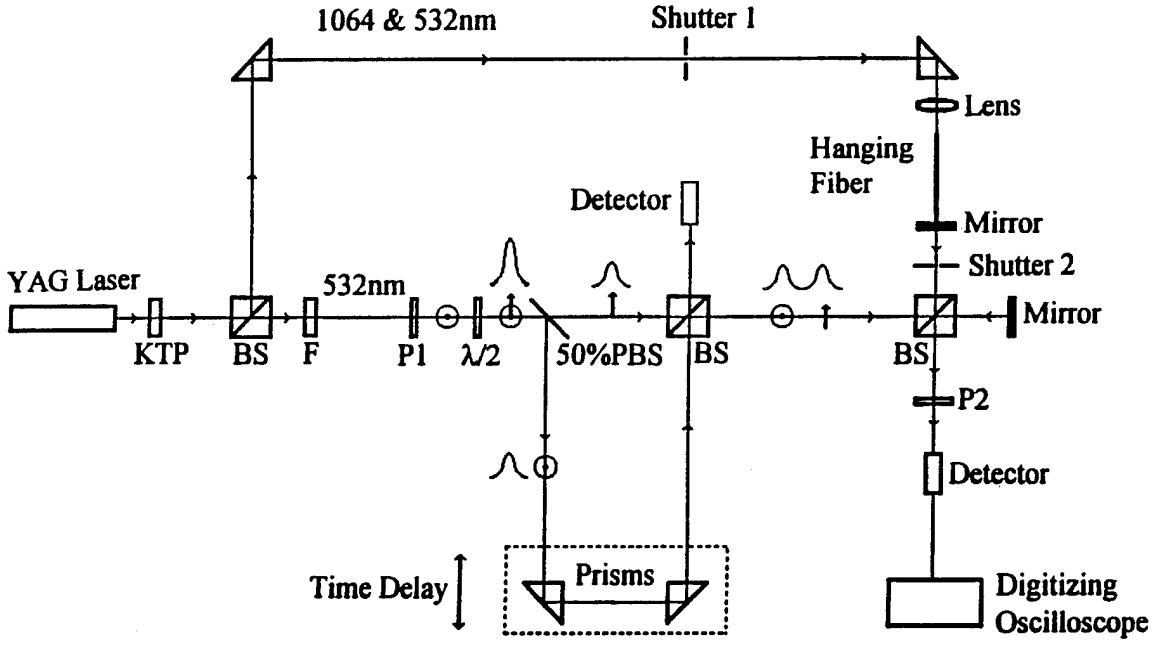

Figure 4: Fast actuator experiment.

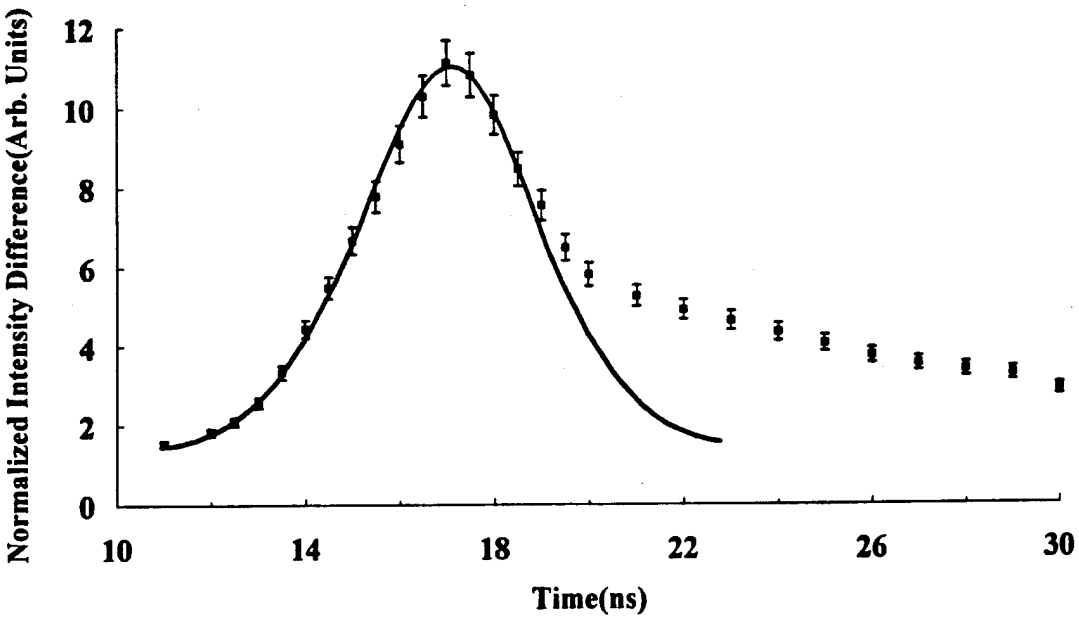

Figure 5: Fractional change in intensity of the probe beam as a function of time due to fiber length elongation that is induced by the pump beam. Solid line represents pump pulse intensity.

lower limit on the mirror acceleration at $4 \times 10^8 m/s^2$.

3 Future Work

We are working on miniaturizing the photomechanical stabilizer/positioner and have designed such a device based on a waveguide Fabry-Perot interferometer. Figure 6 shows a schematic drawing of this device. A set of reflectors can be defined onto the waveguide in the form of a refractive index grating (Figure 6a) or a thickness grating (Figure 6b). When light is launched into the Fabry-Perot device along the cylindrical axis, it will bounce back and forth between the reflectors. The intensity of the light between the reflectors will be determined by their spacing while the spacing will be determined by the light intensity through the photomechanical effect. The feedback loop is thus built into the system. The device's operational characteristics are the similar to the device in Figure 1. An important difference between the device in Figure 1 and 6 is that the miniaturized ones are doped with dyes to enhance the photothermal effect. We have succeeded in making cylindrical waveguides that are 80μm in diameter, less than 1mm in length, and doped with various dyes. We will test the first generation devices made from silvered ends. In parallel, we are developing methods to form index gratings. It is well known that such gratings can be formed in dye-doped polymers with an interference pattern of ultraviolet light that bleaches the dye chromophores in

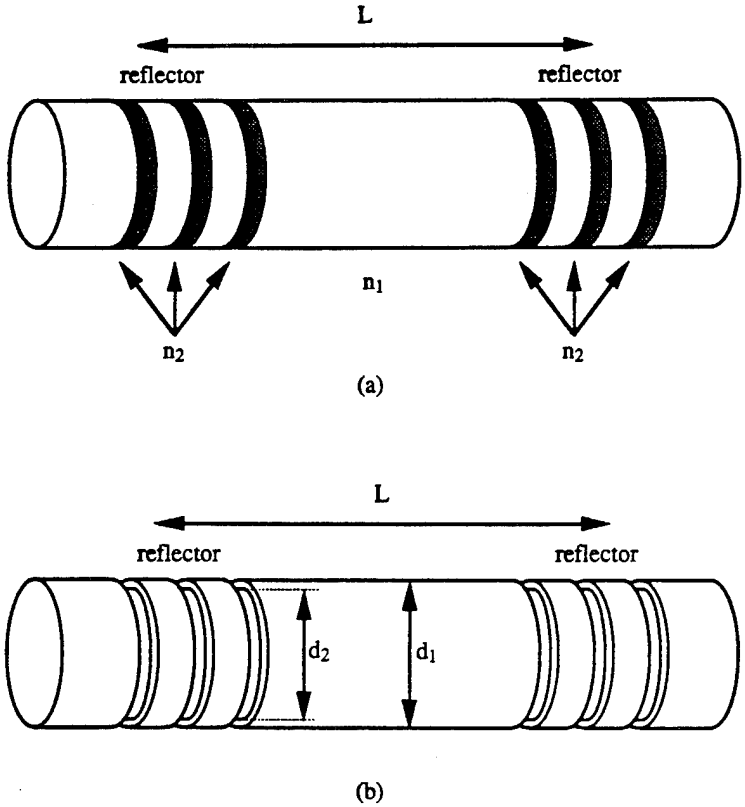

Figure 6: Miniaturized Fabry-Perot interferometer stabilizer/positioner using a) refractive index grating and b) thickness grating.

regions of brightness.

Arrays of such miniature devices can be used as vibration (and sound) suppressors, smart skins, supports for delicate or reconfigurable optics, and sensor sheets for stabilized platforms that can find applications, for example, in high precision manufacturing. Figure 7 shows an array of such devices. Furthermore, the device units can be cascaded in a variety of architectures to perform specialized functions. Aside from acting as a photomechanical unit, the Fabry-Perot cylinder is an optical logic unit that, for a given input intensity, has several possible output states. For a given state, each unit will reflect and transmit a distinct light intensity. Arrays of interconnected Fabry-Perot units could be used as optical memories and powerful associative processors that couple information processing with mechanical sensing/actuating.

4 Conclusion

In conclusion, we have demonstrated that polymer optical fibers can be built into photomechanical devices that include a stabilizer/positioner (both digital and continuous) and a fast actuator. We are in the process of making miniature devices that can be used in arrays to form smart structures and materials that can potentially be built into sophisticated parallel/associative processors that manipulate data and respond to mechanical influence both

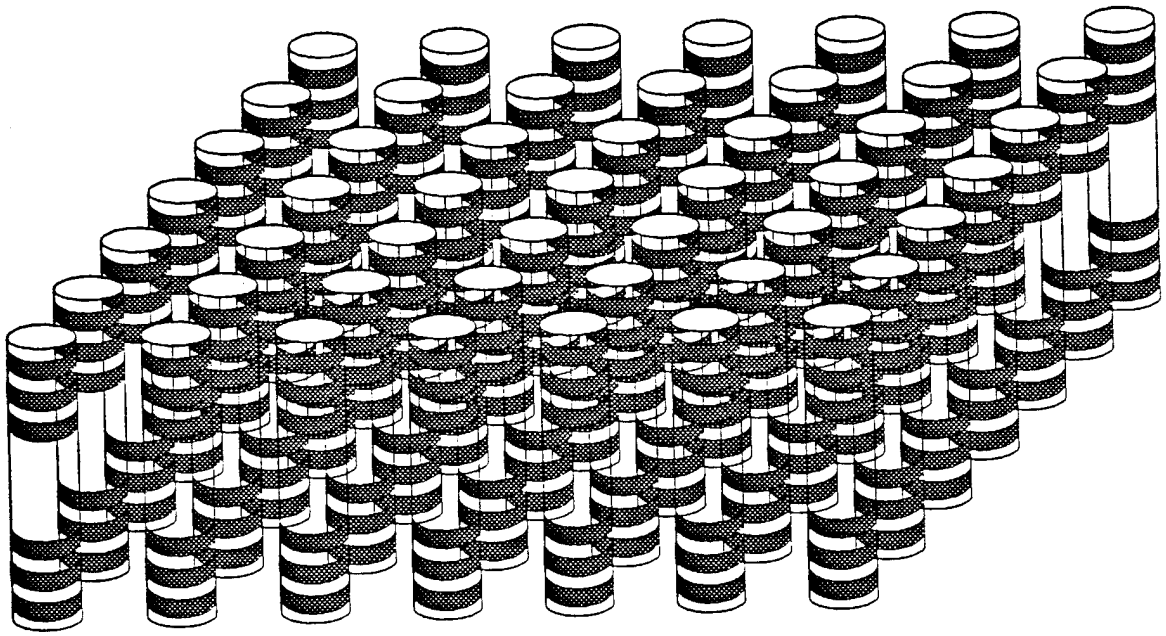

Figure 7: Array of stabilizers used as a smart sheet.

with a mechanical and optical response.

5 Bibliography

1. D. J. Welker and M. G. Kuzyk, "Photomechanical Stabilization in a Polymer Fiber-Based All-Optical Circuit," Appl. Phys. Lett. **64**, 809 (1994).

2. S. Zhou and M. G. Kuzyk "Observation of Fast Photomechanical Effects in a Polymer Optical Fiber," Submitted to Physical Review.

3. M. G. Kuzyk, D. J. Welker, and S. Zhou, "Photomechanical Effects in Polymer Optical Fibers," Nonlinear Optics, in press.

4. M. G. Kuzyk, "All-Optical Materials and Devices," in *Science and Technology of Organic Thin Films for Waveguiding Nonlinear Optics,* F. Kajzar and J. D. Swalen, eds., Gordon and Breach, New York (invited book chapter).

5. M. G. Kuzyk, Q. Li, D. J. Welker, S. Zhou, and C. W. Dirk "All-Optical and Photomechanical Devices in Polymer Optical Fiber," to appear in SPIE Proc. **2143**, EOLASE, Los Angeles (1994).

Fiber Optic Chameleonic Skin

M.L. Myrick, A. Muroski, M.L. McLester
Department of Chemistry and Biochemistry
University of South Carolina
Columbia, SC 29208

Abstract

Optical fibers provide convenient conduits for light; bundles of optical fibers are also commonly used to transfer image-format optical information. We can now conceive materials with a moderate density of optical fibers (e.g., one fiber per 1-4 in^2 surface area) and associated hardware that can serve to passively sense optical data from the surroundings and actively generate optical patterns on their surfaces. The current project aims to combine/develop some key technologies that would make these materials realizable. The major areas in need of development are: (1) high-efficiency, high-tolerance liquid crystal imaging arrays, (2) high-efficiency light harvesting polymer films, and (3) image acquisition, manipulation and display hardware. This presentation will focus mainly on concepts, with added details of current work, results and plans for future work.

Introduction

Camouflage tactics are currently employed to minimize the signatures of surface and air craft in key regions of the electromagnetic spectrum. A simple example of this tactic is the use of camouflage paint to disguise stationary vehicles in a terrain. These paints typically minimize vehicular reflectance signatures in the visible and near-infrared spectral region to frustrate visual or optical cognition/acquisition, and are examples of passive optical camouflage systems.

A major problem with this type of camouflage is that it is stationary (has zero bandwidth). In most battlefield tactical scenarios, acquisition of ground targets by aircraft is dominated by visual or assisted-visual (intensified) sighting. Particularly on varied terrain, the facility with which the human eye can detect motion makes passive camouflage less effective.

While active camouflage systems are available in the radio portions of the electromagnetic spectrum to frustrate acquisition by radar, active optical camouflage has lagged behind in development. This is largely because the task is daunting: the human eye is a relatively high-resolution imaging device, and visual perception is very sensitive to motion. Active optical cloaking systems have developed in nature (e.g., the chameleon), but are typically slow in response (low bandwidth); hence such natural systems are primarily used in a stationary mode to frustrate detection.

A realistic optical cloak for a moving surface vehicle can perhaps be developed along the lines of these natural cloaks, but will necessitate a dramatic increase in the effective bandwidth of the system relative to those in nature. Such a system must satisfy two major demands. First, it must provide full coverage because the resolution of optical detection devices is much greater than that of radio-frequency devices. Second, the bandwidth must be increased to the point that the effects of motion and update lag-time are minimized.

We are working to develop the technology for active chameleonic skins with embedded fiber-optic arrays to generate a real-time-updated image of masking terrain on the material surface. Combined with a real-time or computer-generated video image of the terrain directly beneath a vehicle, the material could generate a "ground-cover" image to mask itself; the perception of motion could be minimized by effectively "scrolling" this realistic mask image down the length of the material opposite the direction of motion during

travel, based on real-time updates or sensor data from engines, power trains, etc. Figure 1 shows in schematic both some of the design elements and capabilities for this system.

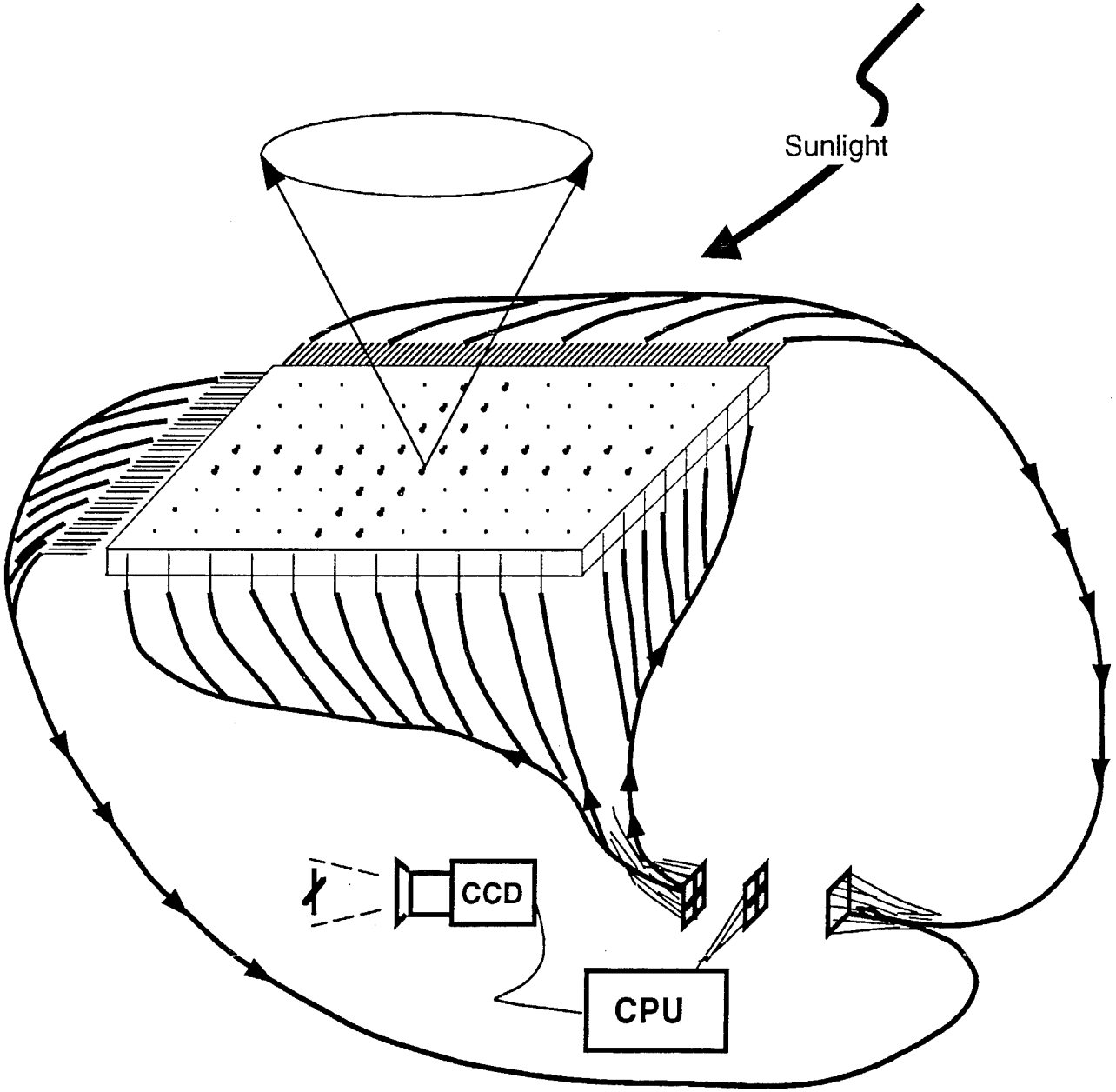

Figure 1: Schematic Diagram of concept. In addition to direct transfer of images to the skin, the optical system could be used to gather optical information from the exterior, transmit images/data optically via line-of-sight to any viewer, or identify concealed material with a narrow-bandbass optical signature.

Key Elements of Concept

As a working example, we will diagnose feasibility and cost for a simple 2 X 3 meter coverage of material viewed from 200 meters under a cloudless sky at the highest solar flux typical for mean sea level. The specific fibers assumed for the array will

be 150 μm diameter including cladding. Spaces between image-broadcast fibers will be assumed to have a reflectance of zero. We assume a high terrain reflectance of 50% across the visible spectrum. We further assume we are designing a system for visible camouflage. Many of these assumptions are made to present a worst-case challenge to the material.

Fiber Optics

Fiber optics are composed of a solid glass core (typical diameter of 25 μm to 400 μm) surrounded by a thin glass cladding of lower refractive index. They can be used to transmit or receive light. In either case, the optical spectrum which can be covered extends from the UV into the Near- to Mid-IR wavelength range.

Coverage

Fiber optics are currently available in large quantities and in high quality, at a cost near $0.50/meter.[1] At this cost, complete coverage of the example area with perpendicular fibers (end-face visible) would amount to more than $75 M per linear meter of fiber. This would also be practically unworkable. Fortunately, this is unnecessary.

If we consider the human eye to be an ideal imaging system producing a diffraction-limited resolution near 1 μm, and a focal length of 2 cm, then the effective minimum resolution element in an object viewed from 200 m is 1 cm.[2] In fact, visual acuity, though great, is not diffraction limited due to lens inhomogeneities, aberrations, and aperture restrictions. Hence, we can consider that the image-broadcasting fiber array (the normal or imaging array) need only consist of fibers spaced on 2-cm centers to provide apparent continuity of coverage on objects viewed from 200+ meters. In this event, fiber cost would amount to less than $8 K per linear meter of fiber, making this expense practical for some purposes.

Optical Source

A more serious consideration is the optical source. The solar radiation striking our sample under our set of imaginary conditions is typically at a power density of $\geq$1000 W/m^2.[3] Total power on our imaginary sample is thus 6000 W. If we take as an approximation that 35% of this power is in the form of visible light (2100 W),[3] then the reflectance of the terrain is such that 1050 W of visible light must emanate from our sample over all angles. If we restrict our interest to those directions from which aerial observation is likely, we can likely reduce our requirements to ~500 W. Unfortunately, lamps have low efficiency (typically $\leq$ 2%), so that nearly twenty-five 1000 W lamps would be necessary to meet even this reduced requirement. While possible, the power consumption of this system would be impractical for any non-dedicated field use. Lasers are not particularly efficient devices either, and are not ideal sources for this application because they generate coherent light; the resultant "speckle" pattern seen by an observer would do more to attract attention to the camouflaged material than to sequester it.

To make an embedded fiber system practical, an energy-efficient incoherent illumination system is needed. The most efficient and elegant solution to this problem would be a solar concentrator, since the need for illumination decreases with solar intensity. Such a solar concentrator can be made by depositing dye-doped or rare-earth-ion-doped polymer films parallel to the external surface of the materials.[4,5] These dopants absorb light and fluoresce in all directions; some of this light is contained and is conducted to the edge of the film where optical fibers can transmit it to the imaging systems. We have shown above that 500 W of visible radiation is needed at a minimum to pump the imaging array. A high-efficiency dye can re-radiate nearly all of the 2100 W of visible solar flux. In a planar optical waveguide with a critical angle of only 75.5°, 25% of this light is contained and transferred.[6] This amounts to 525 W of visible power, sufficient to pump the array. This light harvesting film could cover the large open spaces

between the image fiber array, effectively covering >99% of the surface, and would be relatively inexpensive due to its two dimensional preparation.

Bandwidth Increase

When a material with embedded collector/emitter systems is in place, the remaining requirement (that of generating a high-bandwidth mapped image) can be met by designing a liquid-crystal (LC) dynamic scattering video projection array coupled between the harvesting system and the imaging fiber array. Unfortunately, these arrays are not readily multiplexed due to their linear performance with applied voltage, and would need to be driven with individual thin-film transistors at each pixel. More standard twisted-nematic-type arrays are more applicable for multiplex driver circuitry, though commercially-available arrays suffer from low damage thresholds. This point is addressed below. A video or other detector can be used to image the pattern to be mapped on the surface of the smart material. This can be displayed on the LC array placed in the optical train at the focal point of the imaging array. To obtain multi-wavelength capability, optical filters and dichroic mirrors can be used to split and combine optical frequencies prior to insertion of the light into the image array.

Damage Thresholds

Power damage thresholds for these components are within tolerances required for this application. The damage threshold for optical fibers and polymer films is very large compared to the proposed power densities, as is that of interference filters and dynamic scattering LC devices not utilizing polarizing filters. Standard (e.g., twisted nematic) LC devices commercially available with polarizers are not applicable because of their relatively low damage threshold caused by the absorbance of light in the polarizing films. In addition, these polarizing films restrict the transmission of standard devices to $\leq$25%, typically, whereas dynamic scattering materials can have very large transmissions (>80-85%) in the "on" state.[7]

Major Elements Not Available

Key elements of this system are not currently available, and these are the areas in which research under the current proposal is being conducted. These include preparation of materials with aligned optical fibers, development of a direct video-to-LC-array system, and the passive light-harvesting optical films. The LC arrays are another subject for work because neither of the two major types of arrays (dynamic scattering and twisted nematic) are precisely suitable. The first requires non-multiplexed driver circuitry and is beyond the scope of abilities of this laboratory to address for any reasonable array dimension (e.g., 100 x 100 elements); a corporate partner would be necessary for such developments and one is being sought. The second type normally requires polarizing films in order to work; these restrict the damage thresholds of such devices to unsuitably low values. The LCs themselves have very high damage thresholds, so that one was around the problem with commercial arrays is to identify alternate methods to express the optical rotation induced by the LCs when activated. One area of current work is study of alternate methods for utilizing these devices.

Conclusion

Work in this laboratory is focused presently on interfacing patterned LC arrays to image processing hardware and on developing an alternate method for expressing images on these arrays. In addition, work is being done on distributed sensing using fiber-optic arrays and array detectors. At the outset of this project, a search revealed the existence of a company in Colorado which manufactures fiber-imbedded display screens developed via SBIR funding from the FAA for airport runways - these screens are quite similar to those proposed in this project, and we are currently collaborating with this company to develop fiber-imbedded materials for this project.

References

1. For example, Corning, Inc. (Wilmington, NC) fabricates communications-grade fiber optics for inclusion in communications cables, costing approximately $0.50/meter, of the type used in the working example in this proposal.

2. Based on an effective magnification on the retina of 10^{-4}.

3. J.J. Loferski Nato Adv. Study Inst. Ser. Ser. B B69(1981), 157.

4. A. Gretzberger and W. Greibel Appl. Phys. 14(1977), 123

5. B.A. Swartz, T. Cole and A.H. Zewail Opt. Lett. 1(1977), 73.

6. Based on 4π steradians for random emission, and a planar waveguide that allows light incident on the interface with an angle of 14.5 degrees at either side of the interface to escape. This permits 75% of light striking either interface to escape.

7. For example, the liquid crystal light valves manufactured by Displaytech (Boulder, CO).

Smart Photonic Bandgap Structures

Yang Zhao
Department of Electrical and Computer Engineering
Wayne State University
Detroit, MI 48202
(313) 577-3404
(313) 577-1101 (Fax)
email: yzhao@ece.eng.wayne.edu

Abstract

This research focuses on the study of structure configurations and material compositions for the construction of smart photonic bandgap structures. The performance of three different bandgap structures were comparatively studied. Nonlinear optical films were fabricated using the Langmuir-Blodgett method for realizing these structures.

Introduction

Sensor and vision protection against high-intensity laser beams is very important in many applications. It is highly desirable to design a protection system or device which can sense high-intensity radiation and control its transmittance to block harmful radiation. Such a system should possess fast response time, and reject high-intensity radiation over a broad wavelength range. The system should also be transparent to low-intensity radiation in visible wavelengths for human vision purposes. Current protection systems using the photochromic effect or two-photon absorption can only reject a limited number of laser lines and/or do not depend on the incident laser intensity. Nonlinear one-dimensional photonic bandgap structure (PBS) appears to be a promising candidate for novel protection devices. Such devices will feature high transmission for lower-intensity light, wide-spectral bandwidth protection against high-intensity radiation, and fast response and recovery time.

PBS is an analogy photonic material that performs the same function with light that semiconductors do with electrons, since the wave nature of the electron gives rises to allowed energy bands and forbidden gaps, namely, Bloch bands, for its motion in the solids. The width of bandgap and the central frequency can be designed by choosing the material composition and structure. Microstructures consisting of periodic arrays of high-dielectric spheres or cylinders with diameters comparable to the reflected wavelengths have been shown to exhibit photonic bandgap structure [1-3]. The classic picture of PBS is photon localization. Photon localization is a process involving interference among the multiple scattered waves in a random medium. Interference among these waves in the medium confines the wave within the region of the localization length and no transmission is possible. Photon localization is created by randomly changing the phase shift (optical thickness) [4-6].

The combination of principles of PBS and nonlinear optics can create one-dimensional nonlinear photonic bandgaps, which excludes electromagnetic radiation over a range of frequencies only when the light intensity is high. The system is made up of alternating high and low nonlinear materials with similar linear refractive indices and different layer thicknesses. When the incident radiation is weak, the material system acts as a uniform medium and no photonic bandgap exists. In this case, the system is transparent and can be used for vision purposes. When incident radiation is high, the change in the refractive index in the nonlinear material causes the system to exhibit photonic bandgap and to reject the radiation.

Searching for material structures

There are several material systems for PBS. For one-dimensional nonlinear PBS, three methods have been studied: the quarter-wavelength thickness scheme, modulated superlattices, and the random thickness scheme. Each scheme is made up of alternating high and low nonlinear materials different layer thicknesses (Fig. 1). We have performed comparative study of these schemes. We use the transfer-matrix method by incorporating into the incident-beam intensity dependence on the refractive index of the layered nonlinear materials. Each of the three systems has different features.

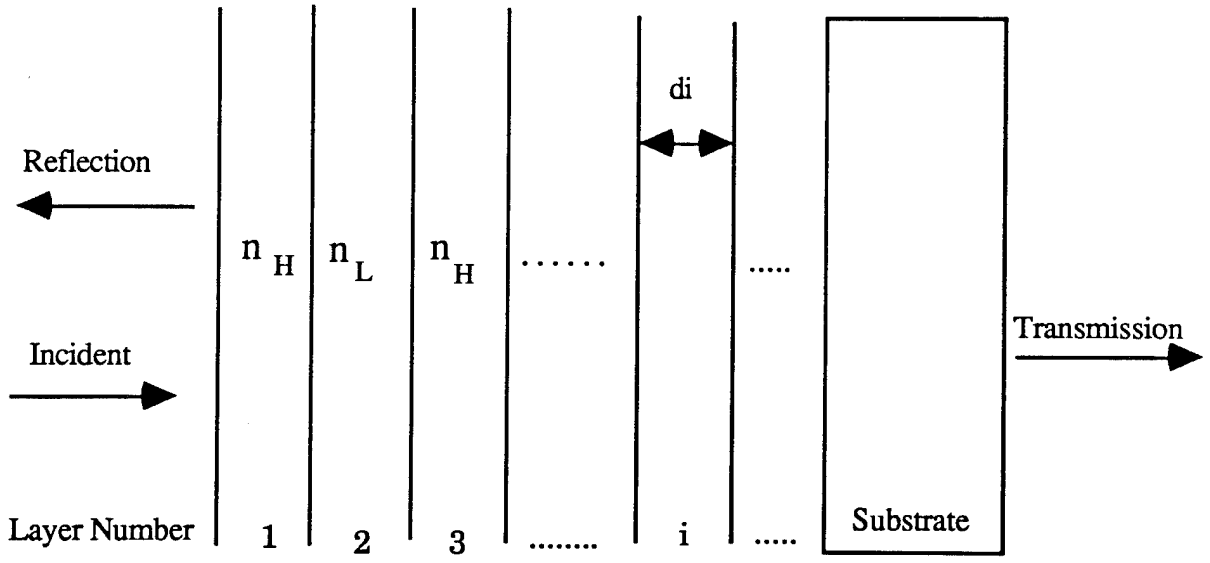

Fig. 1. Multilayers of optical thin films with high- and low- nonlinearity. The optical thickness (d_i) of each layer is (a) quarter of central wavelength for the quarter-wavelength scheme, (b) random between 100 to 200 nm for the random thickness scheme, and (c) sinusoidally modulated between 13 to 40 nm for the superlattice scheme.

For a limited number of layers with given linear and nonlinear optical parameters, it is found that the quarter-wavelength thickness arrangement gives rise to a wide rejection gap in the visible wavelength range. The low-intensity transparency is acceptable for normal vision. This scheme would be the best choice for the construction of 1-D PBS. However, due to fact that the thickness of each layer is larger than the other approaches, it will have some technical difficulties in the fabrication of this structure, especially for Langmuir-Blodgett (L-B) method where large thickness involve the complicated multi-layer depositions.

For the random layer thickness scheme, there is an incomplete rejection gap. The incomplete gap develops into a complete one as the number of layers exceeds 500. This scheme becomes quite transparent in the case of weak incidence of light. Since the thickness of each is in the same order as the quarter-wavelength thickness arrangement, fabrication of this type structure is also a challenge.

The modulated superlattice scheme produces a number of narrow gaps for a set of parameters used in our study. It was found that, by modifying these parameters, it might be possible to obtain a large rejection range. The low-intensity transparency is acceptable for normal vision. Technically, the modulated superlattice scheme is the easiest to fabricate since it involves thin layers.

Searching for nonlinear optical materials

In order to fabricate the smart PBS, the material for the nonlinear layer has to selected. The requirements of the nonlinear material include high third order nonlinearity over broadband, fast response time, and easy and precise control of thickness during the deposition. Although semiconductors and inorganic crystals have high nonlinearity and fast response time, their working wavelengths are in a very narrow range and their deposition processes are complicated. The best material to date for our application seem to be nonlinear bio/molecular and polymeric materials fabricated using the L-B method. Nonlinear optical polymers have many advantages, including subpicosecond response time, large nonlinear resonant nonlinearities, low switching energy, broadband low absorption, and environmental stability. Much progress has been made in the understanding and synthesis of nonlinear optical polymers. We are testing these materials for implementing 1-D PBS devices.

Several nonlinear polymeric and organic materials have been studied and large nonlinearity reported. Our task is to fabricated these materials with different thickness using the L-B method. We have successfully fabricated mono- and multi-layer L-B films of dye-doped PMMA polymers and liquid crystals.

Dye-doped polymers have reasonable high nonlinearity [7]. We have fabricated mono-layer and multilayer PMMA doped with rhodamine. The

system has a nonlinearity χ^3 of around 10^{-5} esu at blue wavelength. Both MMA monomers and Rhodamine 575 were dissolved in butanol. Up to 50 layers of z-type L-B films were made at a pressure of 35 mN/m. Both optical microscope and atomic force microscope pictures show a good uniformity of the films. It should be noted that, in addition to our current application, monolayer PMMA films can be used as resists for high resolution photolithography in semiconductor industry.

Since liquid crystals have very large nonlinearity (χ^3 up to 10^{-3} esu) [8], we also studied the L-B films of liquid crystals. Mono-layer and multilayer films of E7 liquid crystals were made. The liquid crystal was dissolved in butanol and the L-B films were made at a pressure of 15 mN/m. We are currently working the measurement of nonlinear optical properties of these samples. Further investigation is being carried out on the optimization of the fabrication of the above materials, as well as other bio/molecular materials such as bacterio-rhdopsin.

Conclusions

We have comparatively studied the properties of nonlinear films with three different configurations. We have found that the quarter-wavelength thickness arrangement displays a wide gap in the visible light range. The modulated superlattice model shows some narrow gaps in the same range. The random layer thickness arrangement could open a very wide gap for strong incidence of light when more than 500 layers are used and it becomes quite transparent at weak incidence of light at the same time.

We have successfully fabricated monolayer and multilayer L-B films of dye-doped PMMA polymers and liquid crystals. Preliminary testing data show that it is possible to construct smart PBS using the L-B method.

References

1. E. Yablonovitch, Phys. Rev. Lett. 58 2059 (1987); E. Yablonovitch and T. J. Gmitter, Phys. Rev. Lett. **63**, 1950 (1989).
2. E. Yablonovitch, T. J. Gmitter, and K. M. Leung, Phys. Rev. Lett. **67**, 2295 (1991); E. Yablonovitch, T. J. Gmitter, R. D. Meade, A. M. Rappe, K. D.
3. H. O. Everitt, Optics & Photonics News, **20**, Nov. 1992.
4. P.W. Anderson, Phys. Rev. **109**, 1492 (1958). P. Sheng and Z.-Q. Zhang, Phys. Rev. Lett. **57**, 1879 (1986). K. M. Yoo and R. R. Alfano, Opt. Lett. **16**, 1823 (1991).
5. Y. Kuga and A. Ishimaru, J. Opt. Soc. Am. A**1**, 831 (1984) M. P. van Albada, M. P. Van der Mark, and A. Lagendijk, Phys. Rev. Lett. **58**, 361 (1987).
6. W. Chen and D. L. Mills, Phys. Rev. Lett. **58**, 160 (1987). W. Chen and D. L. Mills, Phys. Rev. B**36**, 6269 (1987). L. Kahn, K. Huang, and D. L. Mills, Phys. Rev. B**39**, 12449 (1989).
7. C. J. Herbert, W. S. Capinski, M. S. Malcuit, Opt. Lett., **17**, 1037, (1992).
8. I. C. Khoo, "Nonlinear optics of liquid crystals," in Progress in Optics, Vol. XXVI, edited by E. Wolf, Elsevier, (North-Holland, 1988).

Development of a Liquid Crystal Smart Reflector

Robert B. Meyer
The Martin Fisher School of Physics
Brandeis University

ABSTRACT

A smart reflector is a material which can change its optical reflectivity in response to changes in the intensity of incident light. In particular, we are working on systems that are transparent at low light intensity, and become highly reflective at high incident light intensity. Our systems are based on cholesteric liquid crystals.

We have achieved the first demonstration of a liquid crystal smart reflector, consisting of a cholesteric liquid crystal with temperature sensitive helix pitch, backed by a light absorbing dye layer. Light passing through the liquid crystal is absorbed by the dye, generating heat which raises the temperature of the liquid crystal. The resulting change in the pitch of the cholesteric causes an increase in its reflectivity, reducing the intensity of light reaching the dye layer. This negative feedback stabilizes the reflector for a given light intensity. The smart reflector thus achieves a reflectivity which increases with increasing intensity of incident light. This effect is demonstrated both in experimental measurements and in a mathematical model of the device.

We are currently studying systems with the light absorbing dye dissolved in the liquid crystal. This offers several possibilities for improvements on our initial device, including decreased response time, and even the elimination of the use of temperature changes in the device.

INTRODUCTION

A cholesteric liquid crystal (CLC) is a modification of the nematic liquid crystal in which, due to the presence of optically active molecules, the local optical axis, or director, of the nematic is twisted into a helicoidal structure. The pitch P of this helicoidal structure is often comparable to the wavelength of visible light. The optical properties of CLC's have been widely studied for many years (Chandrasekhar, 1992). One of the most interesting properties is the selective total reflection of light in a band of wavelengths centered on the pitch of the helix, a phenomenon similar to the Bragg reflection of x-rays by a periodic crystal structure. Consider light approximately normally incident on a thin layer of CLC in which the axis of the helicoidal structure is oriented normal to the plane of the layer. One circular polarization of light in the reflection band, which matches the sense of rotation of the helix, will be totally reflected as a circularly polarized beam of the same sense, while the opposite circularly polarized component of the incident will be transmitted by the CLC.

The spectral width $\Delta\lambda$ of the total reflection band is given approximately by the de Vries equation (de Vries, 1951):

$$\Delta\lambda = P\delta n \tag{1}$$

Δn is the birefringence of the CLC, the difference between the indices of refraction parallel and perpendicular to the local nematic director. This reflection band can be typically a few tens of nanometers in width. Its finite width arises from the strong interaction of light with the periodic dielectric structure of the cholesteric, in analogy with the finite band gap for electrons propagating in a semiconductor. The basic physics of this effect has been well studied in both theory and experiment (de Vries, 1951; Chandrasakhar, Ranganath and Surech, 173; Dreher, Meier and Saupe, 1971).

The second interesting property of a CLC which we utilize in this device is the strong temperature dependence of the pitch of its helicoidal structure near the phase transition from the cholesteric phase to the smectic A phase. As temperature T is lowered toward the transition temperature T_{AC}, the pitch diverges toward infinity, with a power law dependence, $P \propto (T - T_{AC})^{-0.67}$ (Pindak, Huang and Ho, 1974). In some materials, this means that the pitch can change from the ultraviolet to the infrared in a range as small as one degree Celsius. The resulting dramatic color change finds application in the well known liquid crystal thermometers and mood rings.

Our smart reflector consists of a thin oriented layer of CLC with a highly temperature dependent helix pitch, backed by a layer containing a light absorbing dye, as illustrated in Fig. 1. The device works in the following way. At ambient temperature, the liquid crystal is in the smectic A phase, and incident light passes through it to the absorbing dye layer, where the light is converted to heat. This raises the temperature of the liquid crystal, converting it to the cholesteric phase, and the pitch of the helicoidal structure of the CLC is initially in the infrared. With further heating, the pitch grows shorter, until the reflection band of the CLC begins to reflect part of the incident light. The resulting reduction of optical power reaching the absorbing layer constitutes a negative feedback mechanism, controlling the temperature of the CLC and allowing just enough light to reach the absorbing layer to maintain the device at its correct operating temperature. Any increase in light intensity results in a compensating increase in temperature and reflectivity, and conversely, any decrease in incident light intensity results in a corresponding decrease in temperature and reflectivity.

In our initial experiments, we limit ourselves to the most favorable conditions, by using monochromatic light of the correct circular polarization, from an Argon ion laser. We have carried out a series of experiments varying the ambient temperature of the reflector and the intensity of the laser beam to demonstrate the intensity dependent change of reflectivity of the device. Moreover, we have constructed a mathematical model of the device with which we can compare theory to experimental results.

We first present the model calculations to give a cleared picture of the details of operation of the device.

MODEL CALCULATIONS

The exact solution of the wave equation for the propagation of light along the helical axis of a CLC was presented by Mauguin, Oseen and de Vries (Mauguin, 1911; Oseen, 1933; and de Vries, 1951). Nityananda and Kini (Nityananda and Kini, 1973) applied this theory and used continuity at the boundary to get the reflectivity when a

CLC is sandwiched between two isotropic media. Berreman (Berreman, 1972) used a 4×4-matrix formulation to solve the transmission problem numerically, and Hajdo and Eringen (Hajdo and Eringen, 1979) proposed a multilayer model to explain the effect of a pitch gradient in the CLC on the reflectivity.

The reflectivity of a CLC for light of wavelength 0.5 μm, as a function of nP, the mean index of refraction times the pitch of the helix, is shown in Fig. 2. We plot long pitch at the left for comparison with experiments below. Notice the steeply rising reflectivity and the total reflection band of finite width, as indicated by the de Vries formula given earlier. The negative feedback mechanism of our device is active on the steeply rising part of this spectrum.

A full model of the device requires the interaction of three variables within the CLC layer: the light intensity, the temperature, and the helix pitch, as functions of distance, from the front to the back of the layer. Light enters the front of the layer, and part of it is transmitted. The light reaching the back of the layer is absorbed and converted to heat. This heat source raises the average temperature of the CLC, and also creates a temperature gradient that conducts heat back to the front of the CLC layer. The temperature change and gradient produce corresponding changes in the mean pitch and a pitch gradient in the helicoidal structure of the CLC. This change in pitch structure changes the transmission of light through the CLC layer. For a CLC in which dP/dT, the change of pitch with temperature, is negative, when operating on the long pitch side of the reflectivity spectrum shown in Fig. 2, this produces a negative feedback, which leads to a stable equilibrium among the three variables in the CLC layer. This is summarized by the equation

$$tW = KA \frac{\Delta T}{\Delta x} \tag{2}$$

in which there is a temperature difference ΔT across the sample of thickness Δx, with area A, characterized by thermal conductivity K, and optical power transmission coefficient t, illuminated by laser power W.

In our model, we assume for simplicity a constant negative dP/dT. We fix the temperature at the front of the CLC layer at the ambient level. Then for a given temperature gradient, we calculate the pitch structure and the optical transmission coefficient of the CLC layer, using the multilayer model to account for the effects of the pitch gradient. From Eq. 2, we then know what incident laser power is required to maintain this temperature gradient. In Fig. 2, we show two curves for the reflectivity of the device at higher power levels, as a function of the pitch of the CLC at the ambient temperature at the front of the CLC layer. As optical power W is increased, the pitch at the back of the CLC layer decreases, due to increased temperature at the back, and the reflection coefficient increases. Note that when the pitch at the front of the CLC is such that the reflection coefficient there is nearly 100%, the relative increase in reflectivity is smaller, since very little light is transmitted in any case. This means that the point at which the reflection coefficient goes to 100% does not shift to longer pitch values. Rather, the reflectivity at longer pitch values increases with increasing power. This is precisely the effect desired for the smart reflector. Notice that on the short pitch side of the reflectivity curves, where the feedback effect is positive, rather than negative, the reflectivity of the CLC decreases with increasing incident light power. This makes the device unstable,

and for a smart reflector, operation in this region must be avoided.

EXPERIMENTS

In our experiments, the choice of the CLC was crucial. It had to have a T_{AC} above room temperature, a large birefringence to give a large reflectivity, and a pitch that varied from the infrared to the ultraviolet in a small temperature range. We used a mixture of the nematics K24 and K30 (EM Chemicals) to get the correct T_{AC} (Gray and Mosley, 1976). We used these materials for their high birefringence ($\Delta n \sim 0.2$). Three chiral dopants, R1011, R811, and CB15 (EM Chemicals) were used to achieve a short enough high temperature pitch. The dopants tend to lower T_{AC}, and each dopant has only a limited solubility in the nematic mixture. This is why we were led to this rather complex composition, in which the three dopants, all with right handed twisting power, work together to reduce the pitch of the CLC to the proper range. The resulting pitch of the CLC as a function of temperature is shown in Fig. 3.

The CLC was sandwiched between two glass substrates separated by a 19μm Mylar spacer. One substrate was coated with polyimide and the other with an orange dye, covered with a layer of UV cured Norland optical adhesive, to isolate it chemically from the CLC layer. Both substrates were then rubbed to induce homogeneous alignment of the CLC molecules at the surface. This helps keep the helix oriented with its pitch axis normal to the plane of the device, which is necessary for achieving high reflectivity. The device was placed in a temperature controlled oven to set the ambient temperature, determining the pitch of the helical structure in the absence of incident optical power.

An argon ion laser (Spectra Physics model 165) with linear polarizer and quarter wave plate, produced an intense circularly polarized light source. We used a power meter to monitor the reflected light intensity from the device at near normal incidence.

Results of our experiments are shown in Fig. 4. We plot reflection coefficient as function of the ambient temperature of the device. This is qualitatively similar to the plots of reflectivity *vs.* helix pitch in Fig. 2, for the model calculations, since pitch decreases with increasing temperature. At the lowest power, the reflection coefficient is essentially that of the CLC with no heating or feedback effect. As power is raised, the reflection coefficient on the low temperature side of the curves increases, just as seen in the model calculations. On the high temperature side, the reflection coefficient at high power drops suddenly below its low power level, indicating the positive feedback that makes the device unstable in this region.

In Fig. 5, we show the increase of reflectivity with power at constant ambient temperature, the essential desired behavior for the smart reflector.

Comparing the experiments with the model calculations, we see several significant differences. First, the reflection coefficient never reaches 100%. This is because the CLC layer is not perfect. There are many disclinations distributed through the CLC layer that scatter light, so the reflection coefficient is less than one in the plateau region of the curves in Fig. 4. Part of the scattered light is back scattered, but some of it is forward scattered, so it reaches the absorbing layer and generates heat, even in the plateau region. This means that the feedback effect does not go to zero at the beginning

of the plateau region, so the beginning of the plateau shifts to lower temperature at high power. This could not happen in the model calculations. Moreover, as temperature is increased, for high incident power, the sample overheats due to transmitted light, even in the plateau region. This results in a sudden drop in the reflection coefficient at some point in the plateau region, as the positive feedback effect drives the sample to higher temperature. This effect is made more evident because the laser power can increase the temperature of the whole CLC layer, rather than just creating a temperature gradient. In the model calculations, the temperature at the front surface of the CLC layer was held at the ambient level, making it more stable than the real device.

CURRENT AND FUTURE STUDIES

There are a number of issues beyond the initial demonstration of the smart reflector that we are pursuing. Before discussing them, let me note that in a related project funded by the DOE, smart reflectors for use as smart windows to control solar radiation were studies, with the resulting demonstration of broad band smart reflectors, potentially covering the whole visible spectrum. These devices were fabricated with several layers of liquid crystal with different reflection bands to cover the visible spectrum.

To achieve faster response times and simpler fabrication, we are studying the incorporation of the light absorbing dye into the liquid crystal layer. We are performing both mathematical simulations of this system and experiments. There is a fundamental question of stability in this sytem; because the reflection process occurs in a finite thickness layer of the liquid crystal, there is also of necessity some absorbtion of light by the dye in that layer, even in the most reflective state of the system. This could cause the sytem to overheat. We are trying to determine the stability of the system in our simulations.

As a much more basic modification of the system we have been studying, we are trying to use dye dissolved in the liquid crystal layer to eliminate the thermal step in the response of the smart reflector. Upon absorbtion of light, certain dyes change their molecular structure. This change of molecular structure can affect the packing of the molecules in the cholesteric liquid crystal in such a way that it changes the pitch of the cholesteric helix. We are studying the interaction of dyes with liquid crystals in an effort to utilize this effect in the smart reflector. If we can demonstrate a smart reflector in which the change of reflectivity is directly coupled to changes in light intensity, rather than through temperature changes, this would be a major achievement. It would make the device temperature insensitive, and could improve response time as well.

REFERENCES

Berreman, D.W. 1972. J. Opt. Soc. Am., 69:502.

Chandrasekhar, S., G.S. Ranganath, and K.A. Surech, 1973. Proceedings of the International Liquid Crystals Conference, Bangalore, Pramana Supplement I:341.

Chandrasekhar, S. 1992. Liquid Crystals, 2nd ed. (Cambridge University Press, Cambridge).

de Vries, H. 1951. Acta Cryst. 4:219.

Drehar, R., G. Meier and A. Saupe, 1971. Mol. Liq. Cryst. 13:17.

Gray, G.W. and A. Mosley, 1976. J.C.S. Chem. Comm. 147.

Hajdo, L.E. and A.C. Eringen, 1979. J. Opt. Soc. Am. 69:1017.

Mauguin, M.C. 1911. Bull. Soc. Franc. Miner. Cryst. 34:71.

Nityanada, R. and U.D. Kini, 1973. Proceedings of the International Liquid Crystals Conference, Bangalore, Pramana Supplement I:311.

Oseen, C.W. 1933. Trans. Faraday Soc. 29:883.

Pindak, R.S., C.C. Huang, and J.T. Ho, 1974. Phys. Rev. Lett. 32:43.

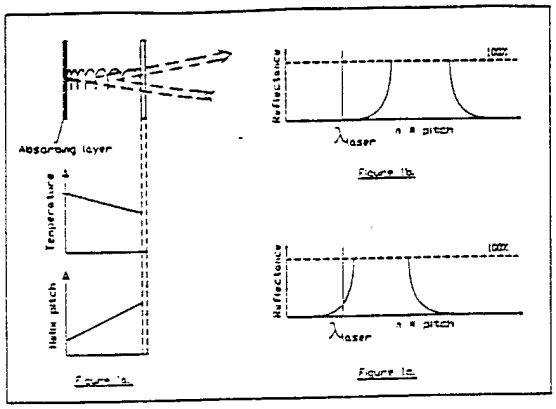

Figure 1: Schematic description of the smart reflector. a) In the feedback control mode, light enters from the right, and part of it reaches the absorbing layer, generating heat. This creates temperature and helix pitch gradients in the CLC layer. The reduced helix pitch results in increased reflectivity. b) At low light intensity the helix pitch is too long to reflect the laser beam. c) In the control mode, the laser beam is partially reflected.

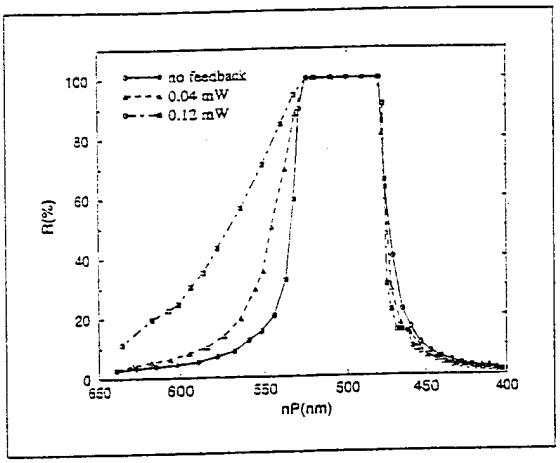

Figure 2: Calculated reflectivity R of the model system as a function of refractive index n times ambient helix pitch P, for three incident laser powers.

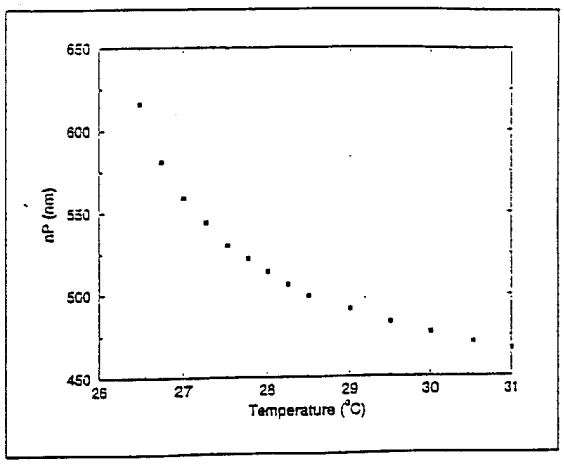

Figure 3: Temperature dependence of the helix pitch P times index of refraction n for the CLC used in our device.

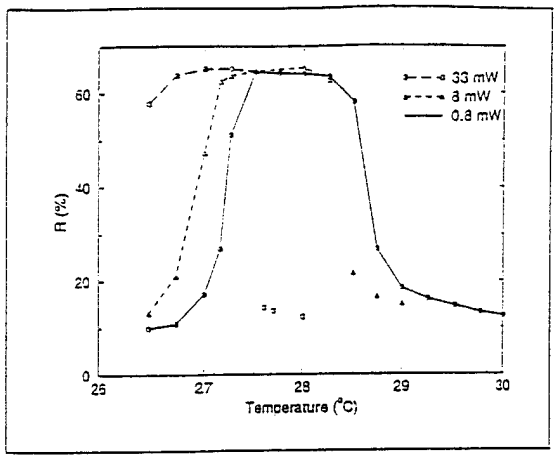

Figure 4: Reflectivity of our device as a function of ambient temperature for three incident laser powers.

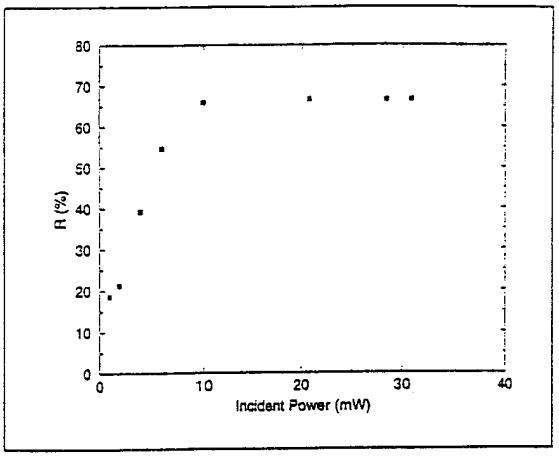

Figure 5: Reflectivity of our device as a function of laser power at an ambient temperature of 27°C.

ABSTRACT

SMART MATERIALS: THE CONCEPT AND REALITY

Richard A. Pethrick
Department of Pure and Applied Chemistry
Thomas Graham Building
University of Strathclyde
Cathedral Street, Glascow G43 2QQ, Scotland

The concept of smart materials will be discussed in a general manner and some of the current activities in Europe and Japan will be used to illustrate the lecture. The idea of smart structures will be introduced and discussed in the context of a high rise building with seismic control. The material issues will be discussed with particular reference to civil engineering projects. Topics considered will include use of shaped memory alloy in ventilation controls, smart windows and monitoring civil engineering structures. The method of making glass reinforced concrete structures smart will be described. Methods of generating self healing alloys for use in high vacuum applications will be considered together with the development of noise damping metallic structures. Other materials concepts will be reviewed; micro activators, fullerenes, conducting polymers, biosensors, smart rope. Thus use of dielectric relaxation techniques to monitor and control the phase separation and cure of thermoplastic modified thermosets will be reviewed if there is time. The future of smart materials development will be briefly reviewed.

Static and Mobile Polymer Surfaces of Well Defined Structrure

William J. Brittain, Wayne L. Mattice and Mark D. Foster
The Department of Polymer Science, The University of Akron
August 16, 1994

INTRODUCTION

A major objective of this research program is to create a "smart" coating with reversible absorptive capacity for biological agents (e.g., proteins). An organic thin film has been synthesized that contains a photoresponsive group (azobenzene). This photoresponsive group induces changes in the thickness and wettability of the surface depending on whether the surface is exposed to visible or ultraviolet light. Wettability is directly tied to the affinity of the surface for biological agents and other surface active agents. The change in wettability is reversible so that biomolecules can be adsorbed and later removed by adjusting the wavelength of light. This concept is illustrated below in Figure 1. Our approach has involved three major components: synthesis of self-assembled monolayers (SAMs) containing azobenzene, development of new experimental methodology for measuring protein adsorption to SAMs, and molecular dynamics simulations of SAMs to aid the interpretation of experimental results.

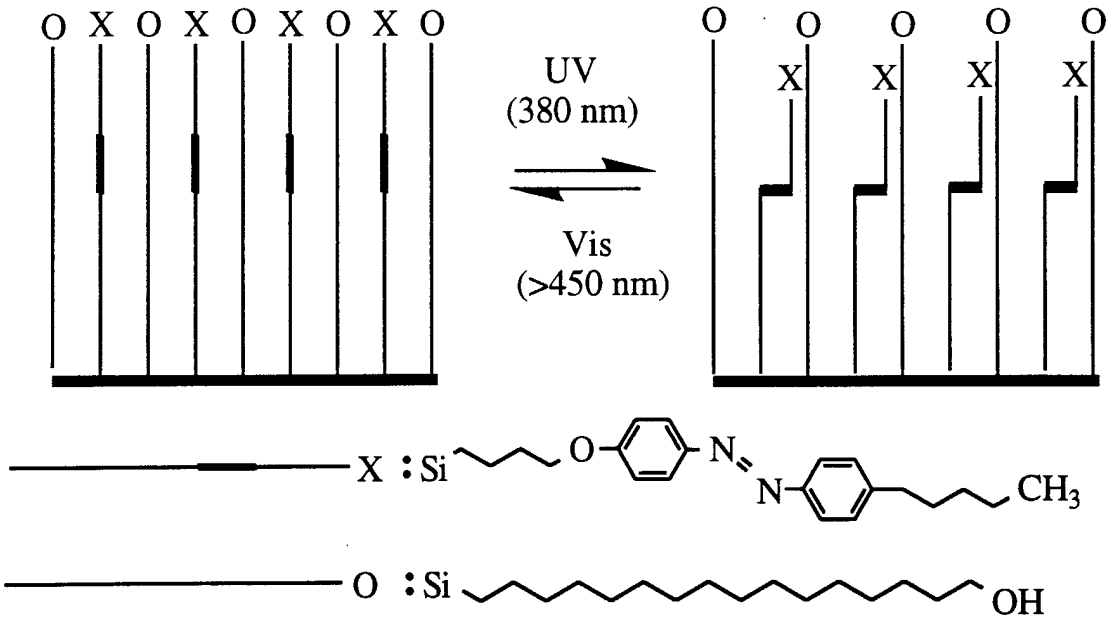

Figure 1. Principle: irradiation will reversibly alter the composition at the surface which will control wettability and adsorption.

RESULTS

Synthesis of Photoactive Thin Films

Three different synthetic routes are being explored for the preparation of SAMs containing azobenzene. The first involves chemisorption of the alkyltrichlorosilane-**1**. The synthesis of **1** is straightforward except for purification of the final product. The reaction mixture from the last step had to be used "as is". Monolayers were prepared on clean silicon or quartz

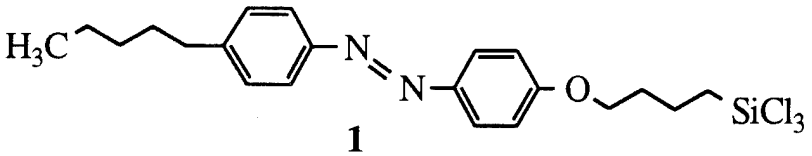

1

substrates. Attenuated total reflectance IR spectroscopy indicated that the alkyl chain and aromatic rings have similar orientations with axes tilted by 15-20° to the surface normal. The X-ray photoelectron spectrum of the SAMs derived from **1** contained a peak corresponding to the nitrogen 1s ionization at 399 eV. Monolayers were also prepared on quartz slides to study the electronic spectra of the azobenzene chromophore. The UV-vis spectrum contains an absorption at λ_{max} = 366 nm which corresponds to the π-π^* transition. Preliminary photoisomerization reactions have been followed using water contact angles. We found that the advancing water contact angle of monolayers prepared from **1** before isomerization was 76 ± 1°. After exposure to UV light for 30 minutes, the contact angle decreased to 72 ± 1°. Thus the wettability of the monolayers increased upon isomerization of the azobenzene moiety. These results are similar to those of related work in the literature. Currently, we are using X-ray reflectometry to study the changes in film thickness upon photoisomerization.

The disadvantage of the trichlorosilane deposition is the difficulty in making high purity silane-**1**. Thus, we have been investigating two alternative routes to azobenzene SAMs. The first is a coupling reaction of an amino-functionalized SAM with compound **2**. The final monolayer contains azobenzene chains coupled to the surface via amide bonds. Preliminary work on this method has indicated that the coupling reaction of the acid chloride-**2** to the amine-functionalized surface is not quantitative and leads to disordered monolayers.

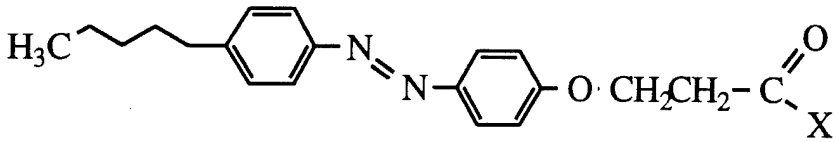

2: X=Cl
3: X=OH

A third approach to an azobenzene SAMs involves reactions with surfaces modified with Cl_3Si-$Co(CO)_4$. We have used this synthetic approach

with compound **3** to prepare azobenzene monolayers. Mirkin and co-workers have established the number density of cobalt sites generated in this method. Assuming quantitative reaction with compounds like **3** allows us to predict molecular surface coverage. Information concerning the number density of azobenzene moieties is important input for the molecular dynamics calculations.

The above discussion has focused on the preparation of monolayers composed entirely of methyl-terminated azobenzene chains. Concurrently, we are developing strategies for making two-chain systems where the chains that do not contain azobenzene will be terminated by a hydrophilic endgroup like hydroxy or amine. Regardless of the deposition technique, the strategy is similar, that is, chemisorption using a solution of both surface-reactive reagents. Depending on the mole ratio of the two reagents, different surface concentrations of azobenzene moieties can be prepared.

Protein Adsorption onto Functionalized Surfaces

A new experimental methodology based on neutron and X-ray reflectometries (NR, XR) has been developed for monitoring *in situ* the adsorption of proteins from solution onto functionalized self-assembled monolayers. X-ray reflectometry measurements in air of the uncoated silicon substrates and subsequently the SAMs after deposition provides precise characterization of the surface topology and layer structure before adsorption. Protein is adsorbed from solution in a sample cell constructed from the 0.5 inch thick silicon substrate and a shallow Teflon® trough, which allows a neutron beam to reflect from the solution/SAM interface on the substrate side. Spectra presenting the reflectivity's variation with scattering vector, q ($Å^{-1}$) provide unrivaled detail of the protein concentration profile to a depth of at least 100 nm in the solution. Measurements of this sort are being used to probe the variation in protein adsorption with changes in surface functionality.

Measurements show that the widely studied protein, Human Serum Albumin (HSA), adsorbs from buffered (pH = 7.0) D_20 solutions onto both methyl and amide terminated surfaces in the concentration range between 0.005 and 0.1% HSA with the amount adsorbed increasing as protein concentration is increased. At the lowest solution concentration studied, 0.0001%, the adsorption to a methyl terminated SAM is imperceptible. XR measurements on adsorbed layers dried after removal from contact with solution provide corroborating information on amount adsorbed and layer thickness. They also providing a point of comparison with established methodologies that quantify adsorption by measuring dried layers.

NR data for the adsorption from 0.1% buffered D_2O solutions to both types of surfaces may be explained by concentration profiles containing two parts, as shown in Figure 2. The first is a region adjacent to the

SAM of roughly 40Å thickness in which the mass fraction of HSA exceeds 0.17. The second is a more diffuse region in which the concentration falls gradually to the bulk value. For the methyl terminated surface, the concentrated region is slightly thinner (35Å) and the outer portion of profile is higher in concentration and substantially thicker (ca. 140Å). The interfacial excess of protein is thus much larger in the case of methyl termination.

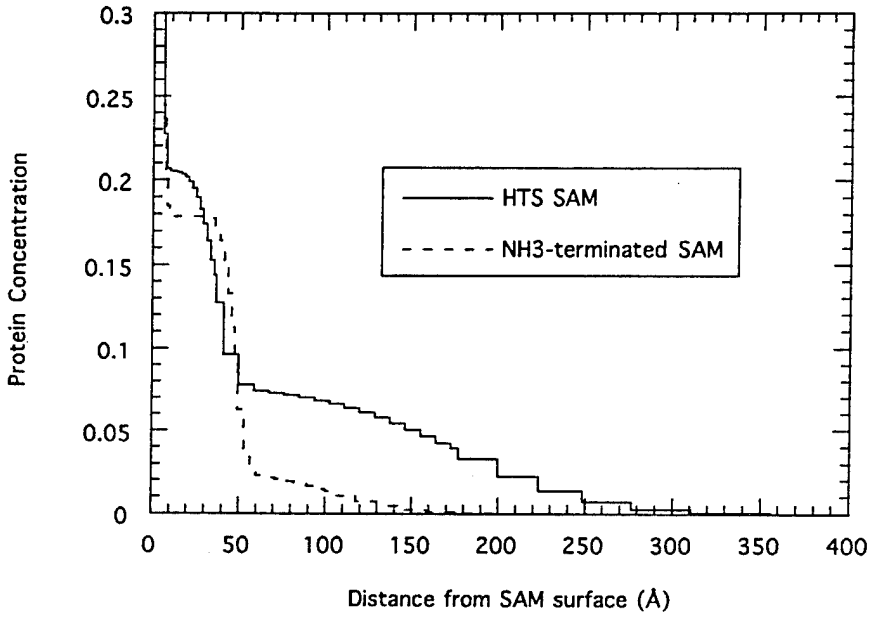

Figure 2. HSA concentration in mass fraction as a function of distance from the functionalized SAM surface. The interfacial excess is considerably higher for the methyl terminated surface.

Molecular Dynamics Simulations

Fully atomistic simulations of the conformation and dynamics have been performed for self-assembled monolayers composed of alkylsiloxanes in which the tails are $-(CH_2)_{16}-OH$ (Zhan, Y.; Mattice, W. L. Langmuir, submitted 7/1/94). These simulations have been performed at 300 K, at a surface density of one chain per 21 $Å^2$, using different patterns of attachment to the surface that are consistent with this surface density.

They demonstrate that several properties of interest (including the tilt angle and average thickness) are not determined by the surface density alone, but are also affected by the pattern of attachment of the siloxane head groups to the surface. For example, the range for the tilt angle is 5-19 degrees, which seems to include the likely experimental range.

Other properties of interest (including the fraction of the bonds in the tails that populate gauche states, the magnitude of the fluctuations of the torsion angles within the preferred trans rotational isomeric state, and the mosaic formed by the hydroxyl groups at the free surface) are much less

sensitive to the pattern of attachment of the head groups. The fraction of bonds in gauche states is about 0.02, with the gauche defects very strongly segregated toward the free ends of the tails. The fluctuation of the torsion angles within trans states is about 9 degrees, which is similar to the fluctuation obtained previously for a long *n*-alkane in another severely constrained environment (*n*-tetracontane in its inclusion compound with perhydrotriphenylene, Zhan, Y.; Mattice, W. L. Macromolecules 1992, 25, 4078.) The hydroxyl groups at the free ends have a radius of movement of about 3 Å, which is sufficient to produce a mosaic of these groups that is nearly independent of the details of the attachment of the siloxane head groups to the surface, so long as the density of their attachment remains at one chain per 21 $Å^2$.

In summary, these simulations with systems in which the tails are $-(CH_2)_{\{16\}}-OH$ are helpful in separating properties of the self-assembled monolayer that may be determined by the surface density alone from other properties which depend on the pattern of the attachment as well as the surface density.

LIST OF ACCOMPLISHMENTS

- Synthesis of an azobenzene-containing monolayers via trichlorosilane chemisorption.
- Observation of reversible wettability for azobenzene monolayer.
- First ever *in situ* measurement of protein adsorption concentration profile with ca. 20Å resolution using neutron reflectometry.
- Quantified differences in form of profile as well as interfacial excess for CH_3 and NH_2 terminated surfaces.
- Molecular dynamics simulations have been performed for hydroxy-terminated SAMs

FUTURE POSSIBILITIES

Current synthetic work is aimed at azobenzene-containing monolayers with different lengths of methylene spacers between the azobenzene and the end-groups. The choice of new spacer lengths is being guided by results of the molecular modeling. We plan to prepare different compositions of SAMs using the azobenzene chain in several different two component systems. We will address how the nature of the end-group (e.g., methyl vs. hydroxyl) and the mole fraction of the azobenzene chain affect the *trans* to *cis* isomerization. The *trans* to *cis* isomerization will be studied using X-ray reflectometry to more precisely characterize the structural changes upon irradiation. Neutron reflectometry will be used to the characterize protein adsorption to azobenzene-containing monolayers and how this changes with the wavelength of light.

The simulations are being extended to self-assembled monolayers in which azobenzene, in its *cis*- and *trans*-conformations, is incorporated into one, or several, of the chains. These simulations are being performed in two distinctly different ways: (1) under circumstances where we enforce a particular surface density and pattern of attachment of the siloxane head groups to the substrate, and (2) under circumstances where the system selects its own surface density, with the option of having that density be lower near the chain(s) that bear(s) the azobenzene. The latter method, which we anticipate may provide simulations that are more pertinent to real systems prepared in the laboratory, makes use of a flexible "net" based on interlocking eight-membered rings, cyclo(Si-O-Si-O-Si-O-Si-O), for attachment of the tails.

SMART MATERIALS BASED UPON OLIGOMERIC MOLECULES

Darrell H. Reneker, Roderic P. Quirk, and Wayne L. Mattice
The Maurice Morton Institute of Polymer Science
The University of Akron

Introduction:

Macromolecular smart materials and structures were designed and characterized. The designs were based on oligomeric modules, each of which is responsible for a particular function in the smart material, or in the structure of which it is a part. Liquid crystals and block copolymers were also characterized for potential use as modules. Computer modeling of molecular architecture and motion was used to identify oligomers that can provide useful functions in a smart molecule system. Networks of oligomers, polymers, and block co-polymers with well defined structures were identified and synthesized. Functional groups at specific locations were used to create the networks. Molecular scale assemblies were attached to mica or graphite and observed by atomic force microscopy or scanning tunneling microscopy. Rubbery networks containing strain sensitive chromophores were characterized by optical spectroscopy.

Functions performed by the various oligomers that were examined include attachment of the oligomer to a graphite or mica surface, incorporation of a chromophore into an elastomeric network, piezochromic effects, formation of bonds that can be broken predictably by forces that do not break the backbone chain, and maintenance of a force transmitting connection between a reinforcing fiber and the polymer matrix in the presence of high strain.

Potential applications of the results of this project include health monitoring of composite structures such as aircraft and land vehicles. This work is an example of the design of materials, based on oligomers, that are sensitive to strain, stress, incident photons, certain small molecules, electric fields, or hydrostatic pressure in networks and can be combined with structures that provide other smart material functions such as signal transmission, signal processing, or actuation of useful changes.

Strain sensitive smart material:

We successfully designed, synthesized and tested a smart material that preserves a record of the maximum amount of mechanical strain that the material has ever experienced.[1,2]

This smart material combines a strain sensitive chromophore (cis-azobenzene), a nylon based system of hydrogen bonds that latch the azobenzene in the cis form, and attachments to a polyurethane elastomer to apply stress to the ends of the nylon segments. The force breaks the hydrogen bonds and helps the azobenzene to transform to the trans conformation, which has a strong ultraviolet absorption band.

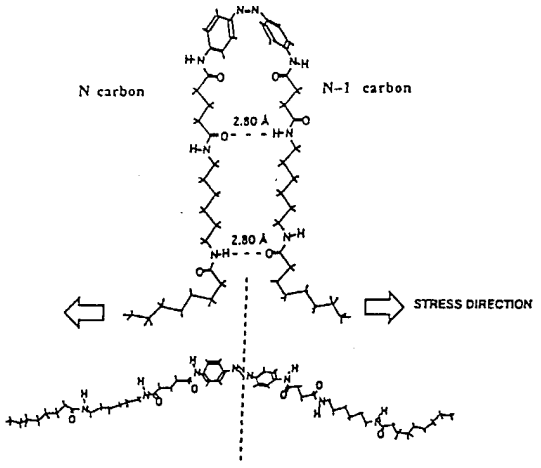

Figure 1. Strain sensitive smart molecule, before stretching (top), and at the maximum stretch (bottom).

Figure 1 shows the structure of the molecule and, in a schematic way, its behavior. Figure 2 shows the increase in the number of trans-azobenzene molecules as the material is stretched three times to 100% elongation and relaxed, then stretched three times to 200% and relaxed and finally stretched three times to 300% and relaxed. The increase in the number of trans-azobenzene molecules in successive stretches was relatively small until the strain exceeded the previous maximum strain, and then many cis-azobenzenes were transformed. The material was recycled to a state with mostly cis-azobenzenes by heating to about 100 C and irradiating with ultraviolet light. It then responded to a second cycle of stretching in essentially the same way as it did to the first. No primary bonds are broken in the material. Its ultimate load bearing capacity is not affected by repeated cycles of use.

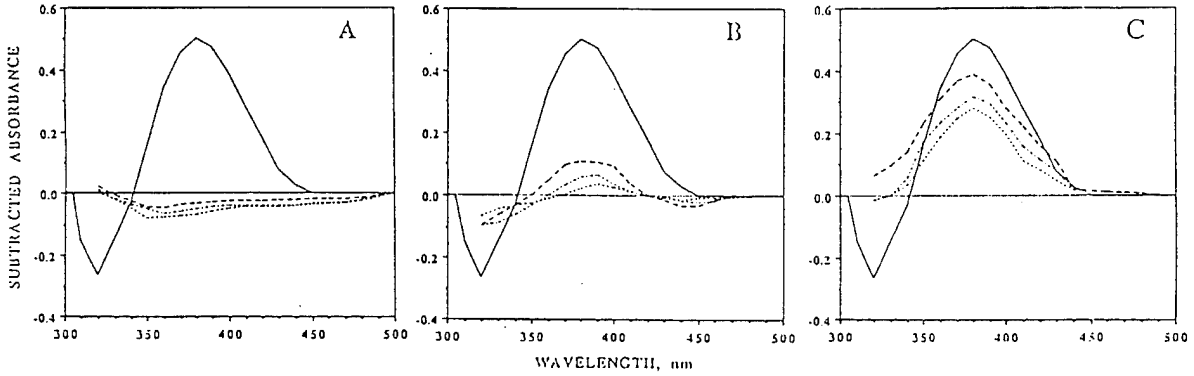

Figure 2. Increase in the number of trans bonds caused by 3 successive stretches to (A) 100%; (B) 200%, (C) 300% elongation.

These results demonstrate the use of the hydrogen bonds on a polymer as weak links to latch a molecule in a desired conformational state. The use of an elastomer network (in this example, polyurethane) as a "test bed" to apply forces along the chain axis is likely to be useful in a number of other investigations of the response of molecules to tensile forces applied through chemical bonds.

Smart materials based on polydiacetylene segmented block copolymers: Polyurethane segmented block copolymers were prepared using polydiacetylene hard segments and polybutadiene soft segments. The soft phase segments were formed by the reaction of well-defined hydroxy- and dihydroxy-functionalized polybutadienes with two equivalents of 4,4'-methylene bis(phenylisocyanate) (MDI) to form the corresponding telechelic isocyanate-functionalized polybutadienes. The segmented polyurethanes were prepared by coupling this telechelic di-isocyanate with the diacetylene, 2,4-hexadiyne-1,6-diol. The resulting segmented block copolymers undergo cross-polymerization of the diacetylene units to form a blue-colored polydiacetylene hard phase upon either heating or photolysis. The sensitivity to heat could be utilized as a sensor, since cross-polymerization of the initially formed, colorless segmented polyurethane to form a blue polymer occurs upon heating. The color of these materials is dependent on the conjugation length of the polydiacetylene, which, can be changed by heating or application of stress after cross-polymerization. This segmented polymer also undergoes reversible thermochromic shifts when heated below 180 C, and an irreversible color change from blue to red upon heating above 180 C. Wide-angle X-ray scattering analysis indicates that the polydiacetylene phase crystalline peaks at a Bragg angle of 9.3 degrees are lost at 180 C. A considerable range of application as thermochromic sensors is provided by the initially formed polymer (colorless), and the cross-polymerized polymer (blue) and the polymer heated above 180 C (red).

The mechanochromic properties of a cross-polymerized segmented block copolymer were investigated by elongation of the samples in the sample compartment of a UV-visible spectrophotometer. The absorption maximum shifted reversibly to shorter wavelengths upon elongation. These segmented polyurethane block copolymers based on a polybutadiene soft phase and a polydiacetylene hard phase have potential as useful thermochromic and mechanochromic sensors. The stress-strain properties of these polymers can be varied systematically by changing the molecular weight of the rubbery block and also by varying the proportion of the hard phase.

Molecular Dynamics calculations:
Molecular dynamics methods were used to model the photoinduced trans-cis isomerization of stilbene in a polybutadiene oligomer. The presence of the attached polybutadiene increases the activation energy of the transition. The changes in the positions of the atoms in the polybutadiene chains caused by the transition extend about 2 nm from the stilbene. It is likely that a relatively simple functional expression of the average changes in position can be obtained and the parameters in the function determined from the results of the molecular dynamics calculation. This analysis provides information of the type needed to predict the "reset", or "initialization" behavior of a smart molecule in which the cis form of a stilbene is created by UV irradiation.

We have published the descriptions of fully atomistic models for amorphous polybutadiene with four microstructures: 1,4-cis,[3] 1,4-trans,[4] vinyl, and a mixed structure composed of 55% trans, 35% cis, and 10% vinyl, all at a density of 0.89 g/cm^3. Figure 3 depicts the arrangement of the chains in one of these models. We have analyzed the manner in which the distribution of free volume depends on the microstructure,[5] and are currently studying the molecular dynamics of the amorphous systems at bulk density.[6,7,8] These models can be analyzed to investigate the storage of strain energy in the elastomer, and the transmission of forces through the elastomer for real polymer molecules. This information is needed to optimize the choice of length and molecular nature of the elastomer.

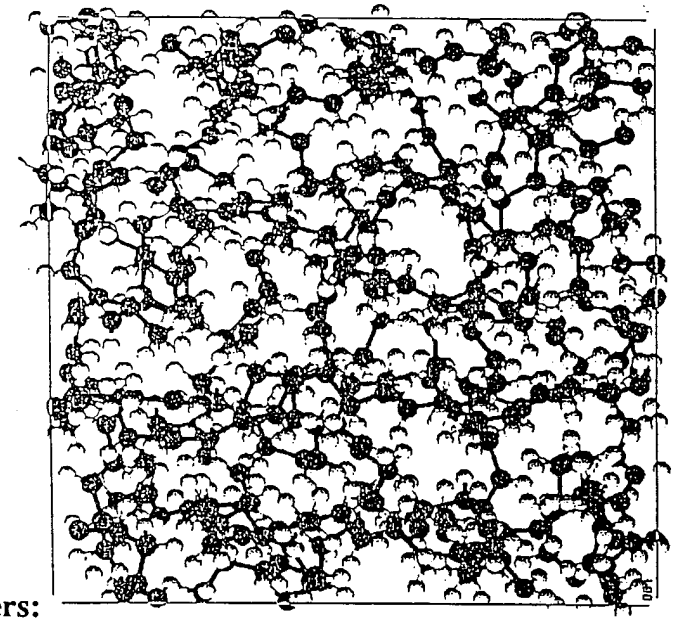

Figure 3. An image of a calculated arrangement of a polybutadiene molecule at a density of 0.89 g/cm^3. The edge of the box is about 2.1 nm long.[9]

Microphase separation in block copolymers:
One of the most important larger scale organizations of synthetic polymers is the separation of the different blocks into separate phases. Block copolymers are used as the basis for moldable elastomers in which a rigid phase serves as crosslinks between elastomeric molecules, memory materials such as heat shrinkable tubing, and for compatibilization of polymer blends. These commercial applications of block copolymers can be viewed as important steps toward the creation

of smart materials. The presence of soft and hard blocks in polymer chains promotes formation of microphases with supermolecular organization as a result of selective segregation of the blocks, driven by their incompatibility. Depending upon composition, chemical structure of the blocks, molecular weight, and presence of a third component such as a selective solvent, a variety of microphase morphologies can occur.

Recently simulations have been developed in which diblock copolymers at high density are seen to spontaneously self-assemble into a variety of structures: spheres, cylinders, oriented bicontinuous double diamond (OBDD), or lamella.[10] The transition from the disordered phase to lamellae has been studied in detail in symmetric diblock copolymers,[11] and the anisotropy of the self-diffusion coefficient has been evaluated for the chains in the lamellar state.[12]

Morphology of liquid crystals and other organized molecular systems:
The surfaces of several kinds of ordered molecular systems which are candidates for use in smart material systems were examined by atomic force microscopy. Monolayer films from discotic liquid crystals showed periodic features of the ordered molecules.[13] The surface morphology of cyanine dye single crystal sheets grown on lipid monolayers was observed.[14] Langmuir-Blodgett films from ladder polyheteroarylenes,[15] from polyglutamate[16,17] and multilayer films[18] were also characterized. In many cases, the mechanical properties of the films were examined by using the atomic force tip to scrape holes in the films.

Calculation of electronic properties of distorted diacetylene and azobenzene:
Quantum mechanical calculations of the changes in the electronic states of polymer molecules were made[19,20] for molecules which were subjected to tension, to bending, or to twist which induced cis-trans isomerization of the azobenzene molecules. The relationships between the deformation and shifts in the electronic states were observed.

Attachment to carbon black or to graphite:
As a part of our study of the attachment of oligomers to graphite, we observed[21] the morphology of carbon black particles. The scanning tunneling microscope showed the greatest detail of the sufaces of the carbon black particles. Hexagonal arrays of individual carbon atoms were resolved on many of the facets of graphitized medium thermal carbon black. These morphological features had never been observed before. Other kinds of carbon black had surfaces with very complicated morphology that contained many ledges and crevices long which a polymer could lie. The transmission electron microscope showed internal structure and the scanning electron microscope showed the overall structure of the particle aggregates. The attachment of polyimides and Nylon 6/6 to graphite[22] was observed.

REFERENCES:

1. "Macromolecular smart materials and structures", D.H. Reneker, W.L. Mattice, R.P. Quirk, and S.J. Kim, *Smart Materials and Structures,* 1, 84-90, (1992).

2. S.J. Kim and D.H. Reneker , *Polymer Bulletin*, 31, 367-374 (1993).

3. Y. Li and W.L. Mattice, *Macromolecules*, 25, 1992, pp. 4942-4947.

4. "Atomistic Models of Amorphous Polybutadiene II: Poly(1,4 trans-butadiene), Poly(1,2-butadiene), and a Random Copolymer of 1,4 trans-butadiene, 1,4 cis-butadiene, and 1,2 butadiene," E.-G. Kim, S. Misra, and W.L. Mattice, *Macromolecules*, 26, 1993, pp. 3242-3431.

5. S. Misra and W.L. Mattice, *Macromolecules*, 26, 1993, pp. 7274-7281.

6. E.-G. Kim and W.L. Mattice, *Polym. Prepr.*, 33(2), (1993), 458-459. Also E.-G. Kim, Ph.D. Dissertation, University of Akron, 1993.

7. "Atomistic Models of Amorphous Polybutadiene. #. Static Free-Volume", Sanjay Misra and Wayne L. Mattice, *Macromolecules,* 26, 7274-7281 (1993).

8. "Local Chain Dynamics of Bulk Amorphous Polybutadienes: A Molecular Dynamic Study", Eung-Gun Kim and Wayne L. Mattice, *J. Chem. Phys.*, 101, 1-13 (1994)

9. Kim, E.-G.; Misra, S.; Mattice, W.L., *Macromolecules* 1993, 26, 3424-3431.

10. R. Balaji and W.L. Mattice, *Polym. Prepr.*, 33(2), 1993, 464-465. Also R. Balaji, Ph.D. Dissertation, University of Akron, 1994.

11. R. Balaji, Y. Wang, M.D. Foster, and W.L. Mattice, *Comput. Polym. Sci.*, 3, 1993, 15-22.

12. T. Haliloglu, R. Balaji, and W.L. Mattice, *Macromolecules*, in press.

13. "Atomic Force Microscopy of Ordered Monolayer Films from Discotic Liquid Crystals," V.V. Tsukruk and D.H. Reneker, *Langmuir*, 9, p. 2141-2144 (May 1993).

14. "Surface Morphology of Cyanine Dye Single Crystal Sheets Grown on Lipid Monolayers," V.V. Tuskruk, D.H. Reneker, V.N. Bliznyuk, S. Kirstein, and H. Mohwald, to be published in *Thin Solid Films*, (1994).

15. "Morphology and Molecular Ordering in Langmuir-Blodgett Films From Ladder Polyheteroarylenes," V.V. Tsukruk, V.N. Bliznyuk, and D.H. Reneker, to be published in *Thin Solid Films*, (1994).

16. "Stability and Modification of Polyglutamate Langmuir-Blodgett Bilayer Films," Vladimir V. Tsukruk, Mark D. Foster, Darrell H. Reneker, Albert Schmidt, Hong Wu, Wolfgang Knoll, *Macromolecules*, 27, 1274-1994 (1994).

17. "Morphology of Langmuir-Blodgett Films from Polyglutamate Observed by Atomic Force Microscopy," V.V. Tsukruk, M.D. Foster, D.H. Reneker, A. Schmidt, and W. Knoll, *Langmuir*, 9(12), 3538-3547, December 1993.

18. "Scanning Probe Microscopy of Organic and Polymeric Films: From Self-Assembled Monolayers to Composite Multilayers," Vladimir V. Tsukruk and Darrell H. Reneker, to be published in *Polymer*, (1994).

19. V.V. Tsukruk and D.H. Reneker, *Polymer Preprints*, 34, 312-313 (1993).

20. V.V. Tsukruk and D.H. Reneker, Ukranian Polymer Journal, to be published in Spring 1993.

21. S.J. Kim and D.H. Reneker, *Rubber Chemistry and Technology*, 66, 559 (1993).

23. S.J. Kim and D.H. Reneker, Plastics Shaping the Future, Proceedings of the 50th SPE Technical Conference (1992), pp. 246-250.

The Preparation and Study of Some Macrocyclic Polyether Substituted Poly(Iminomethylenes): Smart Polymers Having Externally Controlled Complexation Properties

William B. Euler and William Rosen
Department of Chemistry
University of Rhode Island
Kingston, RI 02881

As exemplified frequently in nature, one of the ways to design smart materials is to develop supramolecular complexes that form only under a narrow and specific set of conditions. A typical strategy is to use hydrogen-bond donors and acceptors whose geometry matches so that the optimum interaction can be obtained. Another similar approach to this strategy is to use polymers with the appropriate structure to bind to predetermined substrates. This requires controlling the polymer architecture at both the molecular and macromolecular level.

The literature suggests that the poly(iminomethylene) [PIM, also called poly(isocyanide)] family of polymers have a helical backbone, as shown below, and the result is formation of rigid rod-like molecular entities.

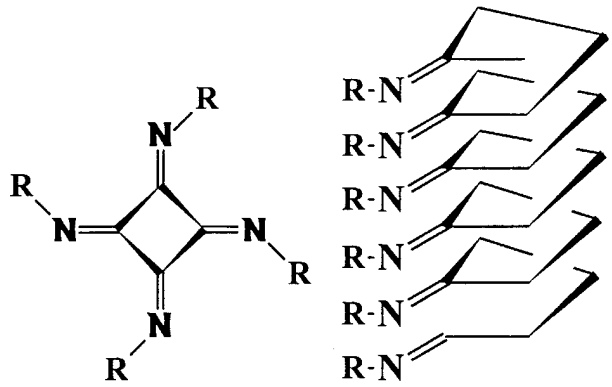

The 4/1 pitch of the helix leads to rigorously enforced stacks of R groups that can be chosen to be one portion of a supramolecular complex. The R substituent can be nearly any alkyl, aryl, or substituted alkyl group. The distance between repeat units along the stack is about 4.5-5 Å.

Our initial proposal was to use a PIM with macrocyclic polyethers (MPPIM) as the R group appended to the helical backbone. The cyclic ether could be used as a hydrogen bond acceptor with the positions and orientations of the oxygen atoms largely enforced by the polymer support. As the hydrogen bond donor we chose 4,4'-diaminodiazobenzene (DADAB) to take advantage of the photochemistry of the diazo linkage. Thus, in the *trans* conformation only a single amine group can bind to the macrocycle while in the *cis* conformation both amine groups can hydrogen bond if the geometry of the substituent groups along the stack is correct. In the *cis* conformation the amine groups are about 9 Å apart (as judged by molecular models) so that a

macrocyclic polyether placed at every other site along the stack is well situated to bind to the *cis*-DADAB. The geometry of the diazo linkage can be controlled with light. The ground state has the *trans* conformation and exposure to UV light switches this to the *cis* form. The *cis* form can be returned to the *trans* form either with visible light or thermally. We predicted that the supramolecular complex formed between the *cis*-DADAB and the macrocyclic polyether PIM would significantly slow down or prevent the thermal reaction while the photoisomerization from *cis* to *trans* would still have sufficient energy to occur, as demonstrated in the scheme shown below. If the predictions were correct, a photoaddressable switch would be realized.

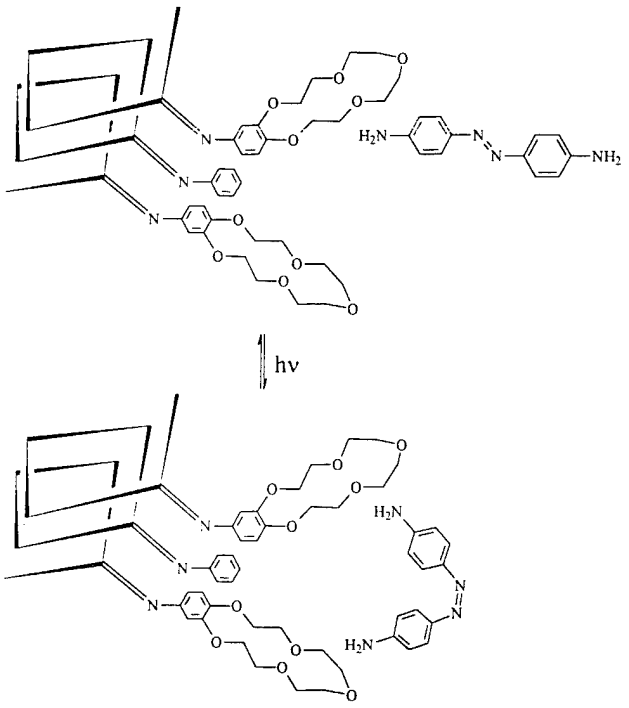

Our initial studies have been of model compounds of both oligomers and simple polymers to establish the geometric parameters necessary to prepare the appropriate MPPIM. We chose R=phenyl (φPIM) as the model since this gives a wide variety of possible substituents off of the aryl ring. We found that φPIM does not form a simple rigid rod. ^{15}N NMR on enriched samples of low molecular weight (M_n ~2000 by GPC) showed that there were three environments for the nitrogen. This is interpreted as regions of helical polymer and regions of linear polymer, of which there are two isomers. The transitions from helical to linear polymer produce regions that allow the polymer to form random coils and this is the likely overall structure for this material.

Despite the absence of a rigid rod, the MPPIM should still interact with DADAB as shown above but only at sites fully exposed to the exterior environment. To test this, we examined the photochemical and dark thermal recovery of the *cis-trans* isomerization of DADAB at both room temperature and 0 °C. In the absence of polymer, the reaction proceeds as expected: photolysis creates the *cis* state and this returns to the more stable *trans* conformation at moderate rates ($k \sim 0.8$ min^{-1} at 27 °C and $k \sim 0.2$ min^{-1} at 0 °C). Upon addition of MPPIM, the reaction

appeared to be completely repressed, i.e., no evidence of the *cis* state is found over the minutes time frame of the experiment. It is not currently known if this is due to elimination of the photo reaction or acceleration of the dark reaction.

In order to test if the observed photoeffect of the MPPIM was due to the macrocycle, a PIM with R = 3,4-dimethoxyphenyl (DMφPIM) was synthesized and coreacted with DADAB. The observed effect for DMφPIM and MPPIM were the same. However, this effect is not due to the phenyl group or the PIM backbone since addition of φPIM to DADAB has no effect on the photoreaction. Addition of THF to DADAB gives a behavior identical to MPPIM or DMjPIM while addition of water gives a similar but not identical response. Thus, it appears that the alteration of the photochemical equilibrium is due to the oxygen atoms and is not geometry specific. The somewhat different behavior of water is probably due to acid/base effects since addition of acid drastically changes the system reactivity. A detailed examination of all of these reactivity differences is in progress.

Novel Applications of Ionic Polymeric Gels As Smart Materials and Artificial Muscles

Mohsen Shahinpoor
Intelligent Materials, Structures and Systems Laboratory
School of Engineering
University of New Mexico
Albuquerque, New Mexico 87131

Extended Abstract

Presented are the results of research and development on a number of ionic polymeric gels, i.e., polyelectrolytes, in order to assess their potential applications as intelligent/smart/active materials and in particular artificial muscles. These results have been obtained during the first 16 months of a 36 months research and development effort, funded by the ARO, on novel applications of such polyelectrolytes. The ionic polymeric polyelectrolyte gels considered in our experimental efforts are, polyacrylonitrile (PAN) fibers (commercially known as *ORLAN* ™ or artificial silk) as pH-controlled muscles, and a number of electrically activated ionic polymeric gels such as polyacrylic acid plus sodium acrylate cross-linked with bisacrylamide (PAAM), poly(2-acrylamido-2-methylpropanesulfonic acid (PAMPS) and a number of chemically-doped polyacrylic acid-polyvinyl alcohol (PAA-PVA) polyelectrolyte mixtures. Described briefly are an ionic polymeric gel linear actuator made with contractile polyelectrolyte fiber bundles, a number of self-powered pH indicators, a number of encapsulated muscles to be used in active musculoskeletal structures as well as an array of fibrous muscles in various configurations. Additionally, a number of engineering models have been developed for numerical simulations of their dynamic behavior with or without solvent exudation. References [1]-[17] present detailed treatments on the subjects briefly reported in this extended abstract as well as methods of preparation of such ionic polymeric gels.

Ionic polymeric gels are three-dimensional networks of cross-linked polyelectrolyte macromolecules capable of collapsing, swelling, bending, flexing and general non-homogeneous large deformations in dynamic ionic environments. Such environments can be produced by pH changes in aqueous solutions, i.e., acidic and alkaline environments, electrodialysis or the passage of electricity in an electrolytic solvent, electrochemistry, as well as electromagnetic waves in the form of light and heat. For a partially swollen polyelectrolyte gel in an aqueous solution, fixed electrical charges (polyions) reside at some cross-links within the macromolecular network of the gel in the presence of unbound charges (counterions). The unbound ions tend to change their spatial distribution within the gel network either by combining with ions of opposite electrical charges that tend to enter the network by molecular diffusion (osmotic effects) or by electrophoretic migration towards other regions within the network. In the former case, the collapse or swelling of the gel is accompanied by solvent exudations or absorption. In the latter case, the deformation induced in the gel does not create any solvent exudation and absorption and the volume of the gel network is essentially unchanged. There are generally four forces competing within the gel network : rubber elasticity, polymer-polymer affinity, ionic Brownian motion or ionic pressure and electromagnetic. These forces collectively create a non-homogeneous osmotic pressure field within the gel network that causes the network to deform accordingly.

Katchalsky [1] and Kuhn [2] originally reported on the possibility that certain copolymers can be chemically contracted or swollen like a synthetic muscle (pH muscle) by the changing the pH of the solution containing them. Hamlen, Kent and Shafer [3] were the first to report that contraction and swelling of these gels can also be obtained electrically. In what follows, we describe briefly an ionic polymeric gel linear actuator made with contractile polyelectrolyte fiber bundles, a number of self-powered pH indicators, a number of encapsulated muscles to be used in active musculoskeletal structures as well as an array of polyacrylonitrile (PAN) fibrous muscles in various configurations.

A Spring-Loaded Ionic Polymeric Gel Actuator

Designed and prototyped is a number of linear actuators in the form of encapsulated, contractile polyelectrolyte gel fiber bundles circumscribed inside a parallel helical compression spring which is sandwiched between two flat end-caps and is filled with an electrolytic solvent (see Figures 1,2 and 3). The design is such that the helical compression spring is compressed by the contraction of the fiber bundle due to either pH or electrical changes in its environment. The helical compression spring not only acts as a source of potential energy for the reverse process of expansion of fiber bundle but also acts as one of the electrodes (anode), while the two end-caps act , collectively, as the other electrode (cathode). For a more detailed description of this actuator see references [10]-[16].

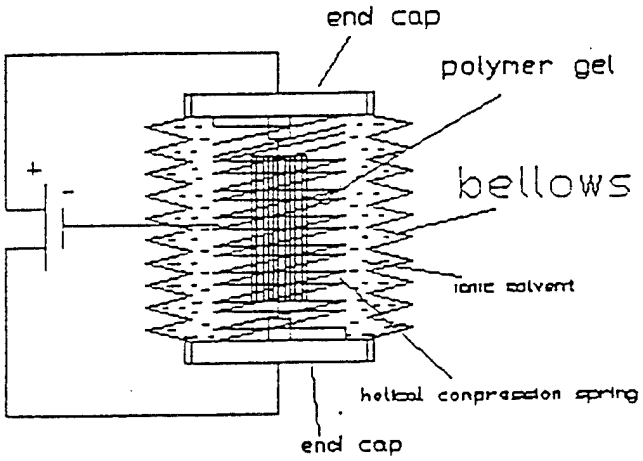

Figure 1- A schematic of the linear polymeric gel actuator

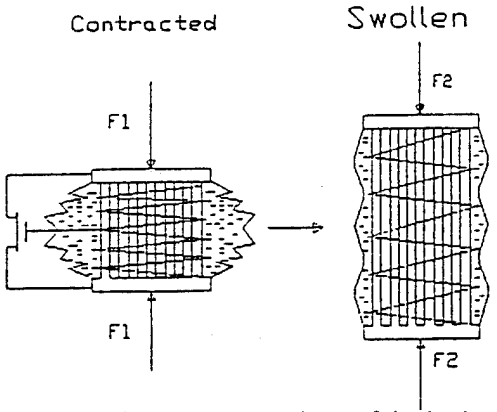

Figure 2- Modes of expansion and counterions of the ionic gel actuator

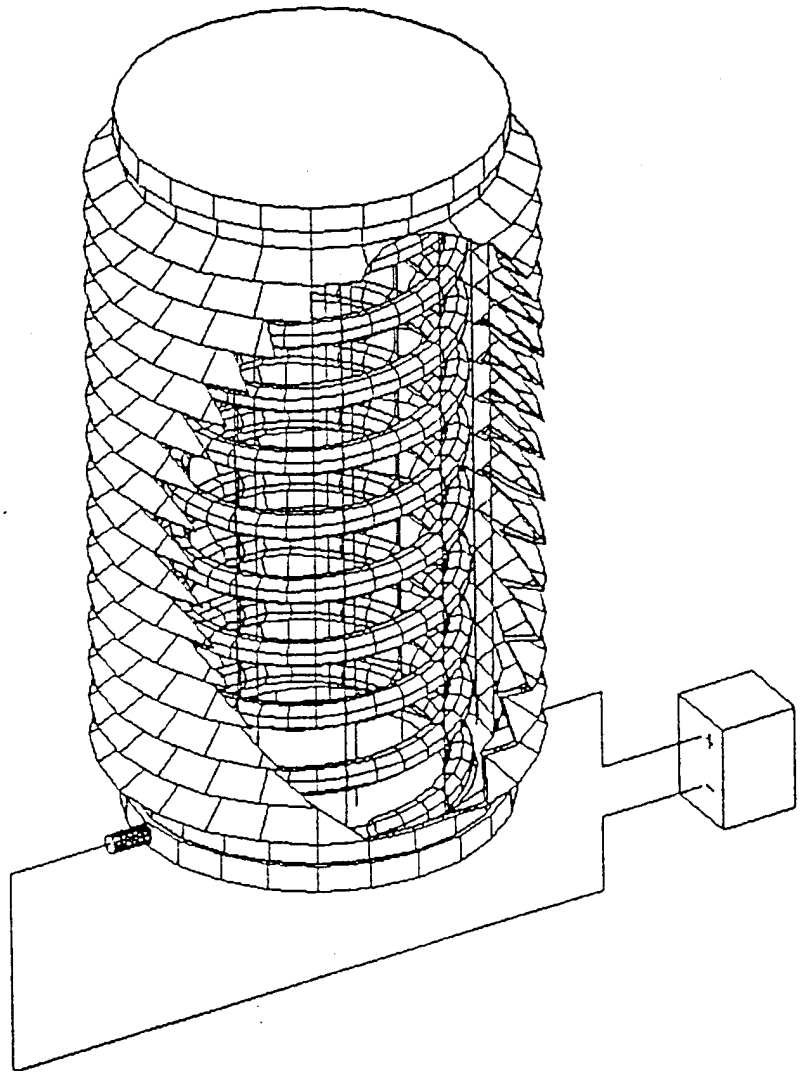

Figure 3- A cut-out view of the ionic polymeric gel actuator

Self-Powered pH Indicator Designs

A number of self-powered pH indicators have been designed and tested. The simplest version is in the form of a linear contractile fiber bundle made with a collection of polyacrylonitrile (PAN) fibers encapsulated inside an open-ended graduated glass tube which is immersed in the solution whose pH is to be determined. The contraction and expansion of the fiber bundle inside the glass case is then a measure of the pH of the solution to be tested. Two other designs have also been fabricated and tested. These newer designs are in the form of either vertical or horizontal torsional spring loaded array of PAN fibers encapsulated between a pair of co-axial and concentric glass cylinders. The inside cylinder, over whose cylindrical mantle the fibers are wrapped, is allowed to pivot about a center of rotation with a dial indicator. Depending on the pH of the solvent passing through the self-powered pH indicator, the fibers contract or expand against the resiliency of the torsional spring, thus indicating the pH of the solvent. The performance of such pH indicators have been observed to be slow compared to conventional powered pH indicators. However, the advantage of such pH indicators is that they require no external power to operate. Figure 4 displays a horizontal version of the self-powered pH indicator.

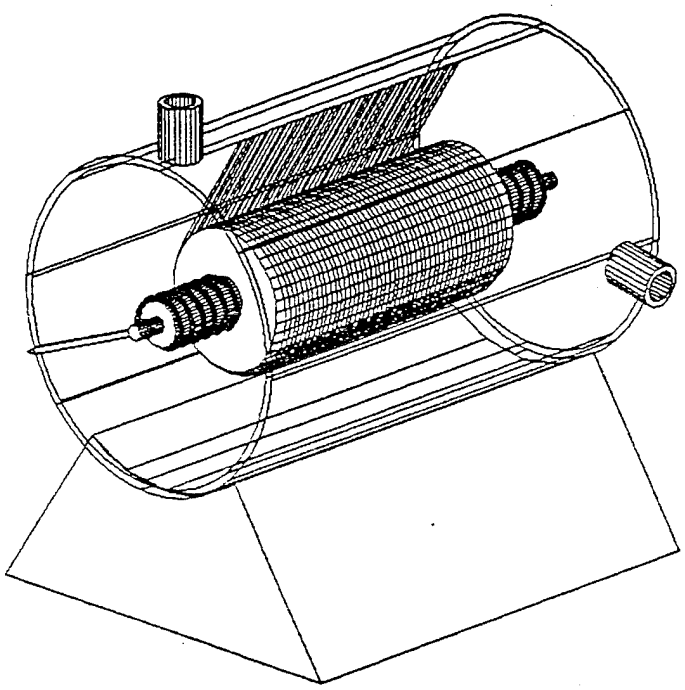

Figure 4- Horizontal version of the self-powered rotary pH indicator

Active Musculoskeletal Structures

In order to study the feasibility of equipping an individual with exoskeletal muscles for additional strength and power, a normal size human skeleton made with synthetic bones have been equipped with a central circulatory system, i.e., an artificial heart in the form of a multi-channel computer-controlled master fluid pump and a collection of solenoid pumps. In addition, a network of plastic veins connect the central circulatory system to a network of encapsulated ionic polymeric gel muscles. These muscles are generally in the form of pairs of antagonist muscles because they are essentially contractile. Thus the ionic environment in an encapsulated muscle can be modified under computer control by selective pumping of either acid, base or de-ionized water in and out of any encapsulated muscle. Figure 5 displays a simple form of such encapsulated muscles. Figure 6 and Photo 1 display the desired arm configurations under the action of bicep-tricep antagonist muscles and the skeleton (Bony) equipped with an encapsulated biceps muscle. The experimental results so far indicate that the response of encapsulated muscles are very slow due to the sluggish nature of circulation of pH solutions in and out of the encapsulated muscles. Efforts are underway to further understand the design parameters and improve dynamic performance.

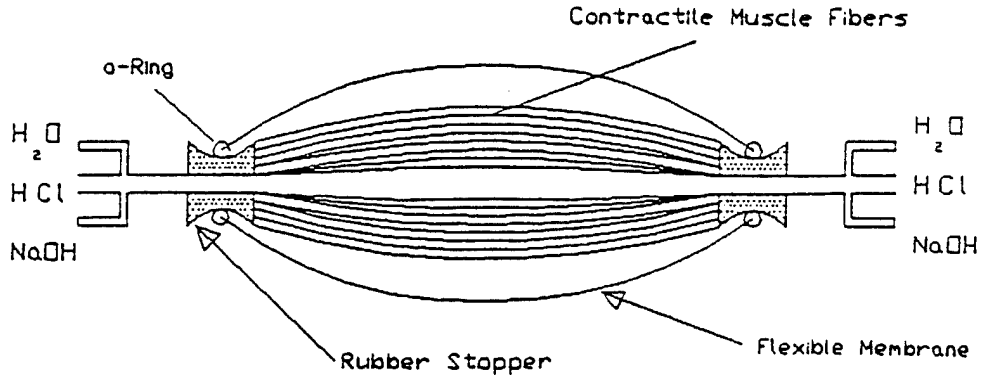

Figure 5- Schematics of a simple contractile encapsulated muscle

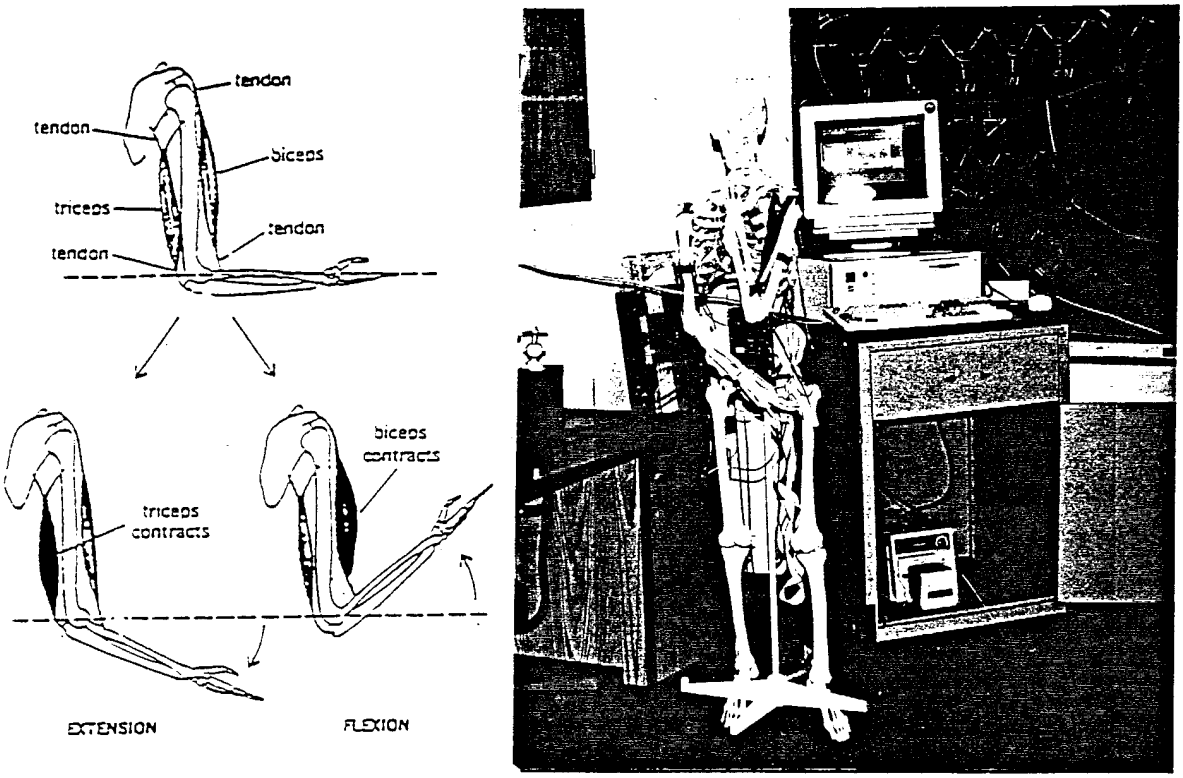

Figure 6 and Photo 1- Ideal placement arrangement of the antagonist muscles in the shoulder and the arm

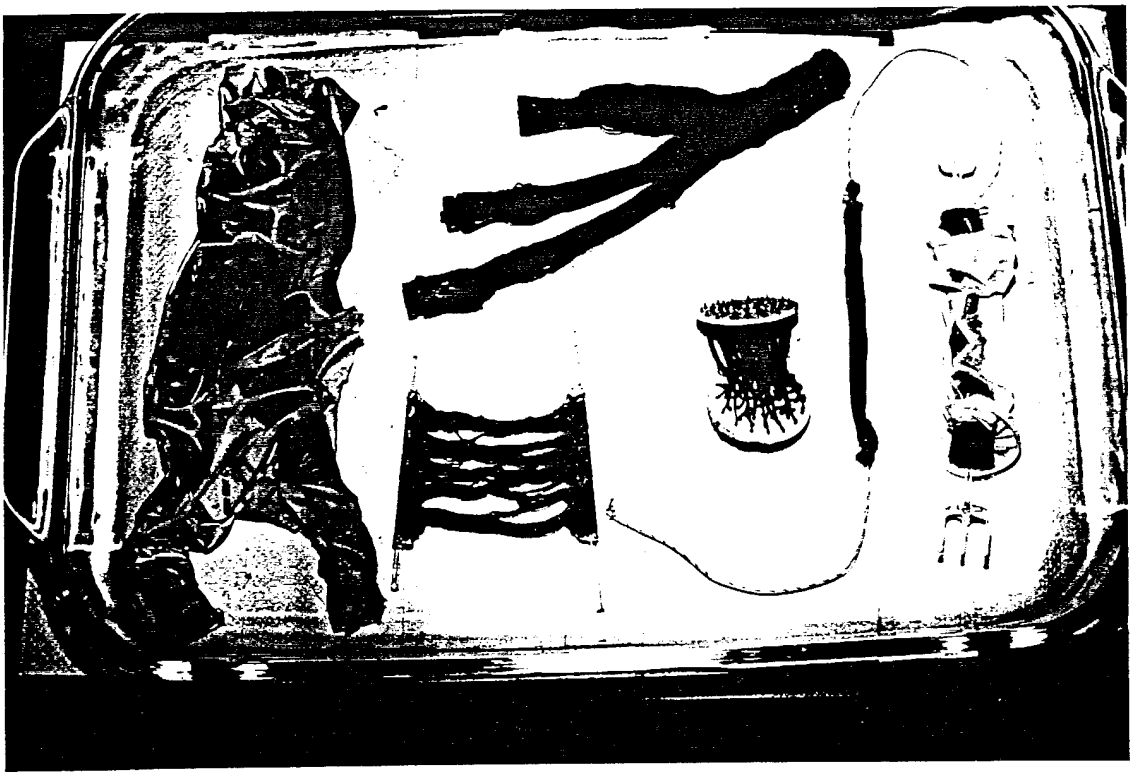

Photo 2- An array of contractile fibrous muscles in various configurations

An Array of Contractile Fibrous Muscles In Various Configuration

Photo 2 displays an array of fabricated muscles in our laboratory. From left to right, the first muscle is an encapsulated biceps muscle with latex membrane as the encapsulation material, a triceps muscle composite fiber bundle which is not encapsulated, a leaf muscle to be used in the torsional self-powered pH meter, the internal structure of the linear spring-loaded ionic polymeric gel actuator, a simple contractile fiber bundle muscle and finally on the right hand side of the photograph an encapsulated linear contractile muscle.

Acknowledgment

Thanks are extended to Dr. Andrew Crowson, Dr. Gary Anderson, Dr. Wilbur Simmons and Dr. Edward Chen for their encouragement and support of this research.

References

1- Katchalsky, A., Experientia, vol. 5, pp.319-320, (1949)
2- Kuhn, W., Experientia, vol.5, pp. 318-319, (1949)
3-Hamlen, R.R., Kent, C.E., and Shafer, S.N., Nature, vol. 206, pp. 1148-1149, (1965)
4-M. Shahinpoor, Int. J. Smart Materials & Structures, vol. 1, no. 1 pp. 91-94, (1992).
5-D. Segalman, W. Witkowski, D. Adolf and M. Shahinpoor, Int. J. Smart Materials & Structures, vol. 1, no. 1, pp. 44-45, (1992).
6-A. Meghdari, M. Jafarian, M. Mojarrad and M. Shahinpoor, ASME Publication DE-vol. 58, Intelligent Structures, Materials, and Vibrations, edited by M. Shahinpoor and H.S. Tzou, vol. DE-58, pp. 21-26, (1993).
7-M. Shahinpoor, ASME Publication AD-vol. 35, Adaptive Structures and Material Systems, edited by G.P. Carman and E. Garcia, vol. AD-35, pp. 11-22, (1993).
8-D. Segalman, W. Witkowski, D. Adolf and M. Shahinpoor, Proc. 1st. Int. Conf. Intelligent Materials, ICIM'92, Tsukube, Japan, July, Technomic Publishing Co., pp. 310-313, (1992).
9-D. Segalman, W. Witkowski, R. Rao, Doug Adolf and M. Shahinpoor, Proc. 1993 SPIE North American Conference on smart Structures and Materials February 93, Albuquerque, NM. vol. 1916, pp. 40-55, (1993).
10-M. Shahinpoor, Proc. 1993 SPIE North American Conference on Smart Structures and Materials., February 93, Albuquerque, NM. vol. 1916, pp. 416-423, (1993).
11-M. Shahinpoor, Proc. 1993 IEEE International Conference on Robotics & Automation, Atlanta, Georgia, May 93, vol. 2, pp. 380-385, (1993).
12-M. Shahinpoor, Proc. SPIE 1994, North American Conference on Smart Structures and Materials, February 94, Orlando, Florida, vol. 2189, paper no. 26, pp. 255-264, and papper no. 27, pp.265-274, (1994).
13-M. Shahinpoor, Proc. SPIE 1994 North American Conference on Smart Structures and Materials, February 94, Orlando, Florida, vol. 2189, paper no. 13, pp.134-142, (1994).
14-M. Shahinpoor, Proc. Thirteenth Southern Biomedical Conference, April 1994, Washington, D.C., vol. 1, pp.31-38,pp.255-264, (1994).
15-M. Shahinpoor, Proc. 1994 Int. Conf. on Intelligent Materials, ICIM'94, June 1994, Williamsburg, VA, pp. 1105-1116, pp.1079-1085, pp. 1095-1104, and pp. 1086-1094, (1994).
16-M. Shahinpoor, Proc. 1994 IEEE International Conference on Robotics & Automation, San Diego, California, May (1994), pp.1502-1507, (1994).
17-M. Shahinpoor, "Continuum Electro-Mechanics of Ionic Polymeric Gels As Artificial Muscles For Robotic Applications," Int. J. Smart Materials and Structures, to appear (1995).

DESIGN AND CONSTRUCTION OF SMART MATERIALS BASED ON PIEZORESISTIVE SENSORS AND MULTILAYER ACTUATORS

Grant # DAAL03-92-G-0374

Institution: NEW YORK STATE COLLEGE OF CERAMICS
ALFRED UNIVERSITY, ALFRED, NEW YORK

Investigators: WALTER A. SCHULZE and WILLIAM B. CARLSON
Res. Assists: JOSEPH CAPURSO, JON FROMMELT

ABSTRACT

The goal of this project is to develop novel piezoresistive sensor/actuator designs and then construct smart mechanical materials that are not dependent on amplifiers or logic circuits. The logic circuits are replaced by a piezoresistive sensor and resistor network that controls power to the transducer by changing current or voltage. Piezoresistivity furnishes a built-in logic by changing resistance with stress and controlling the voltage to a transducer using simple thick or thin film resistor technology. The resistors may be fired or deposited on an insulating surface on either the sensor or transducer and do not need to be mounted separately. Multilayer technology allows low voltage operation and the possibility of multiple interconnections between sensor and transducer.

The principal design goal will be towards tunable anomalously soft ceramic and composite modules. However, the piezoresistive sensor can be used to control other transducer components such as optical, magnetic and thermal devices. Conversely, other types of resistive sensors (varistors, thermistors and photoresistors) can be used to control various transducers.

ACCOMPLISHMENTS

PROCESS DEVELOPMENT

Precipitation Technique - the dopant incorporation technique developed here has proven to be effective in achieving homogeneity of microstructure and composition. Uniform grain size is consistently seen, color is uniform, and PTCR response from batch to batch is invariant. The original coprecipitation process for dopant incorporation has been altered: it was found that excess CO3- effectively precipitates La as well as Mn, thus removing the need for a second precipitating agent, i.e. ammonium succinate.

Trilaminate Structures - laminates consisting of 36 tape layers (two groups of 9 doped layers separated by 18 undoped layers) have been produced with minimal camber and zero delaminations. Density is approximately 95% of theoretical.

Tape Casting Process Development - consistently good results are seen from cast to cast for both doped and undoped powders. A four-foot tape caster was designed and constructed. The primary reasons for building this caster were safety and the ability to control the process. Doctor blade velocity is controllable through a DC motor, and the entire machine is enclosed in a case which is vented to the outside. Nearly flawless casts

of 4' by 3-1/2" with thickness ranging from 4 to 8 mils are obtained using a double doctor blade and a Teflon® casting surface. Organics provided by Palomar-MSI (San Diego, CA) allow a fairly wide processing window, in terms of casting and lamination (conditions: 2500 psi at 80 C for 3 minutes).

Burnout Profile Development - weight loss and reaction points vs. temperature have been characterized for the MSI polyvinyl buterol binder system using TGA and DTA analyses. This information made it possible to reduce the total sintering cycle to 36 hours for laminated structures. Four-hour holds at the temperatures corresponding to the maximum rate and completion of weight loss, together with a 20 C/hour ramp rate throughout the weightloss range result in consistently defect-free laminated structures.

PVA Gelation Trials - medium molecular weight (~50,000) fully-hydrolyzed PVA results in optimum gelling behavior to immobilize precipitated dopants before calcination.

Tube Furnace - a safer, more energy-efficient furnace has been designed and built, having a 5" zone with a temperature range of ~1 C. It is able to withstand 1500 C operation, with 4.8 kW maximum power input, and about 1.0 kW conductive loss. Gas switching is programmable, allowing walk-away operation.

TEST DEVELOPMENT

PTCR Test System - based on an HP 4140B pA meter, this automated over-night test system provides 1 C resolution PTCR sweeps. A MacorÆ-based fixture was constructed using spring-loaded probes: this provides reliable contact to the Al electrodes, previously difficult to obtain.

Piezoresistance Test System - in essence, a four-point bend fixture seated in a programmable Sigma oven, with currently manual application of stress using a micrometer head in line with a 50 lb. load cell. Electroding/Surface Preparation - much effort has been directed at this problem. Using impedance analysis, it was determined that Al electrode contact quality is highly dependent on the condition of the surface. A surface preparation procedure has been implemented which has yielded consistently good contacts (electrically indistinguishable from Ga/In eutectic electrodes) which are stable throughout the testing temperature range.

MATERIAL STUDIES

Final Powder Acceptance - previous lots of $BaTiO_3$ powder provided by Transelco Div., Ferro Corp. (Penn Yan, NY) had an excessive amount of residual $BaCO_3$, resulting in poor microstructure due to CO_2 liberation at or near the peak sintering temperature. They graciously sent two additional lot samples for evaluation. Based on microstructural and macro-defect evaluation, one of these was chosen (lot #920355). An additional 30+ lbs. of this powder was provided, ensuring consistent results throughout this project.

Lanthanum Dopant Level - variation of La content from 0.0 to 0.5 mol% confirmed that a 0.3% level is optimum, in terms of pellet conductivity and microstructure.

Manganese Dopant Level - Mn, the counterdopant responsible for enhancing the PTCR effect, was varied from 0.00 to 0.06 mol%. Pellet color ranged from blue to green to brown; this was consistently repeated from part to part, as was grain size, indicating that dopant distribution is adequate at these extremely low levels. This variation, together with different cooling (grain boundary oxidation) rates from the peak sintering hold, allow engineering of the PTCR curve from flat (no response) to a six order jump. Therefore, it will be an easy matter to fix the size of the potential barrier at the grain boundary as a

variable in piezoresistivity experiments. Trilaminate Interface Study - platinum shavings were embedded between doped and undoped tape layers to act as an immobile 'flag', to determine the extent of dopant infiltration into the insulating region. It was observed that the semiconductor/insulator interface (regions are differentiated by grain size) is quite straight and is basically immobile.

Preliminary Piezoresistivity Results - it was confirmed that the piezoresistive response of the trilaminate is in sign agreement with Heywang's model of the grain boundary potential barrier, i.e. resistivity increases in compression and decreases in tension. It was also seen that as the test temperature approaches the Curie point from above, piezoresistive sensitivity increases (due to Curie-Weiss dependencies on temperature and pressure): this can be viewed as an additional confirmation of the validity of the Heywang model.

Response in Ferroelectric State - a one order of magnitude increase in resistance was seen at 72 C (well below Tc) for a sample under a 20 lb. constant load, as temperature increased. We believe that this was the result of domain reorientation under stress (ferroelasticity). Although this response has not yet been reproduced, it is novel enough to warrant further investigation.

Elastic Modulus - ultrasonic measurements were used to characterize the elastic properties of the insulating and semiconducting barium titanate bodies vs. temperature.

* INDUSTRY CONTACT - discussions have been held with the staff of Transelco/Ferro (Penn Yan, NY) concerning lab tape casting procedures and barium titanate powder requirements; they have donated several lots for evaluation. We have also maintained contact with Texas Instruments (Attleboro, MA). They have provided a series of PTCR pellets for comparative evaluation, and given assistance in specifying equipment for the piezoresistance test system.

MODELING

* PERCOLATION MODELING - modeling the resistivity and the piezoresistive effect via closed-form effective property relations continues. Only limited success was achieved with surface conducting/insulating models due to variation in conductor phase geometry from that assumed in models.

* ANSYS 5.0 - the newest version of Swanson Analysis Finite Element package has been installed and is being tested. "Real-time" simulation of potential smart materials packages will be achieved by including externally written programs or macros in the analyses. Currently, system software is being upgraded to allow the full potential of macro capabilities to be realized. Hardware upgrades are also being considered since piezoelectric and piezoresistive analysis of a three-dimensional body is memory and microprocessor intensive.

* LOADED POLYMER SENSOR - carbon/epoxy matrix composites have been investigated for use as piezoresistive sensors. Variation in resistivity with applied load showed orders-of-magnitude decreases with increasing pressure. These responses demonstrated that such a material may be feasible in a smart material package.

FUTURE PLANS

* The effect of counterdopant acceptor level and density on trilaminate piezoresistive response will be studied by varying the dopant species/concentration and cooling rates.

* Theories of PTCR behavior will be applied to the piezoresistivity phenomenon.

* Semiconducting layer thickness will be varied to determine the optimum thickness ratios for the trilaminate layers.

* Investigation of the uniaxial response of PTCR pellets will continue.

* The microstructural evolution of insulating and PTCR barium titanate will be examined in some depth.

* Trilaminate response in the ferroelectric state will be scrutinized.

* The epoxy resin will be replaced with a lower stiffness compound for shifting the resistivity change further into the critical range with lower conductor loadings.

* Better quality control on the mixing of agglomerated particles will beattempted.

* Different aspect ratio carbon conducting particles will be tested to delineate surface area effects.

PUBLICATIONS:

1) J.S. Capurso, A.B. Alles, and W.A. Schulze, "Processing of Laminated Barium Titanate Structures for Pressure-Sensing Applications," submitted to the Journal of the American Ceramic Society.

2) J.S. Capurso, A.B. Alles, and W.A. Schulze, "Piezoresistive Ceramic Sensor Based on Barium Titanate," to be published in Ceramic Transactions. Presented at the International Symposium on Materials for Intelligent/Smart Systems & Adaptive Structures, Nov. 8-10, 1993 PAC-RIM Meeting, Honolulu, Hawaii.

3) W. B. Carlson, S. M. Pilgrim, W. A. Schulze, Y. S. Kato, J. M. Frommelt, "Flexi-Distortional Piezoelectric Sensor Results,", Proc. of the 9th Int'l Symp. on Applications of Ferroelectrics, The Pennsylvania State University, University Park, PA.

4) J. M. Frommelt, S. M. Pilgrim, W. B. Carlson, W. A. Schulze, "Modeling of Piezoresistively-Controlled Electromechanical Smart Material," submitted to J. of Intelligent Materials, Systems, and Structures.

PRESENTATIONS/POSTERS:

* Paper and Poster presented at the 95th Annual Meeting of the American Ceramic Society, held April 18-22 in Cincinnati, Ohio.

* Paper presented at the 2nd Int'l. Conf. on Intelligent Materials sponsored by ARPA/ARO/NSF, held June 1994 in Williamsburg, VA.

* Poster to be presented at the 8th International Meeting on Ferroelectrics, held on August 8-13 at NIST, Gaithersburg, Maryland.

* Poster to be presented at the 9th International Symp. on Applications of Ferroelectrics, held in August at University Park,PA.

PATENTS/DISCLOSURES:

* U.S. Patent Number 5,225,126: Piezoresistive Sensor; A.B. Alles and W.A. Schulze, Alfred University, Alfred, New York, July 6, 1993.

* "Flexi-Distortional Piezoelectric Composite Sensors," W. B. Carlson, W. A. Schulze, R. E. Newnham, L. E. Cross, P. Chalk, Alfred University disclosed May 1993, The Pennsylvania State Univ. disclosed June 1993.

A STRESS-SENSING CERAMIC DEVICE BASED ON PTCR BARIUM TITANATE

Joseph S. Capurso and Walter A. Schulze
New York State College of Ceramics at Alfred University
Alfred, New York 14802

Abstract - Positive temperature coefficient of resistance (PTCR) barium titanate is used as the base material for a ceramic sensor which employs piezoresistivity to detect changes in applied stress. Tape-cast sheets of undoped (insulating) and PTCR (semiconducting) $BaTiO_3$ are laminated to produce a three-layer "trilaminate" - a sintered structure which has two PTCR layers separated by an insulating layer. The trilaminate is exposed to mechanical stress in a four-point bend configuration (placing one semiconducting layer completely in tension, the other in compression), and the resistivities for both stress states are measured concurrently as functions of the applied stress magnitude. The piezoresistivity coefficient (π) is calculated from the slope of the linear resistivity-stress response. Piezoresistivity results are presented versus PTCR layer composition (counterdopant species) and furnace cooling conditions (grain boundary oxidation level). These results are interpreted with respect to Heywang's model of the grain boundary potential barrier.

INTRODUCTION

Semiconducting barium titanate is a well-studied material which may exhibit a large increase in resistivity over a relatively small temperature range beginning near its Curie temperature (T_C). It also exhibits *piezoresistivity* (stress-sensitive resistivity), making it a potential base material for stress-sensing applications.

The PTCR phenomenon was first observed in the mid-1950's [1], and was explained by Heywang in terms of a double Schottky potential barrier existing at the boundaries between semiconducting barium titanate grains [2]. He derived an expression for the height of the barrier (ϕ_O):

$$\phi_o = \frac{e n_s^2}{8 \varepsilon_r \varepsilon_o n_o} \tag{1}$$

where n_S is the number of electrons trapped at the grain boundary per unit area, n_O is the number of conducting electrons per unit volume in the bulk, ε_r is the relative permittivity (dielectric constant), and ε_O is the permittivity of free space. The resistivity of PTCR barium titanate ceramic with z grains per unit length is exponentially dependent on ϕ_O:

$$\rho = \rho_b \left(1 + \frac{zbkT}{e\phi_o} e^{\frac{e\phi_o}{kT}} \right) \tag{2}$$

where ρ_b is the resistivity of the bulk (Ω·cm) and b is the electron depletion region half-width.

Below T_C, these barriers are partially compensated by surface charge resulting from discontinuity of the normal polarization components of ferroelectric domains terminating at the grain boundary, according to Jonker [3]. This causes a suppressed resistivity in the ferroelectric state, resulting in an abrupt increase in resistivity once the domains vanish (barrier compensation disappears), above T_C.

The temperature dependence of ε_r for paraelectric barium titanate (above T_C) follows the Curie-Weiss law [4]:

$$\varepsilon_r = \frac{C}{T - \Theta} \tag{3}$$

where C and Θ are constants. So, as temperature increases, ε_r decreases; causing an increase in barrier height and thus a dramatic rise in resistivity. Samara [5] showed that an analogous hydrostatic pressure dependence exists:

$$\varepsilon_r = \frac{C'}{P - P_o} \tag{4}$$

raising the possibility that the grain boundary potential barrier may be adjustable through application of stress.

Relatively little attention has been focused on the piezoresistive effect in PTCR barium titanate. Early investigations of the stress sensitivity of semiconducting barium titanate disks [6,7] indicated that piezoresistivity is maximized at temperatures near T_C in the paraelectric state under uniaxial compressive stress, although discrepancies in the direction (sign) of resistance change were seen. Specifically, hydrostatic compression resulted in a positive change in resistance, while negative piezoresistivity was observed under uniaxial compression (indicating a non-uniform stress state). More recent work [8-11] further reinforces the concept of piezoresistivity being due to the temperature and stress sensitivity of ε_r near the Curie temperature, through its effect on the magnitude of grain boundary potential barriers.

In this work, a four-point bending apparatus is used to apply stress to a *trilaminate* structure [12], which consists of two layers of PTCR barium titanate separated by a layer of insulating barium titanate. A photograph

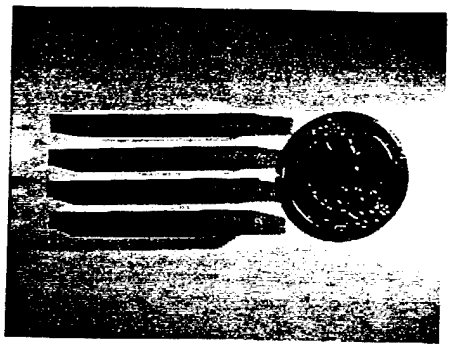

Fig. 1. Photograph of several trilaminates.

of several trilaminates is shown in figure 1. Using this configuration, the effect of stress on resistivity in both the compressive and tensile modes may be observed. This is an approach which minimizes shear stresses, and gives results which agree with the aforementioned model of the grain boundary potential barrier.

EXPERIMENTAL

Processing

Trilaminates are produced by laminating tape-cast sheets of barium titanate together and sintering at 1350°C to form a structure which can withstand a moderate mechanical stress. The composition of the trilaminate with respect to its thickness is determined by the stacking sequence of green tape layers, which are either insulating or semiconducting. Insulating tape is produced from as-received powder*, while semiconducting tape consists of the same powder plus precipitated dopant(s): a 0.3 atom% lanthanum addition causes semiconductivity, and transition metal counterdopants (e.g. manganese, iron, cobalt) result in the formation of acceptor traps at the grain boundaries, enhancing the PTCR effect [13]. Details of dopant incorporation procedures, trilaminate formation, binder burnout, and sintering/cooling are described elsewhere [14].

Testing

The four-point bend configuration is used to stress the trilaminate. This configuration provides a region of constant longitudinal stress between the two inner contact points (Fig. 2). Trilaminates are lightly ground on a 600M SiC pad to minimize surface flaws and to provide a clean, smooth surface for electroding. Electrical contact to the trilaminate is made by evaporating aluminum metal onto either side, leaving a gap on each surface which is well within the region of constant longitudinal stress.

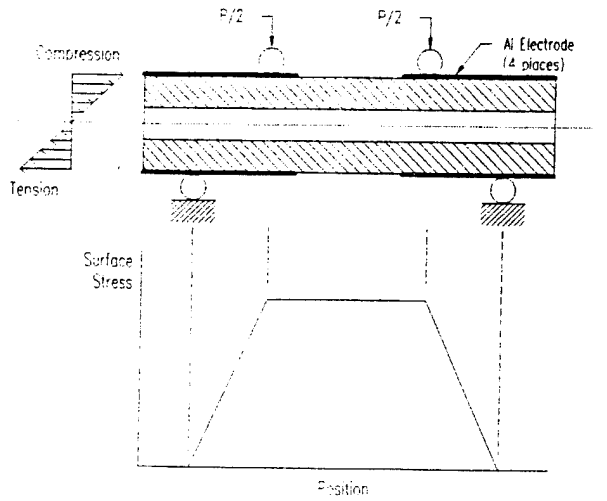

Fig. 2. Application of stress on a trilaminate in four-point bend.

Note that the upper semiconducting layer is in compression only, since it lies completely above the plane of zero stress. This layer undergoes a volumetric decrease, resulting in an overall constriction of unit cells and thus a decrease in relative permittivity (ε_r). Conversely, the lower semiconductor layer is strictly in tension, experiences a volumetric increase, an expansion of unit cells and therefore an increase in ε_r. From Heywang's model (described earlier), one would therefore expect a resistivity increase in compression and a decrease in tension, due to the effect of ε_r on the barrier height.

Piezoresistance testing is performed using a computer-controlled system which acquires resistance versus load data at 1°C intervals over a ten-hour ramp from 107°C to 143°C. Resistance is measured at 0.1 VDC†. The four loading points also act as electrical contacts to the aluminum electrodes on the trilaminate under test. Load is applied at 4.45 N intervals from 8.90 N to 26.7 N, then back down to 8.90 N; using a closed-loop load sensing/driving system which employs a stepper motor to drive the loading column. The slope and y-intercept of the least-squares regression line through these nine data points are calculated, and the isothermal piezoresistivity coefficient π is determined by dividing the slope by the intercept (resistance at zero stress, R_O):

$$\pi = \frac{1}{R_o}\left(\frac{\partial R}{\partial \sigma}\right)_T \qquad (5)$$

* Code 219-9, Transelco Div., Ferro Corp., Penn Yan, NY.

† 4140B pA meter, Yokogawa-Hewlett-Packard, Ltd., Tokyo.

RESULTS AND DISCUSSION

Microstructure

A typical semiconductor-insulator interface microstructure is shown in figure 3. Note that the semiconducting material has a significantly larger grain size (40-60 μm) than the insulating material (10-30 μm),

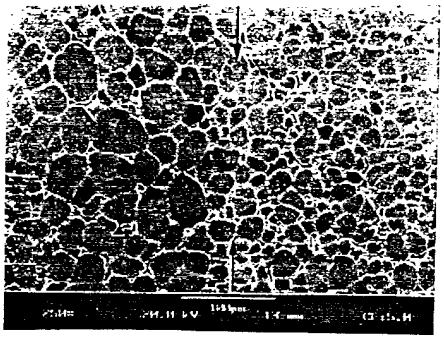

Fig. 3. SEM micrograph of a typical semiconductor/insulator interface (secondary electron image).

and that the interface is continuous and well-defined, with no lamination defects or abnormalities with respect to porosity. Grain boundary relief was obtained by thermal etching at 1325°C for 30 minutes in air.

Piezoresistance

The piezoresistive response of a trilaminate is shown in figure 4, for several temperatures. Note that in all cases, the resistance ratio (resistance at some stress divided by unstressed resistance, R_O) is greater than unity in compression and less than unity in tension, substantiating the arguments stated previously. Also note that the responses are linear, and are more pronounced in tension at these temperatures.

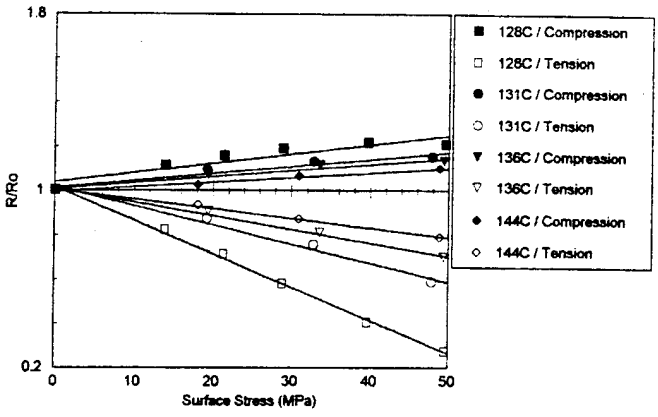

Fig. 4. Normalized resistance of a 9/18/9 layer trilaminate (0.30 at% La, 0.04 at% Mn) vs. surface stress at several temperatures above T_C.

It can be seen that the piezoresistive effect is reduced in magnitude as the temperature is increased above T_C ($\approx$123°C). This is another confirmation that piezoresistivity is a result of changing relative permittivity, since ε_r is most sensitive to pressure and temperature changes as T_C is approached from above, according to the Curie-Weiss dependencies (eq. 3,4).

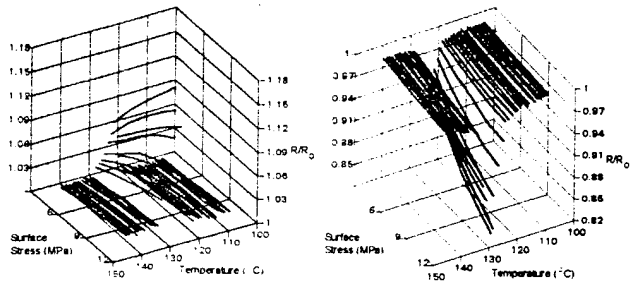

Fig. 5. Normalized resistance of a 3/30/3 layer trilaminate (0.30 at% La only) vs. surface stress and temperature, for regions under a) compression, b) tension.

Similar data were obtained for another trilaminate, over a wider temperature range extending both above and below T_C. These data are illustrated in figure 5 (a,b), where resistance ratio is plotted as a function of both temperature and applied stress: each line corresponds to a constant-temperature resistance-stress plot. Observe that the magnitude of piezoresistivity (slope) maximizes in the vicinity of T_C; and that a smaller, yet non-zero slope is seen below T_C.

Trilaminates having differing counterdopants in the PTCR regions were produced to evaluate the effect of acceptor state level and density. Manganese is known to cause "deep" acceptor states [13], and was added at a 0.04 atom% level. Iron causes formation of shallow states, and was added at a 0.02 atom% level. Cobalt forms states between these two extremes, and was added at the 0.04 atom% level. Optimum counterdopant levels

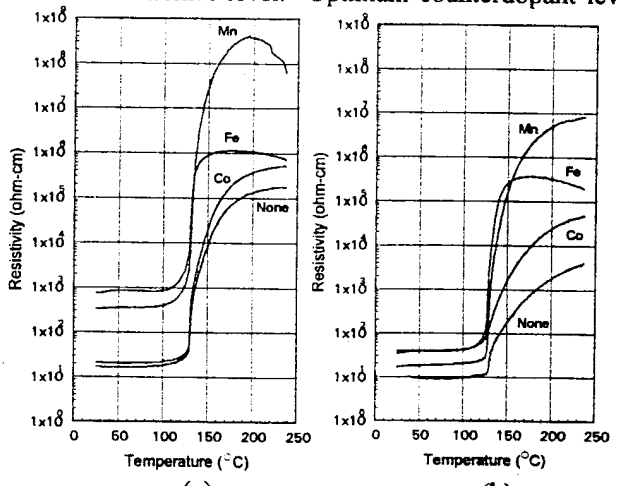

Fig. 6. PTCR response of pellets with different counterdopants, cooled from 1350°C to 500°C at (a) 1°C/min., (b) 10°C/min.

were obtained by increasing the addition until room temperature resistivity began to rise rapidly. The density of acceptor states can be adjusted by variation of the cooling rate from the 1350°C peak sintering temperature to 500°C, and is indicated by the steepness of the PTCR curve above T_C.

PTCR responses for these materials for two cooling rates are shown in figure 6, and figure 7 contains piezoresistivity plots for the same materials and conditions. Note that the piezoresistivity peak is basically equal and cooling-rate-independent for the Mn- and Fe-counterdoped trilaminates, but that cooling rate has a significant effect on the Co- and non-counterdoped samples. It is interesting to note that the Co- and non-counterdoped samples also show a change in initial PTCR slope with change in cooling rate, but the Mn and Fe

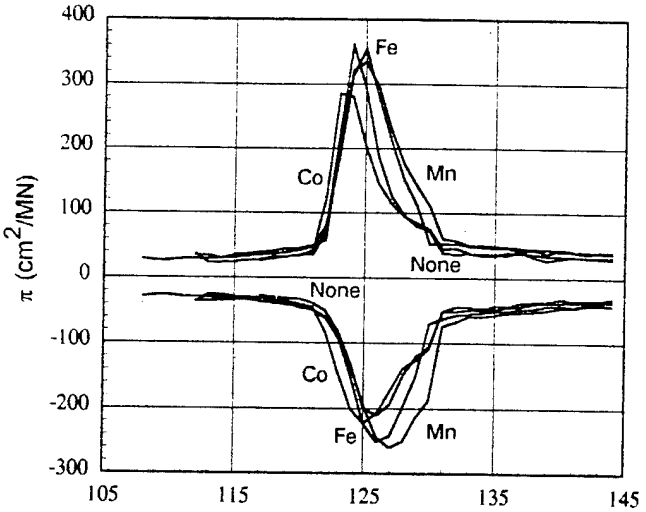

(a)

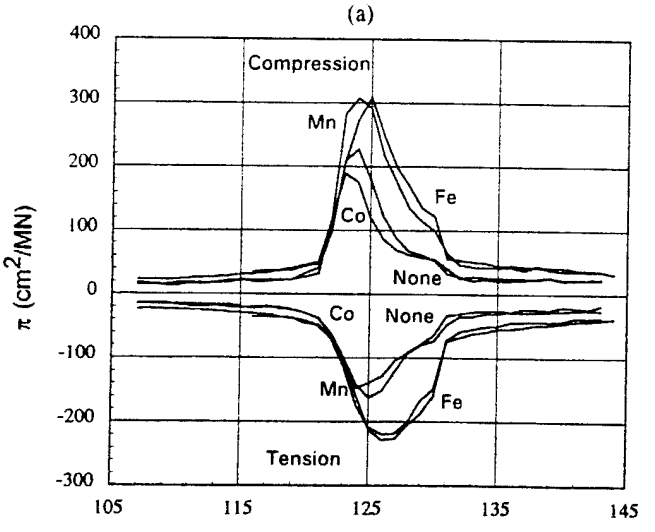

(b)

Fig. 7. Piezoresistive response of 4/28/4 layer trilaminates with different counterdopants, cooled from 1350°C to 500°C at (a) 1°C/min., (b) 10°C/min.

samples do not. These results indicate that piezoresistive response appears to be independent of acceptor level, but is somewhat sensitive to density of states.

SUMMARY

A new type of stress-sensing device based on barium titanate - a *trilaminate* - has been described. The piezoresistive response of the trilaminate is in sign agreement with Heywang's model, and is more pronounced at temperatures near the Curie point, indicating that the basic mechanism responsible is a change in the relative permittivity of the material in the vicinity of grain boundaries. It was also seen that the piezoresistive response of PTCR barium titanate can be engineered to some degree through variation of counterdopant species and cooling conditions.

REFERENCES

[1] P.W. Haayman, R.W. Dam, and H.A. Klasens, "Method of Preparation of Semiconducting Materials," West German Patent 929,350, June 23, 1955.

[2] W. Heywang, "Barium Titanate as a Semiconductor with Blocking Layers," *Solid State Elec.*, **3** [1] 51-8 (1961).

[3] G.H. Jonker, "Some Aspects of Semiconducting Barium Titanate," *Solid State Elec.*, 7, 895-903 (1964).

[4] B. Jaffe, W.R. Cook, Jr., and H. Jaffe, *Piezoelectric Ceramics*, p. 77, Academic Press, New York, 1971.

[5] G. Samara, "Pressure and Temperature Dependences of the Dielectric Properties of the Perovskites $BaTiO_3$ and $SrTiO_3$," *Phys. Rev.*, **171** [2] 378-86 (1966).

[6] H.A. Sauer, S.S. Flaschen, and D.C. Hoesterey, "Piezoresistance and Piezocapacitance Effects in Barium Strontium Titanate Ceramics," *J. Am. Ceram. Soc.*, **42** [8] 363-6 (1959).

[7] O. Saburi, "Piezoresistivity in Semiconductive Barium Titanates," *J. Phys. Soc. Japan*, **15** 733-4 (1960).

[8] H. Igarashi, M. Michiue, and K. Okazaki, "Anisotropic Resistivity Under Uniaxial Pressure in PTC Ceramics," *Jpn. J. Appl. Phys.*, **24** [suppl. 24-2] 305-7 (1985).

[9] A. Amin and M.B. Holmes, "Pressure and Temperature Dependencies of the Direct-Current Resistance of Semiconducting $(Ba,Sr)TiO_3$ and $(Ba,Pb)TiO_3$," *J. Am. Ceram. Soc.*, **71** [12] C482-3 (1988).

[10] A. Amin, "Piezoresistivity in Semiconducting Positive Temperature Coefficient Ceramics," *J. Am. Ceram. Soc.*, **72** [3] 369-76 (1989).

[11] A.B. Alles, M. Murphy, J.J. Symanski, C.L. Tremper, and W.A. Schulze, "Piezoresistivity Modeling of Grain Boundary Junctions in PTCR $BaTiO_3$," submitted for publication.

[12] A.B. Alles and W.A. Schulze, "Piezoresistive Sensor," United States Patent 5,225,126, July 6, 1993.

[13] H. Ihrig, "PTC Effect in $BaTiO_3$ as a Function of Doping with *3d* Elements," *J. Am. Ceram. Soc.*, **64** [10] 617-20 (1981).

[14] J.S. Capurso, A.B. Alles, and W.A. Schulze, "Processing of Laminated Barium Titanate Structures for Stress-Sensing Applications," accepted for publication in *J. Am. Ceram. Soc.*.

TWO DIMENSIONAL CRYSTALS AND SMART MATERIALS

Craig J. Eckhardt
Department of Chemistry
University of Nebraska-Lincoln
Lincoln, NE 68588-0304

The relationship of structure to function remains one of the vital themes of chemistry and has application to both fundamental processes as well as technological applications. With the increasing interest in the creation of new materials, chemists have been confronted with challenges which often require expansion of their traditional emphasis on structure to considerations that have been more in the realm of physics and material science. Since macroscopic behavior is often what must be designed for a new material, it has proven necessary to exploit other interactions than molecular structure to achieve desired properties. Frequently, it is the collective interactions of a material that stimulate interest and permit exploitation for technological ends. Coupled with this need for engineering such properties for a material is the acceleration toward increasing miniaturization. The latter has piqued chemists' interests and molecular diodes, molecular wires and the like have been sought as the ultimate in the miniaturization. Such molecular devices lie well within the province of chemists' skills. There is, however, much more difficulty associated with the deliberate creation of materials that will exhibit desired collective properties.

It is in the solid state that collective properties obviously manifest themselves and thus it would be logical for chemists to synthesize crystals possessing required properties. Unfortunately, it remains impossible for a chemist to create, with any reasonable degree of certainty, a molecule that will form a desired crystal. Much of this can be attributed to the myriad possibilities of crystalline forms available for crystallization. There are 230 three dimensional space groups and, when considerations of variability of lattice motif are made, the possibilities are many-fold more than this. However, a significant reduction in choice of lattices can be achieved if the crystals are forced to be two dimensional. Because there are only 17 two dimensional space groups, over an order of magnitude reduction of possibilities is obtained. Further, two dimensional systems are inherently miniaturized since they can be only a few molecules thick. It is the appreciation of these possibilities that informs our research in creating organized molecular monolayers that exhibit two-dimensional crystallinity and, by extension, collective properties such as ferroelectric phase transitions that are associated with crystalline materials.

Langmuir-Blodgett films have been traditionally formed from long-chain fatty acids which may often be substituted with pendant groups to introduce desired physical properties. Because the basic unit is the fatty acid, it is unsurprising that they have led to formation of only two or three of the possible 17 two-dimensional space groups. Our research centers on creating new planar lattices (nets) by the design of new film-forming molecules (amphiphiles). The design is primarily based on close-packing principles used to rationalize the formation of molecular crystals.[1,2] By designing the molecules to form two-dimensional crystals, the collective properties of solids can be exploited. An additional benefit is that the specific nets depend largely upon the

cross-sectional geometry of the amphiphile thereby making the prediction of the crystal structure more certain than in the three-dimensional case.

The synthesis of new amphiphiles is extremely expensive both monetarily and in investment of time. To alleviate some of this we have developed some theoretical approaches which have proven effective in predicting the packing of amphiphiles in two-dimensional arrangements. Initial investigations used atom-atom potential calculations[3,4] and were met with some success but were limited by the complexity of the calculation. The results of these studies suggested that the cross-sectional geometry was more important to the prediction of the planar lattice so a model potential, the cross-section potential, has been developed which, when used in a Monte Carlo simulation, has proved to be quite powerful in not only predicting the two-dimensional packing but also in following the phase behavior of the two-dimensional crystals.[5,6] The phase behavior is particularly important since many three-dimensional smart materials evince their response to input through a change of phase, *e.g.* the response of a ferroelectric to an electric field. The simulation with the cross-section potential has proven particularly important since it gives much theoretical credence to the posited restricted rotor to free rotor (S → LS) phase transition in fatty-acid monolayers.

One of the great problems of traditional monolayers is mechanical stability. We have designed a lock-and-key amphiphile where the molecule, the trinorbornyl carboxylate (TNBC) shown in Fig. 1, is designed such that it will have both an "acceptor" and a complementary "donor" site. Atomic force microscopy (AFM) has shown that TNBC packs in a nearly perfect hexagonal array which exhibits extensive translational order over areas as large as square microns.[7] Such long-range order is most desirable for the fabrication of any smart material. In addition, TNBC is remarkable in that the AFM shows it to be extremely crystalline with images that reveal that the monolayer shatters into small crystalline shards which show regular interlinear angles identical with those of the planar unit cell.[8]

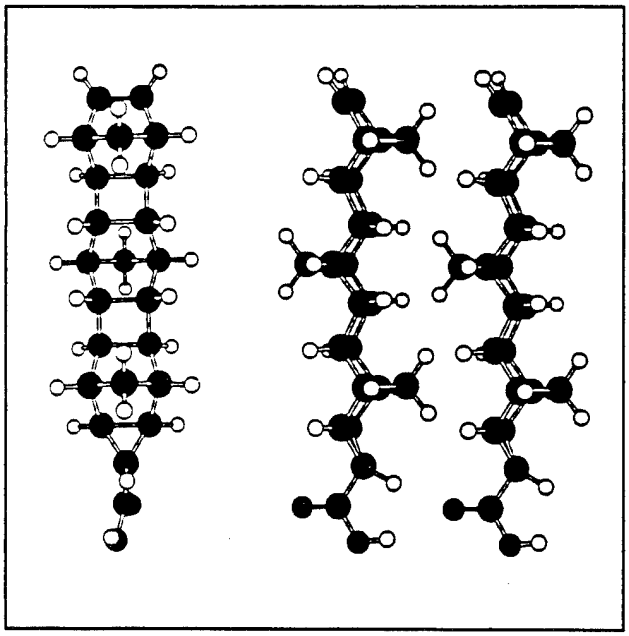

Figure 1: TNBC Molecules

Chirality has also been exploited to control the packing in a monolayer film. A pure enantiomer requires a two- or three-dimensional unit cell that is noncentrosymmetric. A crystalline film comprised of acentric unit cells would necessarily cause second harmonic generation for light waveguided through the film and enhance the response for light reflected from the film. Thus the racemate of a tetracyclic alcohol (TCA) of four fused cyclohexane rings has been synthesized and its structure is displayed in Fig. 2. Symmetry arguments establish that the film of racemic TCA should pack in a rectangular array. The film formed by this molecule is rich in its phase behavior and, on water, shows at least three different phases. Transfer of the film was effected for each phase and AFM studies performed on the film on the mica substrate. The lowest pressure phase was found to be highly disordered such as found in a glass. The

intermediate pressure phase was found to exhibit the expected rectangular packing. However, the high pressure phase showed regions of oblique lattices in mirror-image relationships that were separated by clear grain boundaries. The latter can only be rationalized as resulting from a chiral phase separation of the two enantiomers of the TCA and is the first observation of this phenomenon in two dimensions.[9] The observation of chiral separation has proven to be an important experimental confirmation of the theory of chiral phases in monolayers.[10]

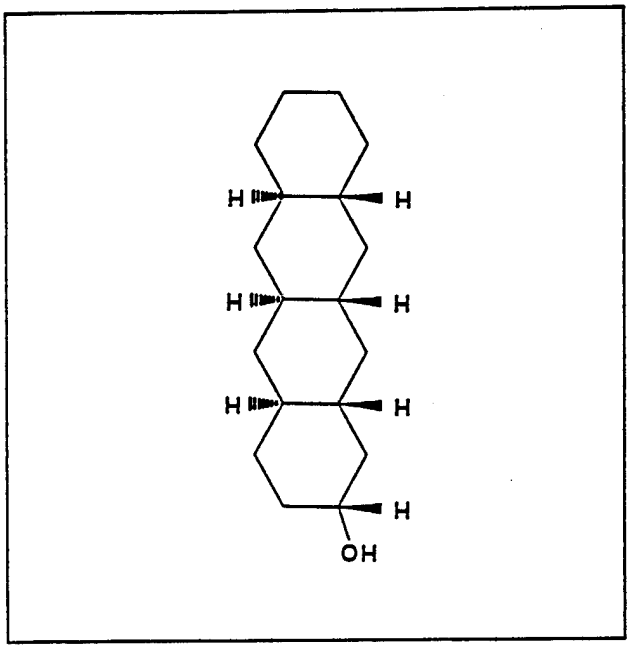

Figure 2: TCA Molecule

Examination of more extensive areas of the high pressure oblique phase reveal that the grain regions show catastrophic disorder. From this it is concluded that the chiral separation occurs on transfer of the film from the aqueous subphase.[8, 9, 10]

The results for both TNBC and TCA indicated that although the rigidity of the amphiphiles confers stable cross-sectional geometries with which to control the packing, they structurally suffer upon vertical transfer to the solid subphase. To introduce some flexibility into the amphiphile and yet retain desired characteristics of chirality and some structural rigidity, another amphiphile has been designed. This consists of a binapthyl core to which short alkyl chains are attached (Fig. 3). The arene core is rigid but otherwise the molecule has much flexibility. Because it is synthesized as a racemate, it too is expected to form a rectangular net. Although the material spreads, it is difficult to obtain a consistent surface isotherm. Nevertheless, at sufficiently low temperature such a film can be made and transferred to mica. AFM studies show that the packing of the film is essentially that shown by fatty acid amphiphiles. Recognizing that the AFM can only see the top atoms of the monolayer and cannot reveal the packing of the binapthyl moieties, atom-atom potential calculations of the structure were performed. The results showed that although the tails packed as the fatty acids, the binapthyls did assume the expected rectangular array. In essence, the *single* BHBN amphiphile produces *three* commensurate planar lattices. Currently, diffraction by TEM is underway to confirm the structural results of the calculations. X-ray reflection studies will also be attempted.

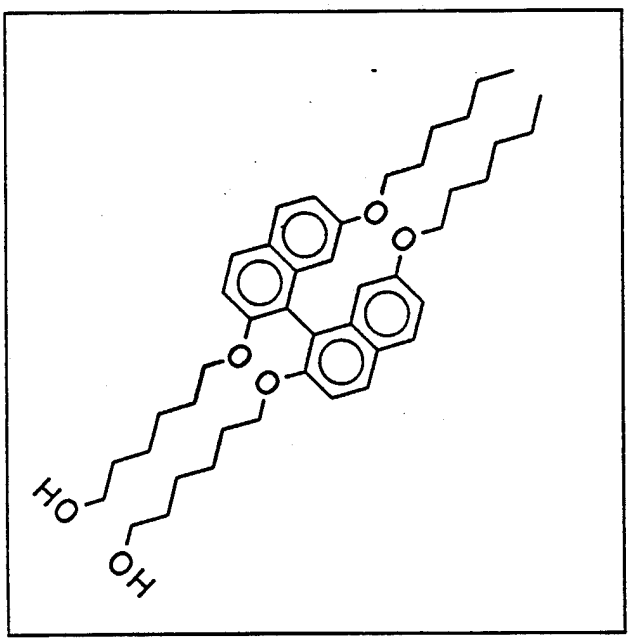

Figure 3: BHBN Molecule

These studies clearly demonstrate the efficacy of the approach of creating two-dimensional solids by control of the geometry of the amphiphiles. In addition, all three of the films display phases which show the nanoscale order so necessary for materials applications. The work has further demonstrated that amphiphiles can be designed to yield films of great mechanical stability such as in the case of TNBC. With these aspects of the materials now under control, the current research thrust is aimed at creating interesting materials.

The present amphiphiles are being chemically modified to produce amphiphiles that will produce films that will behave as smart materials. The first goal is to produce pure enantiomers such that we can assure the formation of acentric unit cells. This is required both for second harmonic generation and two-dimensional ferroelectrics. Unfortunately, and against expectation, the TCA has proven resistant to chiral resolution and a new stereospecific synthesis has had to be devised. The binapthyl series of amphiphiles has proven more amenable to enantiomeric separation although the films are not as robust as those for TCA or TNBC. However, a suitable number of binapthyl molecules have been quite recently produced in enantiomerically pure form. Concurrently, the synthesis of some TCA related pure enantiomers has been completed. These new amphiphiles are now being studied for their film-forming abilities and monolayer properties.

Among the enantiomerically pure systems that have been recently produced are two that possess net dipole moments. This is particularly exciting since our previous work has shown that the theoretical prediction that acentric nets will be formed by enantiomerically pure molecules is valid. Thus, films formed by the polar amphiphiles will have unit cells that are acentric and which must, therefore, possess net dipole moments. Given the long-range order that seems to be associated with our rigidified amphiphiles, such films are anticipated to display ferroelectic behavior and are expected to be switchable by very small electric fields. In the case of one of the amphiphiles, the switching is expected to be associated with a significant change in the optical properties of the film. The electrical field can then be used to switch the polarization of light If the inverse effect can be induced, it will mean that a photoferroelectric material will have been created. Either response will produce a material capable of extremely rapid switching and which, because of its scale, will permit rapid dissipation of the switching energy.

Of the several enantiomerically pure materials that have been made, acentric nets are expected to be formed. Such films should show nonlinear optical (NLO) behavior. Of particular importance are the binapthyls and it is on these systems that the NLO effort is focussed. Such films can generate NLO response in two ways. The first is the traditional one achieved by reflection of light from the surface of the film. Here, the NLO response will be enhanced because of the greater polarizability of the film and the greater asymmetry of the surface due to the acentric net. The incorporation of electron donor-acceptor interactions in the amphiphiles will further enhance such NLO response for second harmonic generation (SHG). The second use of such films for NLO materials is in a waveguide mode. In this application the light is waveguided in the plane of the film. We have found that the binapthyl *monolayers* exhibit what appear to be waveguide-like properties but are not truly so. Nevertheless, these can be exploited and multilayers will be built where true waveguiding is possible through layers of the acentric nets.

There are some other technological applications which are now being pursued. The TNBC molecule is quite rigid and its interlocking appears to form an extremely regular monolayer both in terms of orientational and rotational ordering as well as in height. The lock-and-key geometry effectively prevents any of the amphiphiles from being extruded out of the monolayer. This means that films of the molecule can serve as excellent standards for the

calibration of the height scales for AFM and possibly for scanning tunneling microscopy. The problem of vertical height calibration looms large in AFM studies and use of the TNBC films may prove effective in addressing the problem. To accomplish this an accurate X-ray diffraction study of TNBC crystals will be undertaken to establish the length of the molecule. Then a methodology will be developed to form stepped multilayer films of TNBC. The regularity of the step heights will be studied by X-ray reflectivity measurements.

Another technological application centers on miniaturized devices such as accelerometers. The production of such devices depends crucially on the use of a sacrificial layer which is subsequently removed during fabrication. Removal of these inorganic layers usually involves extreme treatment such as with hydrofluoric acid. Such violent processing severely hampers the number of successful components that can be produced. By engineering amphiphiles as acrificial layers for specific device applications, it may be possible to have a higher success rate. In addition, by proper design of the amphiphiles it may be possible to enhance the response of the device beyond that now available using more conventional materials.

1. A. I. Kitaigorodsky, "Molecular Crystals and Molecules," Academic Press, New York, 1973.

2. C. J. Eckhardt, "Crystal Engineering in Two Dimensions: Design of Amphiphiles Using the Close-Packing Principle," *Acta Chim. Hung.-**Models in Chemistry***, **130** (1993) 235.

3. C. J. Eckhardt and D. R. Swanson, "Crystal Engineering in Two Dimensions: A Calculative Investigation," *Chem. Phys. Lett.*, **194** (1992) 370.

4. D. R. Swanson and C. J. Eckhardt, "Crystal Engineering in Two Dimensions: Close-Packing Applied to a Langmuir-Blodgett Film," *Langmuir*, **9** (1993) 22.

5. D. R. Swanson, R. J. Hardy and C. J. Eckhardt, *J. Chem. Phys.*, **99** (1993) 8194.

6. D. R. Swanson, R. J. Hardy and C. J. Eckhardt, "A Cross-section Potential for Calculation of Close Packing Geometries of Monolayer Films," *Thin Solid Films*, **244** (1994) 824.

7. C. J. Eckhardt, N. M. Peachey, D. R. Swanson, J.-H. Kim, J. Wang, R. A. Uphaus, G. P. Lutz and P. Beak, *Langmuir*, **8** (1992) 2591.

8. C. J. Eckhardt, N. M. Peachey, J. M. Takacs and R. A. Uphaus, *Thin Solid Films*, **242** (1994) 67.

9. C. J. Eckhardt, N. M. Peachey, D. R. Swanson, J. M. Takacs, M. A. Khan, X. Gong, J.-H. Kim, J. Wang and R. A. Uphaus, "Separation of Chiral Phases in Monolayer Crystals of Racemic Amphiphiles," *Nature*, **362** (1993) 614.

10. J. V. Selinger, Z.-G. Wang, R. F. Bruinsma and C. M. Knobler, *Phys. Rev. Lett.*, **70** (1993) 1139.

Dimensionally Self-Regulating Structures

J. E. Furneaux
University of Oklahoma, Department of Physics and Astronomy, Norman, OK, 73019
E. H. Aifer and B. B. Goldberg
Boston University Physics Department, Boston, Ma, 02215

ABSTRACT

We have developed a way to produce a self-tuning detector for the $10-12\mu$m wavelength region in the infrared, consisting of a modulation doped field effect transistor (MODFET) which has a novel gate structure. Our system is an improvement over methods based on 2-dimensional inter-subband absorption in heterostructures. The essential new feature is the introduction of voltage controlled 1-dimensional confinement to the 2-dimensional layer of electrons. By tuning the confining potential one can selectively localize the 2D ground state between 1D barriers while the excited states remain free. In addition, as the confinement potential is varied, the energy difference between levels will also be modulated. With the confinement direction transverse to the MODFET channel, the FIR photoconductivity response will then reflect a large increase in mobility as well as be tunable in wavelength.

INTRODUCTION

Absorption between subbands in quasi-2-dimensional electron systems (2DES) formed in quantum heterostructures, has been investigated for a number of years for its potential in long-wavelength detectors. The GaAs/AlGaAs heterostructure system in particular has been widely studied[1-5]. These types of photoconductors however have two main limitations: First, they have a relatively large dark current due to the carriers in the system which give rise to the 2DES. Secondly, only far infrared radiation (FIR) which has polarization normal to the crystal surface is absorbed, making the coupling of the radiation into the device challenging.

We have developed an approach which modifies the basic design of inter-subband absorption infrared devices with the specific aim of producing an electronically tunable, narrow band detector. These modifications also have the potential of reducing the dark current and improving the optical coupling. As a result, we feel that these ideas may produce a detector for integrated far-infrared spectroscopy.

1D MODIFICATIONS of 2D DEVICES

In order to produce a tunable detector based on intersubband absorption in the $10-12\mu$m wavelength region of the infrared, it is advantageous to use 2D electron systems with asymmetric wells rather than an approach based on a multi-quantum well structure with square potential profiles. In a square well system the energy splitting between 2-D subbands is fixed by the choice of well width, as indicated in figure 1[1].

Photovoltaic quantum well infrared detector

K. W. Goossen and S. A. Lyon
Princeton University, Department of Electrical Engineering, Princeton, New Jersey 08544
K. Alavi
Siemens Research and Technology Laboratories, Princeton, New Jersey 08540

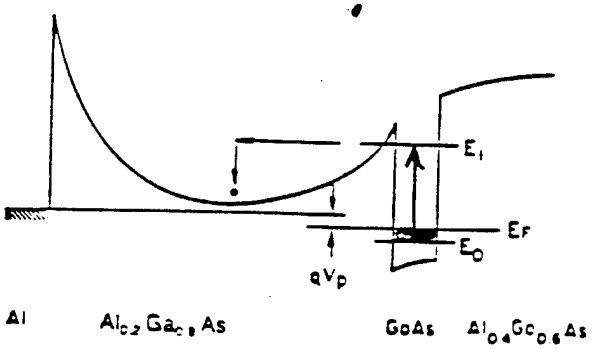

FIG. 1. Schematic of the conduction band of our sample, showing the photoemission process. Electrons are photoexcited to the higher level, upon which they tunnel into the AlGaAs, causing a splitting of the Fermi level across the spacer region.

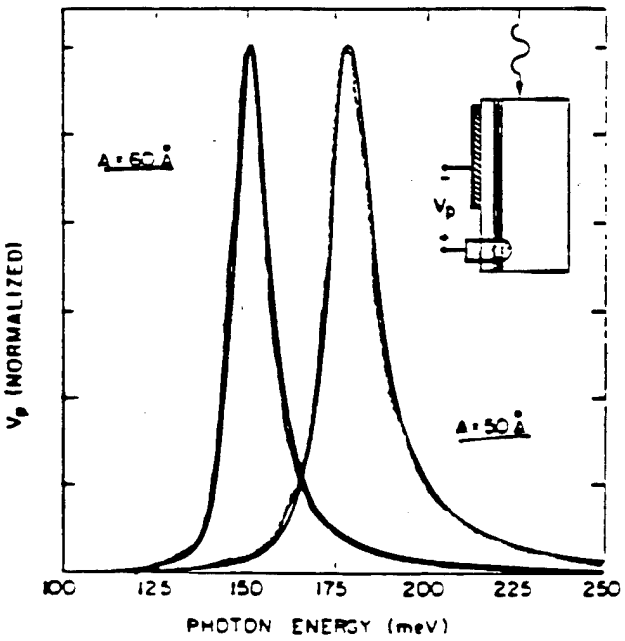

FIG. 2. Photovoltage spectra of samples with well widths equal to 50 and 60 Å, taken at 77 K using a Fourier transform spectrometer. The inset shows our sample geometry and indicates the sign of the photovoltage V_p.

1702 Appl. Phys. Lett. Vol. 52, No. 20, 16 May 1988

Figure 1: Bandstructure and FIR optical response of single quantum well with square potential profile.

In a modulation doped heterojunction however, energy level spacings are influenced by the curvature of the asymmetric well which is a function of electron density at the interface

and can be controlled by gate voltage (Fig.2). We have performed subband spectroscopy of such structures and confirmed that they are capable of tunable absorption in the infrared region of interest (Figs.3).

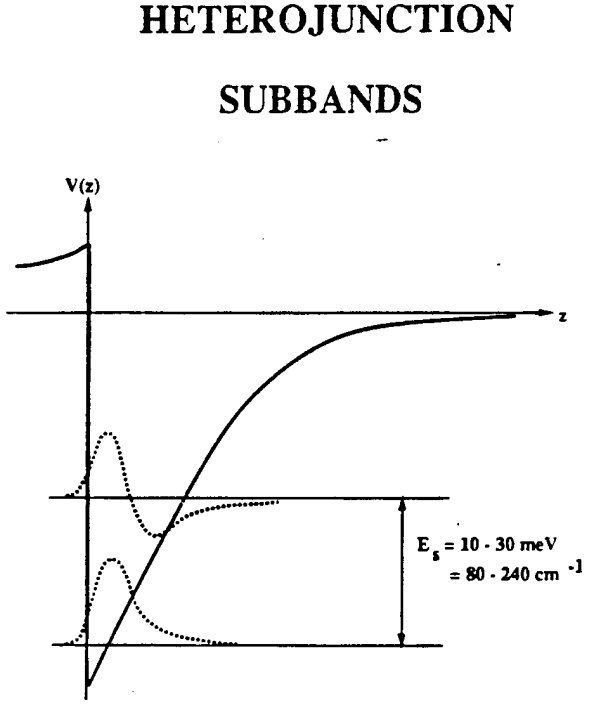

Figure 2: Heterojunction potential at interface with 2D ground and first excited states.

Since heterojunctions have only a single 2DES layer, absorption in them tends to be quite weak. This trade-off in sensitivity for the sake of tunability is exactly what our design seeks to address. We reduce the impact of the low absorption by minimizing the dark current of the device, which is the primary source of background noise associated with these structures. We cannot limit the dark current however simply by reducing the electron concentration, since this would also reduce our absorption signal. We therefore have produced a design which reduces the conductivity for the 2DES in the ground state by adding 1D barrier gates to the sample perpendicular to the direction of current flow (see Fig. 4). The potential on these gates will be large enough that the lowest 2D subband in the patterned 2DES will be further confined into 1D subbands, with the confinement greatly reducing the dark current. At the same time, we feel that this confinement can be adjusted such that the wavefunctions for the higher excited 2D subbands will have significant overlap in the 1D confinement direction. This will result in the absorption of

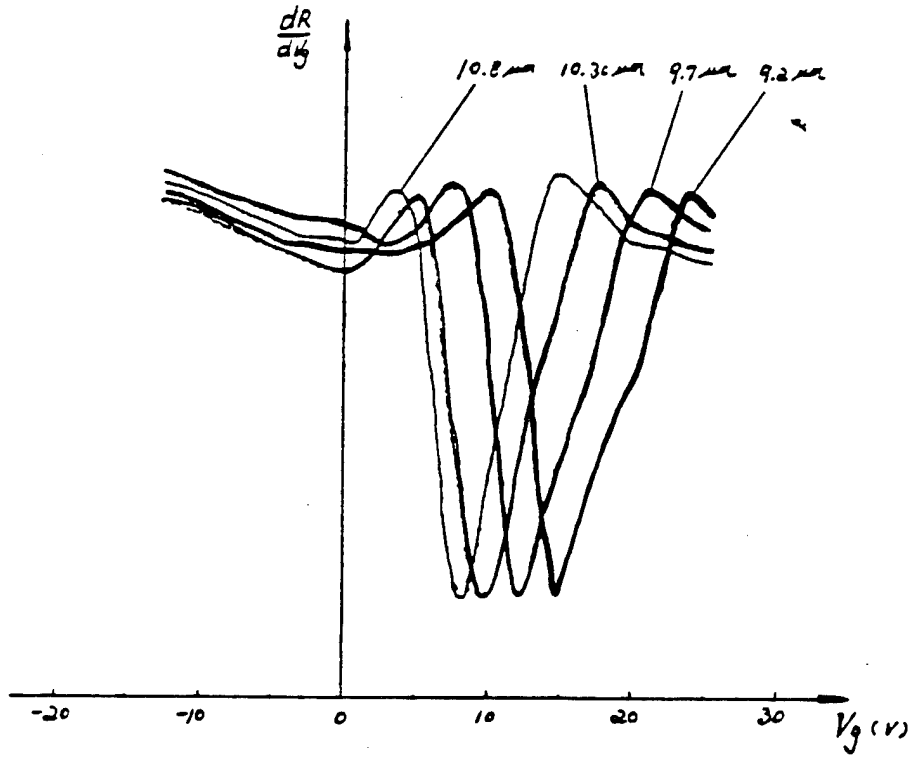

Figure 3: Differential photoresistivity of P-type MOS inversion layer vs gate voltage showing wavelength tunable response in a 2DES with asymmetric potential profile as in figure 2.

a photon corresponding to a transition from a 1DES to a 2DES with a large increase in mobility.

In addition to facilitating confinement, the presence of wires at the surface forms a grating that can greatly enhance coupling of FIR to the device. This is due to the fact that at normal incidence to the heterostructure, with the electric polarization lying in the plane of the 2DES, FIR transitions are forbidden by optical selection rules. The grating serves to generate components of the electric field normal to the 2DES, thus enabling first order transitions.

DEVICE DESIGN AND CONSTRUCTION

Our design is essentially a modified Modulation Doped Field Effect Transistor or MODFET whose gate consists of an array of wires running perpendicular to the direction of current flow in the channel. In the actual device (FIGS.5,6), we extend the channel region to

1D Wire Array

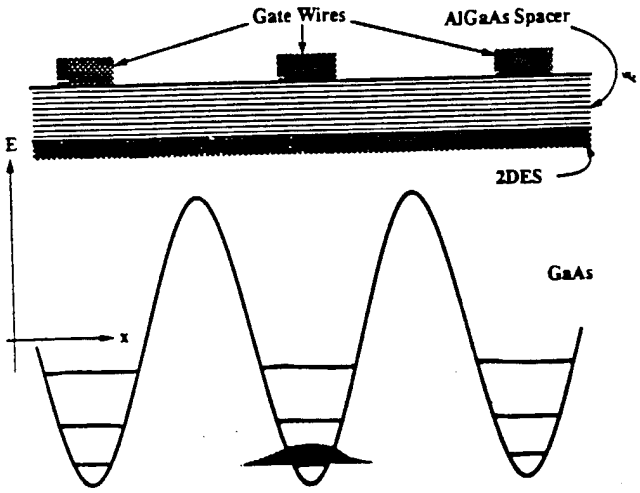

Figure 4: Cross-sectional view of gate wires over the 2DES layer with plot of 1D confinement potential.

accommodate five separate gate arrays, allowing for testing of different geometries on the same sample.

Upon close inspection a typical gate array can be seen to incorporate two different length scales (FIGS. 7,8). The wires, which have $60nm$ width with $180m$ periods are optimized for 1D confinement. These are then grouped in bars of nine that repeat with a 3μm period to produce an optimal grating configuration for FIR coupling in the $10 - 12\mu$m range.

The devices are fabricated using optical lithography to define the mesa, ohmic source and drain contacts, and the gate electrodes. Electron beam lithography is then used to write the sub-micron features of the gate arrays. The gratings present the main technical challenge as we approach the optimal design specifications of 20nm wires with a 60nm period.

CURRENT STATUS AND OUTLOOK

Progress in fabrication has enabled us to produce devices with 60nm wires and 180nm periods as shown above, which are ready for performance testing. Calculations[7] indicate however that this is somewhat far from the optimal period which is on the order of the depth of the 2DES from the surface at 60nm, so efforts will also continue in device fabrication.

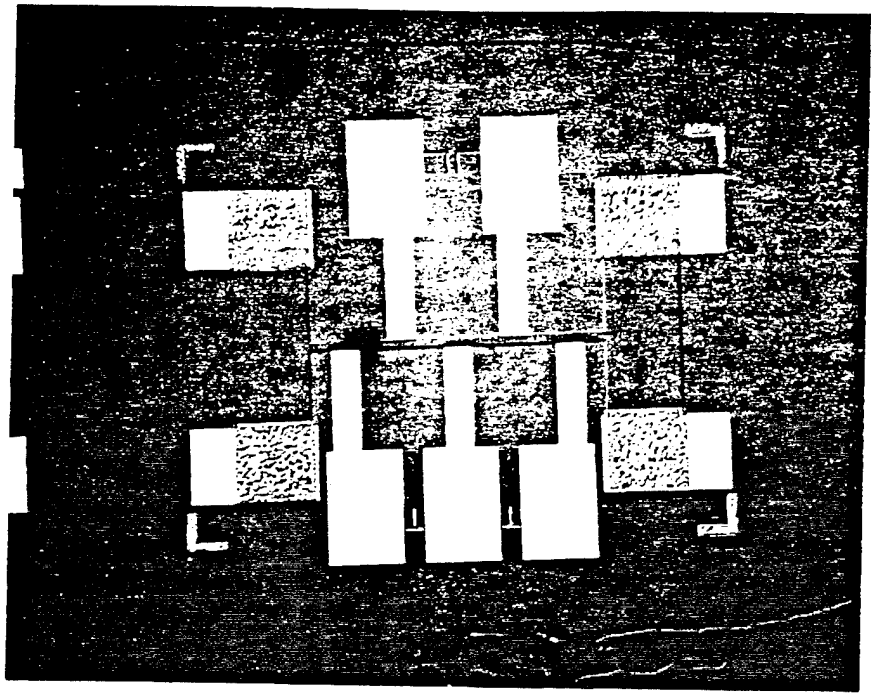

Figure 5: FIR detector prior to patterning and deposition of gate arrays.

With the goal of further improving the tunability, we are also planning to fabricate devices on AlGaAs/GaAs heterojunctions that are "back-gated" which will enable us to control confinement and energy splitting independently.

In the immediate future however we will be measuring FIR photoconductivity of these initial devices and monitoring the need for additional design refinements.

Research supported by the Army Research Office, grant number #DAAL03-91-G-0046.

REFERENCES

1. K.W. Goosen and S.A. Lyon, Appl. Phys. Lett. 52, 1702, (1988).
2. A. Kastalsky, T. Duffiel, S.J. Allen and J. Harbison, Appl. Phys. Lett. 52, 1320, (1987).
3. B.F. Levine, R.J. Malik, J. Walker, K.K. Choi, C.G. Bethea, D.A. Kleinman and J.M. Vandenberg, Appl. Phys. Lett. 50, 273, (1987).
4. G. Hasnain, B.F. Levine, C.G. Bethea, R.A. Logan, J. Walker and R.J. Malik, Appl. Phys. Lett. 54, 2515, (1989).
5. C.P. Lee, K.H. Chang and K.L. Tsai, Appl. Phys. Lett. 61, 2437, (1992).
6. J.E. Furneaux, private communication (1994).

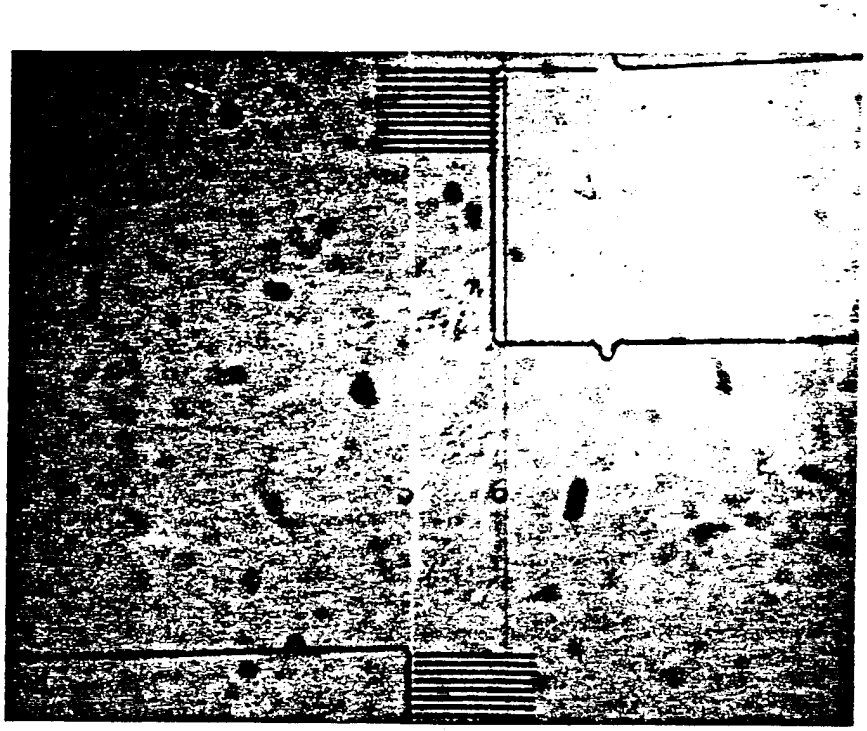

Figure 6: Gate arrays attached to gate electrodes span the mesa where channel is defined. Each of the ten bars is comprised of nine wires.

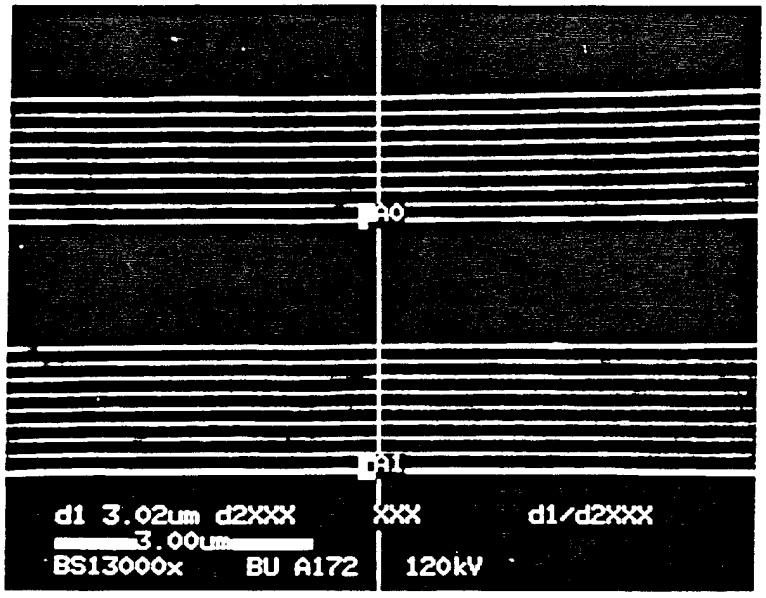

Figure 7: Electron micrograph of gate array showing 3μm periodicity of bars

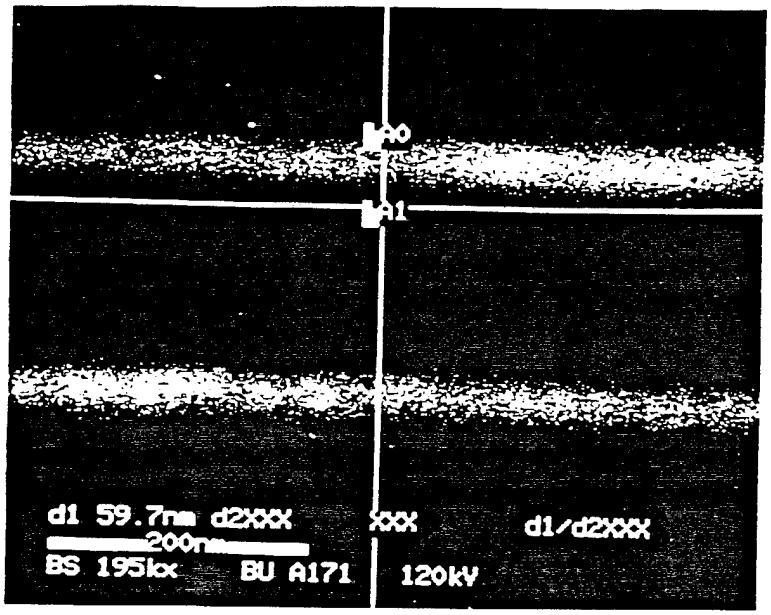

Figure 8: Electron micrograph showing 60 nm wires with 180 nm period

THE GENIUS CHIP: THREE-DIMENSIONAL FERROELECTRIC INTEGRATED CIRCUITS, PROTOTYPE FABRICATION AND INTERFACE STUDIES

R.F. Pinizzotto, E.G. Jacobs, Y.G. Rho, P. Pena, G. Wang and Y. Wu
Center for Materials Characterization
University of North Texas
Denton, TX 76203

B.E. Gnade, S.R. Summerfelt and R. Tsu
Materials Science Laboratory
Texas Instruments Inc.
Dallas, TX 75265

S. Bilodeau and J. Roeder
Advanced Technology Materials Inc.
Danbury, MA 06810

Research personnel at the Center for Materials Characterization of the University of North Texas are designing and building three-dimensional ferroelectric integrated circuits (3d-FICs) using coupled thin film ferroelectric devices. The program has 4 specific goals: (1) demonstration of reproducible cell-to-cell interactions; (2) characterization of electrode/ferroelectric interfaces before and after electrical fatigue testing; (3) studies of the electrical and physical characteristics of thin ferroelectric films and electrodes; and (4) observation of atomic motion in the ferroelectric due to application of electric fields.

The work is being performed in collaboration with the Materials Science Laboratory of Texas Instruments, and with the participants of the Advanced Research Projects Agency consortium working on the development of high dielectric constant materials for integrated circuit applications.

A cross-section of a proposed device structure is shown in Figure 1. The substrate consists of a silicon wafer with a thermal oxide dielectric. A ferroelectric layer is deposited on the oxide. Metal electrodes are deposited onto the ferroelectric and patterned into parallel lines using standard integrated circuit fabrication techniques. A second ferroelectric layer is deposited over the first metal lines, but the contact areas of the electrodes are protected during this deposition so that electrical contact may be made to them later. A second set of electrodes is deposited and patterned perpendicularly to the first set. The overlap areas of the two sets of lines define ferroelectric capacitors, as shown in Figure 2.

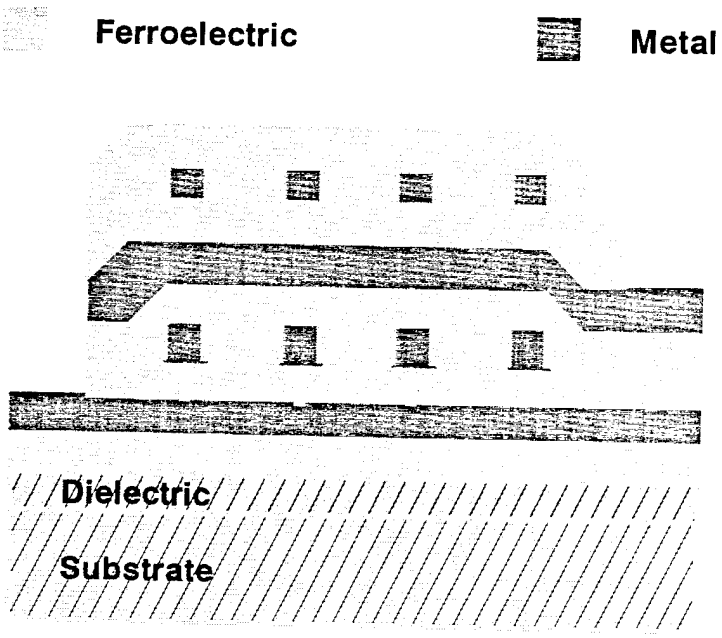

Figure 1. A cross-sectional schematic of a proposed 3-d FIC.

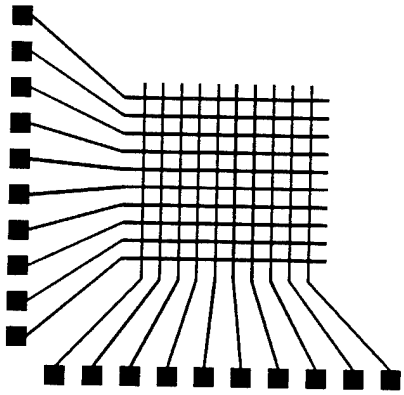

Figure 2. Schematic of capacitor definition by the intersection of the electrodes.

The above sequence may be repeated as many times as desired to build the 3-d FIC with no limitation on the number of vertical layers. The arrows in Figure 1 are the stacked capacitor regions. In this symmetric three layer structure, the central capacitor is surrounded by 6 nearest neighbors, 12 second-nearest neighbors and 8 third-nearest neighbors, for a total of 27 capacitors in a 3 x 3 array. If the array is a closely packed cube, all 26 neighboring capacitors will affect the polarization state of the central capacitor. This is equivalent to a "neuron" in that the polarization state of the central device is a function of the integrated electrical field at that position. Thus, the polarization state of each position depends on the particular polarization pattern applied to the entire device. In addition, the polarization state may change over time at a rate determined by the kinetics of ferroelectric domain switching. This is a form of learning.

The prototype 3-d FIC will consist of three stacked 10 x 10 layers of capacitors for a total array size of 300. There will be 4 sets of 10 electrodes each. Even this small device has a large number of parallel inputs/outputs. The final state of the device will be a direct function of its previous input experiences and the input response will be highly non-linear. It is possible to view the 3-d FIC as an exceptionally "smart" material that learns over time. This ability has led us to term the device "the Genius Chip."

We have developed a fabrication process for the proposed 3-d FIC structure that does not require etching. The electrodes are deposited and patterned using a lift-off lithographic process. The electrode contacts are protected by the use of shadow masks during ferroelectric layer deposition.

Initially, ferroelectric films were formed using pulsed laser ablation deposition (PLD). However, electrical and physical characterization of PLD films showed that stoichiometry control was a major problem. In addition, layer thickness control was also lacking due to instabilities in the laser pulse power and variations in the energy deposited on the target caused by deposition of material on the system windows.

We have subsequently examined ferroelectric films fabricated using sputter deposition, metal-organic chemical vapor deposition (MOCVD), sol-gel processing, and metal-organic decomposition (MOD). Sputter deposition is no longer being considered for this project. The MOCVD films are being fabricated by Advanced Technology Materials Inc. (ATMI). The sol-gel and MOD films are fabricated at Texas Instruments (TI). We are currently installing the equipment needed to perform sol-gel and MOD processing at UNT. We have also begun construction of a sample chamber to perform annealing either in vacuum or in controlled atmospheres.

We have successfully fabricated and tested single layers of capacitors using the facilities at TI. The three-d arrays are currently being processed and should be completed within 30 days.

The physical characterization of the ferroelectric and electrode films is the most advanced part of the program at the present time. Figure 3 is a cross-sectional TEM micrograph of MOCVD material (A) deposited on a Pt electrode (B) on a ZrO_2 adhesion layer (C) on SiO_2 (D) on Si. The ferroelectric is approximately 480 Å thick, the Pt is 1130 Å thick and the ZrO_2 is 320 Å thick. The interfaces are essentially defect free. The grains are columnar are extend throughout the thickness of the film. There are no crystallographic defects observed either at the interface or within the film itself. The ferroelectric used for these samples is $(Ba,Sr)TiO_3$, since BST is also being considered for use as a high dielectric constant material.

Figure 4 is a plane view, bright-field TEM of similar MOCVD BST material. In this particular sample, the ferroelectric grain boundaries are completely coated with a second phase. Selected area and micro-diffraction experiments showed that this second phase is amorphous. The volume fraction of second phase is dependent on the target stoichiometry used during the deposition process. If the metal/Ti ratio is close to 1.00, the second grain boundary phase does not occur.

We have recently purchased a Radiant Technologies ferroelectric electrical test system which has been installed at UNT. We are negotiating for the purchase of a ferroelectric testing sample holder for a JEOL TEM with Gatan, Inc. This holder will have the ability to tilt in two directions, will be able to heat the sample to 1000 °C, and will have 4 electrical inputs. The stage will be used in both JEOL 100 CX and 200 CX Scanning Transmission Electron Microscopes. The drawings needed for the construction of a high resolution ferroelectric sample holder for the top-entry stage of the Hitachi H-9000 High Resolution TEM have been obtained from the manufacturer. A standard sample holder, already obtained from Hitachi, will be modified for this application.

Future Research Plans

The highest priority for this program is the fabrication and testing of an actual 3-d FIC. Demonstration of reproducible cell-to-cell interactions is mandatory. The transfer of MOD and sol-gel technology from TI to UNT for both BST and PZT will facilitate this task. Electrode deposition and lithography will continue to be done at TI. The physical and electrical characterization of thin ferroelectric films will continue at UNT since we believe that we have developed substantial expertise in this area. The sample holders needed for observation of atomic motion due to application of electric fields are in construction and should be available within the next 12 months. As soon as they are available, experimental electron images will be compared to calculated images to measure the crystallographic changes caused by external electric fields.

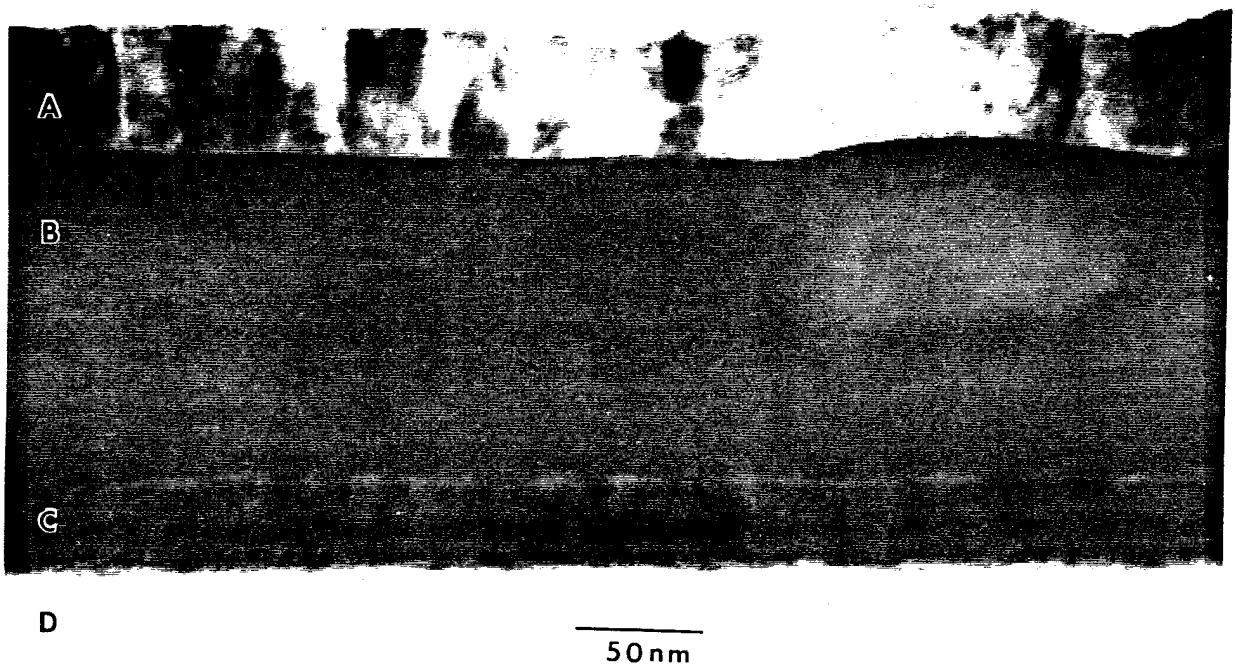

Figure 3. Cross-sectional TEM showing (A) BST ferroelectric, (B) Pt electrode, (C) ZrO_2 adhesion layer and (D) SiO_2.

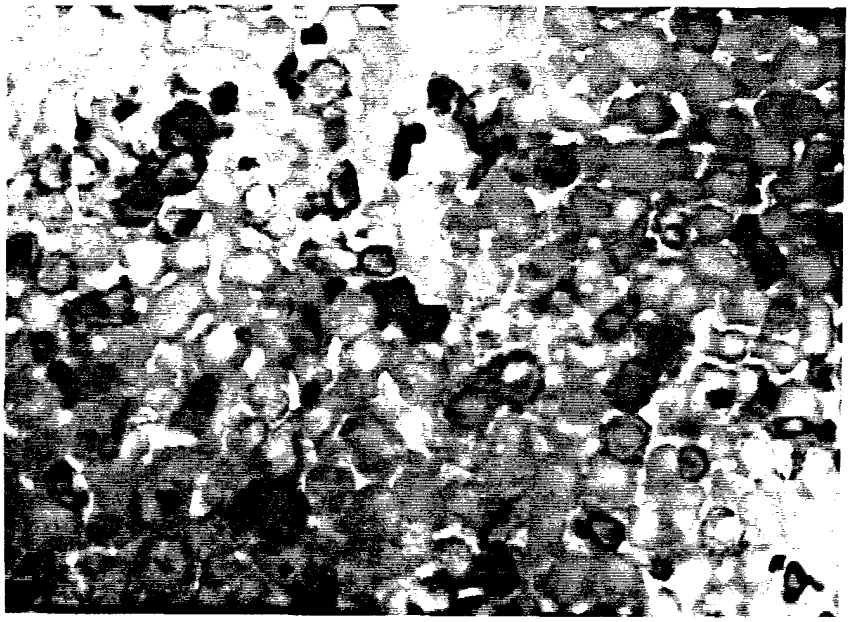

Figure 4. Plane view TEM of a ferroelectric film showing that the grains are surrounded by a second amorphous phase is the stoichiometry is not controlled during deposition.

Extended Abstract
ARO Workshop on Smart Materials

A.Peter Jardine
Dept. of Materials Science
SUNY Stony Brook
Stony Brook, NY 11794-2275

Current Research on Ferroelastic-Ferroelectric Heterostructures

Through the coupling of ferroelastic Shape Memory Alloys and ferroelectric ceramics, a hybrid heterostructure can be fabricated that utilizes the active properties of the individual bulk materials to create a hybrid structure which possesses a new property, which is control. (thus smartness of the system is achieved). Ferroelectric ceramics are very sensitive to applied stresses through the piezoelectric effect and have fast response times, but displacements are very small (in the order of a few micrometers) due to the small strain magnitude. Ferroelastic materials in contrast, have larger displacements and are able to drive larger loads, however, cycling time is much slower since it is dependent upon the dissipation of latent heat of transformation. A natural choice for these composite materials are Ti-based ferroelastic alloys and titanate based ferroelectrics, since the Ti-based alloys typically have an 80 Å layer of passivating Titania.

Smart active damping of mechanical vibrations is a possible application for these heterostructures. This requires the heterostructure to be able to sense the incoming stress wave and to actively respond. The logic of active damping by a ferroelastic-ferroelectric structure can be explained by considering an approaching stress wave shown in Figure 1. The stress wave propagates into the TiNi producing a martensitic-austenitic phase transformation where some of the mechanical energy converts into heat. As the wave continues to propagate, it produces a voltage across the first ferroelectric layer which can be used to produce an out of phase stress wave by the second ferroelectric layer and in turn attenuate the stress wave. By varying the TiO_2 layer between the ferroelectric layers (PZT), it is possible to control the resistance and capacitance of the resulting circuit. To account for the possibility of the velocity of the stress wave to exceed the system's response time, a mechanical metallic impedance buffer (such as Al, Ti and TiNi) can be added to provide time for the counter-stress actuation to occur.

Synthesis issues involved in FFH materials

Synthesis of TiNi was accomplished using powder metallurgy. There are some advantages to using powder metallurgical techniques as opposed to other techniques including a better control of stoichiometry and the ability to produce near-net shapes. However, the major points is that using powder techniques, one can exploit two factors not realized in commercial TiNi, first that compositional coring of the material can be

realized and secondly, that a porous microstructure, suitable for passive damping, can also be realized.

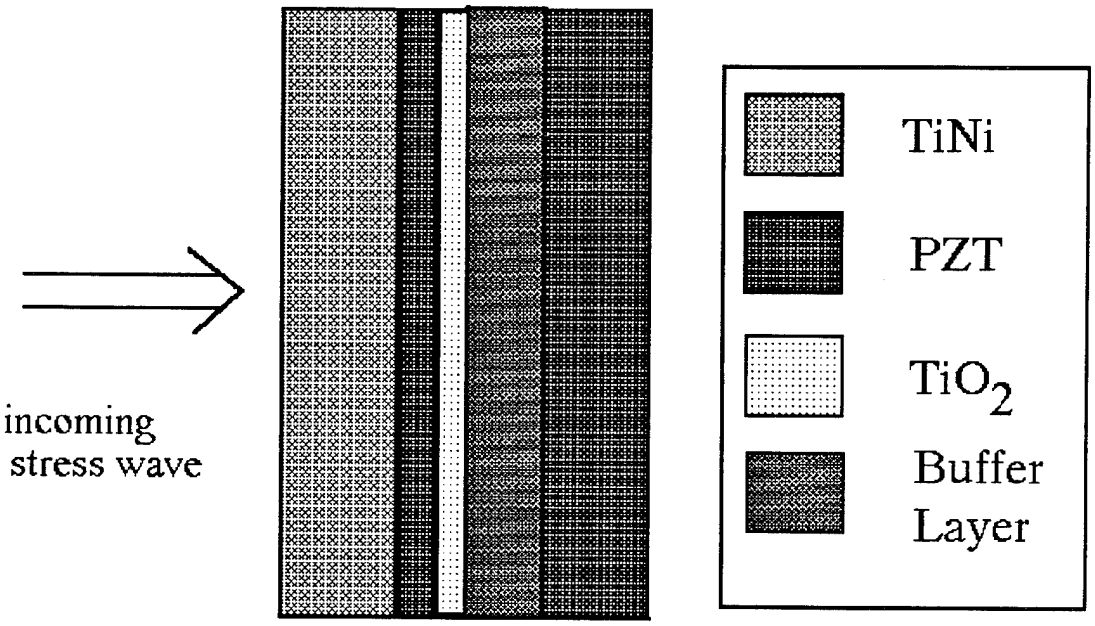

Figure 1: Schematic of the FFH heterostructure:

Using classical powder metallurgical techniques, we have developed TiNi with densities less that half of the conventional powders. From examination of SEM micrographs, there is a considerable amount of microvoidage at the micron level, as well as larger pores generated by packing the powders. This porous microstructure implies that the material will be a better acoustic adsorber than a dense microstructure. Further improvements in decreasing the density where made with the inclusion of NH_3I powders into the Ti-Ni powder mixture, with final sintered densities approaching 0.8 gm/cm^3. The rationale for developing light weight TiNi material is also two-fold; first a lighter material implies better compatibility with aerostructures, for examples helicopters and secondly, there is a decrease in the effective modulus of the material on loading.

We had originally chosen PZT as both sensor and actuator layers due to its superior piezoelectric properties. PZT with a Zr/Ti ratio of 53/47 atomic percent was deposited onto TiNi and $TiNi/TiO_2$ substrates by sol-gel and spin-on process. The PZT sol was prepared using commercially available lead acetate, Zr n-propoxide and Ti-isopropoxide metallorganic solutions. The lead acetate was dissolved in acetic acid and heated to 105 °C to remove the water byproducts. The Zr-Ti precursor was prepared by mixing appropriate amounts of metallorganic solutions with acetic acid and isopropanol. The lead precursor was then combined with the Zr-Ti mixture and mechanically stirred while

water was added to hydrolyze the solution. Ethylene glycol was also added to minimize cracking during annealing cycles.

The PZT solution was spun onto the Si/Au and TiNi substrates at 4000 rpm and prebaked at 300 °C for 15m. This process was repeated twice and then the film was annealed at 650 °C for 15 - 30 m. The final film thickness was approximately 2 μm. The TiNi foils were initially etched to remove existing oxides and cleaned in an ultrasonic bath with acetone and methanol. The TiNi/TiO_2 substrate was also synthesized by the sol-gel process. The TiO_2 film was prepared by dissolving Ti-isopropoxide in isopropanol and spinning onto the TiNi foil at 4000 rpm. After each spin coat, the film was prebaked at 300 °C for 15m to remove most of the organics. This was repeated 5 times before annealing at 600 °C for 15m to produce a film with a thickness of 3.3 μm.

A problem in the characterization of these heterostructures has been the difficulty in growing high quality films onto TiNi. TiNi was exploited as both a passive damping medium and as a structural material; it was necessary to deposit a sensor layer of PZT onto this structure. Difficulties arose in that the PZT layers grown tend to have pinholes which allow for leakage currents to be developed. As seen in Figure 2, the effect of synthesis of PZT onto the a ground surface of a TiNi using sol-gel processing resulted in mud-crack like patterns and this did not allow for a uniform coating on the surface.

There are several mechanisms which can be responsible for these effects. We investigated the effects of substrate surface roughness, various piezoelectric layers, layer thickness and the effect of cooling rate on the thin film quality. Characterization of these materials was done using both optical microscopy and Scanning Electron Microscopy.

Using the appearance of thin-film defects as a qualitative criteria, there was a general trend to improved ferroelectric thin film quality when the TiNi substrate was smoother, though improvements in film quality where not found when polished below 600 grit paper. Improvements where observed on slow cooling of the heterostructure after crystallization, especially the Barium Titanate material, and this may be due to a slow transition through its phase transformation at 400C. When the substrate is rough, the film quality is largely independent of the ferroelectric thin film thickness. When the substrate was smooth, a similar observation was observed.

These observations point to some important lessons in the generation of the thin film structure. Both PZT and BaTiO3 seem to be fundamentally incompatible with TiNi, despite the good thermal expansion compatibility of the materials. Thus, a search for better ferroelectrics is continuing with SrTiO3.

Different FFH Geometries:

The study shown has demonstrated that there are difficulties in synthesizing planar TiNi. One possible clue to developing better heterostructures is to expand beyond planar geometries and persue fundamentally different geometries. As TiNi is available as wire, hence a cylindrical geometry could be exploited. Onto TiNi wire was deposited the PZT solution by dip-coating, which after firing was subsequently poled and the ferroelectric characteristics analysed using an Radiant Technologies RT-11 Ferroelectric test station. The ferroelectric behavior of the PZT was found to be similar to that of bulk material, indicating that the coating was continuous.

Future Research Plans

The key to the development of successful FFH heterostructures lies in controlling the pinhole defects which have prevented successful characterization. Further work is required to completely eliminate certain thin film ferroelectric as viable thin film materials, which should include more detailed studies of both heating and cooling rates of the structures. Finally, defect characterization of the thin film coatings by exploring different geometries will also be important.

Once these issues are addressed, the electro-mechanical response of the system will be characterized and optimization of the structure through modeling can be accomplished.